GEORG-AUGUST-UNIVERSITÄT GÖTTINGEN

Max Planck Institute for Biophysical Chemistry

Roles of *miR-137* in Muscular Dystrophy and Muscular Dystrophy-Related Phenotypes in *Drosophila melanogaster*

Doctoral Thesis

Dissertation for the award of the degree
"Doctor rerum naturalium (Dr. rer. nat.)" in
the GGNB program: "Genes & Development" of
the Georg August University Göttingen
Faculty of Biology

submitted by

Shruti Chhetri
born in Kathmandu, Nepal

Göttingen, March 2019

Members of the Thesis Committee

Thesis Committee Members

Prof. Dr. Halyna Shcherbata (Supervisor, reviewer)
Max Planck Research Group for Gene Expression and Signaling
Max Planck Institute for Biophysical Chemistry
Am Fassberg 11, 37077 Göttingen, Germany

Prof. Dr. Stefan Bonn (2nd Reviewer)
The Center for Molecular Neurobiology Hamburg (ZMNH)
Institute of Medical Systems Biology
Martinistr. 85, 20251 Hamburg, Germany

Prof. Dr. Jörg Großhans
University Medical Center Göttingen
Department of Developmental Biochemistry
Justus-von-Liebig-Weg 11, 37077 Göttingen, Germany

Extended Thesis Committee Members

Dr. Roland Dosch
University Medical Center Göttingen
Department of Developmental Biochemistry
Justus-von-Liebig-Weg 11 37077 Göttingen Germany

Prof. Dr. Martin Göpfert
Schwann-Schleiden Research Centre
Department of Cellular Neurobiology
Julia-Lermontowa-Weg 3, 37077 Göttingen, Germany

Prof. Dr. Ahmed Mansouri
Max Planck Institute for Biophysical Chemistry
Molecular Cell Differentiation Group
Am Fassberg 11, 37077 Göttingen, Germany

Date of Oral Examination: 04.04.2019

Affidavit

I, Shruti Chhetri, confirm that the work presented in this thesis is my own. This thesis was written independently and no other sources or aids were used except the mentioned ones. This thesis has not already been published and is also not concurrently submitted for any other degree.

Göttingen, 01.03.2019

Table of contents

List of figures

List of supplementary figures

List of tables

List of supplementary tables

Abstract

Muscular dystrophies (MDs) are a group of diseases that cause muscular and neurological disorders in human patients. They are associated with a multi-component complex called the Dystrophin Glycoprotein Complex (DGC). The DGC connects the extracellular matrix to the cytoskeleton and is well-conserved in animals. Perturbation of this complex is associated with various kinds of MDs, leading to a diverse range of muscle and nervous system abnormalities. Dystroglycan (Dg) is a central DGC component, mutations of which are associated with a heterogeneous group of MDs also known as dystroglycanopathies.

MiRNAs are small, noncoding RNAs that function in posttranscriptional gene regulation and often represses their target mRNAs. Previous work has shown that similar to MD, stress itself causes muscle degeneration, and altered miRNA expression profiles have been detected in dystrophic as well as stressed wild type flies. These results indicate that miRNAs influence a common regulatory pathway between stress and MD. Though much is known about the DGC and its relevance to MDs, the molecular and genetic pathways underlying MD pathogenesis remain largely unknown.

To understand the role of miRNAs in DGC signaling and their contribution to MDs, in particular during stress, we screened several miRNAs that are predicted to target multiple components of the DGC study their potential roles in MD development, particularly upon various stresses. We found that *miR-137, miR-966,* and *miR-927* affect muscle integrity upon stress and aging. Our study further reveals that *miR-966* and *miR-137* are required more during adult muscle maintenance than developing muscles. *MiR-137*, in particular, is a stress-responsive miRNA, as the severity of the phenotypes related to muscle maintenance progressed in a stress- and age-dependent manner.

We further show that levels of Dg must be regulated to sustain healthy muscle, and this regulation includes targeting of *Dg* by *miR-137*. The *Dg-miR-137* interaction is required to address negative effects of stress in adult muscle maintenance. Our results also demonstrate that a perturbed blood-testis barrier (BTB) in testes is a novel phenotype related to MD, and *miR-137* regulates the expression of *Dg* in early somatic cells of *Drosophila* testes to maintain the BTB. Our results highlight the importance of miRNAs in the regulation of the DGC and MD, particularly on muscle maintenance that is accelerated upon stress.

1 Introduction

Muscular Dystrophies (MDs) are a group of genetic disorders mostly characterized by progressive muscle degeneration and wasting. The condition often begins by affecting a particular group of muscles, such as the limb, facial, and axial muscles, as well as respiratory and cardiac muscles, before affecting the overall musculature to variable degrees. In some cases, the disorder can affect other tissues such as the brain, inner ear, eye, or even skin. More than 30 different types of MDs have been characterized so far. The severity, age of onset, consequences, and disease progression vary from patient to patient, as well as from the type of disorder. Unfortunately, there is neither a cure nor adequate treatments for this group of diseases, making it more critical to understand disease-specific complications and pathogenesis as well as the implementation of medical-related advances. Duchenne muscular dystrophy (DMD) is the most severe type of MD. It affects 1/3500 males worldwide and is an X-linked, fatal disorder. Loss of Dystrophin (Dys) is associated with DMD. Patients with DMD die in their early twenties because of respiratory or cardiac failure (Durbeej and Campbell, 2002). Dys is also associated with a less severe form of MD called Becker MD (BMD), which also affects males with mean age of onset of 12 years old, resulting in a loss of ambulation and cardiac defects (Wilson et al., 2017). *Dys* is the largest gene in the human genome at 2.5 Mb and is a part of a membrane-associated protein complex called the Dystrophin Glycoprotein Complex (DGC) (Hoffman et al., 1987; Kunkel et al., 1986). Mutation in any of the components in the DGC (Chapter1.1) is associated with various kinds of MDs, namely limb-girdle MD (LGMD), congenital MD (CMD), DMD, BMD, muscle-eye-brain disease (MEB), Walker-Warburg syndrome (WWS), and myotonic dystrophy. All of these diseases share the common symptoms of muscle degeneration, reduced lifespan, cardiomyopathy, as well as some extent of neuronal disorders. The involvement of the DGC in MDs, affecting various tissues causing individual symptoms are due to mutations in different proteins of the DGC that share similar cellular functions. Most of the components of the DGC are well-conserved throughout the animal kingdom and are well-characterized, making them easier to study in different model organisms in order to highlight their molecular function and regulation in the disease state.

1.1 The DGC

The DGC is a large, oligomeric complex that connects the extracellular matrix to the cytoskeleton. In mammals, it is composed of transmembrane dystroglycan (α- and β-),

sarcoglycans (α-, β-, γ-, and δ-), cytoplasmic dystrophin, syntrophins (α1-, β1-, β2-, γ1-, and γ2-), α-dystrobrevin, and neuronal nitric oxide synthase (Durbeej and Campbell, 2002). α- and β-dystroglycan connect the extracellular matrix (ECM) component laminin-2 to the cytoskeleton via dystrophin, which in contractile muscle cells accounts for the mechanical stress resistance and the stability of the muscle sarcolemma (Ervasti and Campbell, 1993). Thus, the DGC in muscles has very important roles: 1) to account for the flexibility and the durability of the resilient plasma membrane to maintain its structure in each contraction and retraction; and 2) to act as a signal transduction platform to maintain the link between the inner and outer environments of the cell. Syntrophins, having various protein-protein interaction motifs, are famous as adaptor proteins capable of binding to heterotrimeric G proteins, adaptor protein Grb2, and neuronal nitric oxide synthase (nNOS) (Cacchiarelli et al., 2010; Xiong et al., 2009; Zhou et al., 2006) among other signaling molecules. Recently it has been shown that α-syntrophin can bind directly to multiple spectrin-like repeats in dystrophin and mediate its binding to nNOS (Adams et al., 2018).

The DGC components are associated with various forms of MDs. α2-laminin is associated with CMD, sarcoglycan deficiency is linked to LGMD, and hypogycosylation of dystroglycan is associated with severe forms of congenital (Fukuyama CMD, FCMD; WWS; CMD type 1C/1D, MDC1C/MDC1D), and late-onset muscular dystrophies (MEB; hereditary inclusion body myopathy (HIBM)) (Cohn, 2005). Progressive muscle degeneration is a hallmark of many of these MDs; however, clinical traits for these group of diseases are not limited to the muscles. They are also associated with structural brain defects, abnormal neuronal migration, as well as mental retardation (Balci et al., 2005; Muntoni et al., 2002; van Reeuwijk et al., 2006; Waite et al., 2012; Zhou et al., 2006). The main classes of proteins involved in MDs can be subdivided into groups: 1) extracellular matrix proteins, or external membrane proteins (laminin, collagen VI); 2) enzymes or proteins presumably with enzymatic function that are either involved in glycosylation of α- Dystroglycan, and those that are not involved in glycosylation of α-dystroglycan; 3) sarcolemma-associated proteins; a major subcomplex of the DGC (dystroglycan, dystrophin, and sarcoglycans); 4) nuclear membrane proteins (lamin A or C, emerin *etc.*), sarcomeric proteins (titin), and others (DUX4) (Mercuri and Muntoni, 2013).

MDs, in general, affect various types of tissues causing individual symptoms among patients. Moreover, the genetic and molecular pathways underlying MDs' pathogenesis remain poorly understood. Recent advances in the understanding of MDs' pathogenesis suggests that variable symptoms of MDs are due to the different components of the DGC and their isoforms

being expressed in many tissues. For example; Apo-dystrophins-1 and 3 are regulated by a promoter situated between the exons 62 and 63 of the dystrophin gene. It is expressed in tissues such as brain, lung, liver, and kidney. Apo-dystrophin-2 is regulated by a promoter positioned between exons 55 and 56 of the dystrophin gene and is expressed in peripheral nerves. α- and β-dystroglycan are also expressed in the brain, lung, liver, and kidney (Tinsley et al., 1994). Each of the five homologous isoforms of syntrophins has a unique tissue expression. α1-syntrophin is primarily expressed in skeletal muscles but also in heart, brain, and other mammalian tissues; β1- and β2-syntrophins are broadly distributed; γ1- and γ2-syntrophins are highly expressed in brain, but the γ2 isoform also has a broader distribution in mammalian tissues (Bhat et al., 2013).

Dystroglycan is one of the essential components of the DGC. Dg has two subunits, α- and β-dystroglycan. α-dystroglycan connects extracellular matrix proteins to the muscle sarcolemma, and β-dystroglycan is a transmembrane subunit connecting α -dystroglycan to various cytoskeletal adaptor proteins, such as dystrophins and syntrophins. Defects in glycosylation of α-dystroglycan is one of the major causes of CMD and LGMD. Disorders due to mutations in dystroglycan, or in the genes encoding the proteins and enzymes involved in the glycosylation of α-dystroglycan are collectively known as dystroglycanopathies. The dystroglycanopathies are described as a group of diseases caused by the loss or reduced binding of α-dystroglycan to its extracellular ligands, such as laminin, agrin, neurexins, perlecans, pikachurin, and Slit (Brown and Winder, 2017). Mutations in these proteins share the clinical features of dystroglycanopathies, which widens the horizons of how crucial and selective the role of Dg is in various kinds of MDs. α-Dystroglycan is glycosylated mostly by O-mannosylation (Mercuri and Muntoni, 2013). Glycosylation overall has many enzymatic steps that are regulated during development and in a tissue-specific manner. α-dystroglycan glycosylation has a fundamental role in muscles as well as in basal membrane maintenance (Jimenez-Mallebrera et al., 2009). It is also required for the development of the central nervous system, as many MD patients experience cognitive impairment and learning disability and develop behavioral and neuropsychotic disorders (Waite et al., 2012).

Neuromuscular junction (NMJ) shares a structural function, by stabilizing the muscle sarcolemma from various excitations and contractions through the coupling from neurons. Many motor neuron disorders such as in spinal muscular atrophy (SMA) and amyotrophic lateral sclerosis (ALS) can cause progressive degeneration of muscle fibers which occurs due to loss of innervation in muscle tissues (Kreipke et al., 2017). Dystrophin is found at extrasynaptic and synaptic regions of muscle fibers and is required for NMJ development,

and Dystroglycan is required for synaptic maturation as well as synaptic Utrophin, Laminin α5 and Laminin γ1 concentration (Grady et al., 2000). In *Drosophila,* proper localization of glutamate receptors is mediated by the binding of Dg to Coracle (Cora) (Bogdanik et al., 2008; Marrone et al., 2011b).

In mammals, it has been shown recently that Dystroglycan sequesters phosphorylated Yap (Yes-associated protein) to prevent the actions of activating phosphatase as a mechanism to regulate cardiomyocyte proliferation (Morikawa et al., 2017), broadening the role of Dystroglycan in muscle maintenance and muscle-related diseases. Trim32 (tripartite motif-containing protein 32)**,** a ubiquitin ligase, is critical for muscle atrophy. Mutations in the third repeat of Trim32 cause LGMD -2H (Frosk et al., 2002; Shieh et al., 2011), and inhibition of Trim32 enhanced plakoglobin binding and induced fiber growth, while down-regulation of plakoglobin caused muscle atrophy (Cohen et al., 2014). Since muscle weakness is often due to muscle atrophy, hypertrophy, or both, as seen in DMD patients, it is important to investigate the relationship between Trim-32, plakoglobin, and the DGC to identify further players in MDs and their disease relevance.

1.2 *Drosophila* as a model for Muscular Dystrophy

Drosophila melanogaster has many advantages as a model organism. Besides the relatively low cost of the cultivation, the forward and reverse genetic tools in *Drosophila* are much more advanced and sophisticated than in many other model organisms. The relatively fast life cycle (~ 9 days in ambient temperature and humidity), and short lifespan (~ 3 months) of *Drosophila* makes it easier to cultivate large numbers of flies in a short amount of time, which is a great advantage in studying the developmental aspects of disease progression, as well as in creating a large amount of basic material required for biochemical and molecular assays. There are fly homologs of more than 75% of human genes that are associated with various kinds of disorders ranging from bacterial infections, metabolic disorders to aging, and cancer. Therefore, *Drosophila melanogaster* is an ideal model for studying the DGC, identifying its novel functions, interacting components, and factors involved in the physiological and molecular dynamics of its signaling and regulatory systems. Many of the core components of the DGC are evolutionarily conserved but with less diversity. *Drosophila* has only two syntrophins: syntrophin-like-1 (Syn1) homologous to α1/β1/β2-syntrophins, and syntrophin-like-2 (Syn2) homologous to γ1/γ2-syntrophins in mammals. Dystrophin (Dys) is a sole homolog to mammalian utrophin and dystrophin, and a single copy of Dystrobrevin

(Dyb) is homologous to α-, and β-dystrobrevin in mammals (Greener and Roberts, 2000). As in mammals, DGC components in *Drosophila* (Figure 1) are expressed not only in the muscle but also in the nervous tissues (Bhat et al., 2013; Bogdanik et al., 2008; Deng et al., 2003; Marrone et al., 2011a; Shcherbata et al., 2007; van der Plas et al., 2006; Yatsenko et al., 2007). Many of the MD-related phenotypes in the muscle and nervous systems reported in mammals can be easily phenocopied in flies. Flies lacking *Dg* or *Dys* (further dystrophic flies) experience a shortened lifespan, age-dependent muscle degeneration, decreased mobility, and defective photoreceptor path-finding (Shcherbata et al., 2007), hyperthermic seizures (Marrone et al., 2011b), as well as decrease in presynaptic glutamate release at neuromuscular junctions (NMJs) (Bogdanik et al., 2008; van der Plas et al., 2006). Both *Dg* and *Dys* are required in both glial cells and neurons for correct neuronal migration (Muntoni et al., 2002; Shcherbata et al., 2007). In recent years, the roles of the DGC have not been limited to muscle or nervous tissues. Studies have shown that lack of the DGC complex, in particular Dg, in patients is associated with elevated levels of creatine kinase in the blood, ataxic gait, learning disabilities, dilated cardiomyopathy, complete lissencephaly (type II), and autism spectrum disorder and are diagnostic features of dystroglycanopathies (Astrea et al., 2018; Bonnemann et al., 2014), broadening the horizon of *Drosophila* as a model organism to study the pathogenesis of MDs.

DMD is the most severe form of MD and has been studied quite extensively. As a consequence of muscle fiber damage in DMD, specific muscle-microRNAs (myo-miRs) are found to be released into the bloodstream of DMD patients, as well as in mammalian model of DMD (*mdx* mouse), and their levels correlate with the severity of the disease (Cacchiarelli et al., 2011b). The same study also proposed *miR-1*, *miR-133*, and *miR-206* as valuable biomarkers for the diagnosis of DMD. In fly models of cobblestone lissencephaly (similar to type II lissencephaly in humans), *miR-310s* has been reported to play an important role as a buffering agent to establish the proper level of *Dg* level by targeting its alternative 3'untranslated region (3'UTR) (Yatsenko et al., 2014). The same miRNA is also known to play an important role in Hedgehog signaling in response to nutritional changes (Cicek et al., 2016). Similarly, *miR-9a* has been shown to target *Dg* to maintain the precise level of Dg to establish myotendinous junction (MTJ) formation, and flies lacking *miR-9a* have defective muscle architecture (Yatsenko and Shcherbata, 2014). Overall, miRNAs targeting the DGC can influence many signaling pathways, illustrating a molecular mechanism by which miRNAs serve as a quick and robust response in many signaling pathways. These studies show that miRNAs play a fundamental role in MDs.

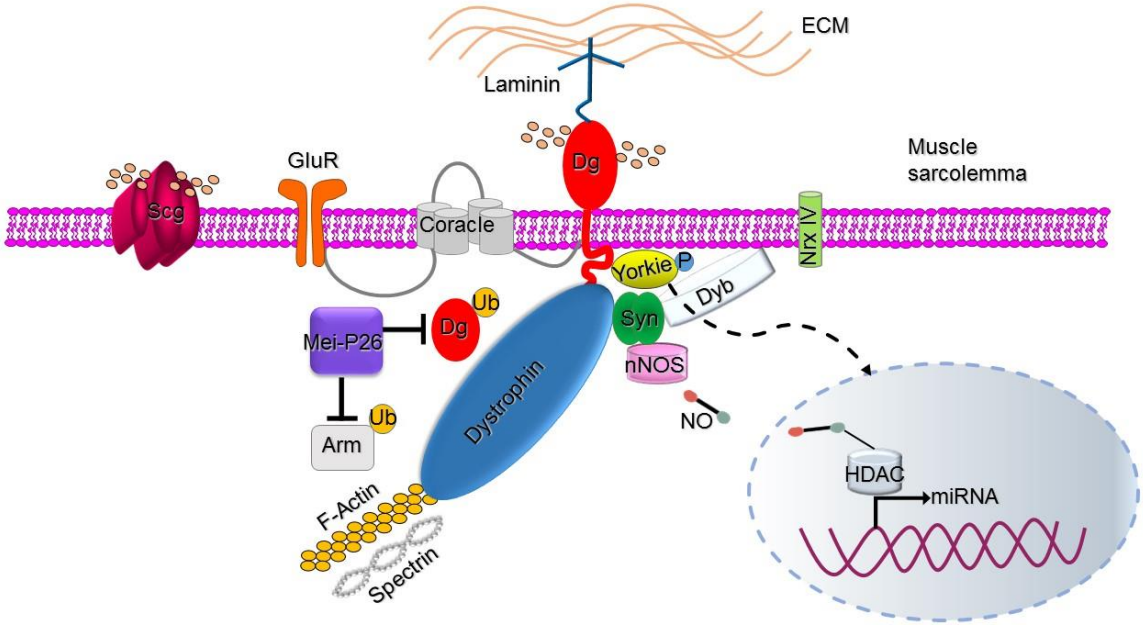

Figure 1. The Dystrophin Glycoprotein Complex (DGC) and its associated components in *Drosophila melanogaster*

The transmembrane protein Dystroglycan (Dg) is a key component of the complex connecting the extra and intracellular environment by binding to laminins extracellularly and Dystrophin (Dys) intracellularly. The DGC acts as a scaffold for many signaling molecules such as syntrophin (Syn) and neuronal nitric oxide syntase (nNOS). nNOS produces nitric oxide (NO) which is involved in nitrosylation of histone deacetylases (HDACs), which in turn influences the gene expression. At the neuromuscular junction (NMJ), Dg is required for proper localization of glutamate receptor (GluR) which is mediated by Dg binding to Dys and coracle (Cora). Similar to the mammalian model, Dg sequester phosphorylated Yorkie (fly ortholog to Yap), and can influence muscle maintenance. Similarly, we also hypothesize that *mei*-P26 (Trim-NHL protein in fly) can ubiquitinate arm (armadillo, fly ortholog of plakoglobin) or Dg, promoting the DGC stability in skeletal muscle.

1.3 MicroRNAs (miRNAs)

MiRNAs are small, ~ 22bp long, endogenous, non-coding RNA molecules that regulate gene expression post-transcriptionally in diverse cellular and developmental processes in a tissue-specific manner. They bind to 3'UTRs of targeted messenger RNAs (mRNAs) with partial complementarity and mediate gene expression via translation inhibition or mRNA decay (Bazzini et al., 2012; Djuranovic et al., 2012; Guo et al., 2010). Under certain conditions, they are also known to activate gene expression (Vasudevan, 2012). The miRNA field is relatively new with the discovery of the first miRNA just over two decades ago in the relatively simple eukaryote *C. elegans* (Lee et al., 1993; Wightman et al., 1993). They are the most abundant non-coding gene family, distributed widely in plants and animals. Since

the discovery, 253 miRNAs in *C.elegans*, 258 miRNAs in *Drosophila*, and 1917 miRNAs in humans have been annotated so far (www.miRBase.org, as of 2/11/2018). The number of miRNAs present in a species has been shown to positively correlated with organismal complexity (Grimson et al., 2008), suggesting that miRNA-dependent fine-tuning of gene expression was necessary for the evolution of higher organisms (Heimberg et al., 2008). MiRNAs' functions can be extended from fine-tuning effects to significant alterations in the gene expression profile. They are known to control basic cellular processes such as cell growth, differentiation, proliferation, and apoptosis (Dhahbi, 2014), or to moderate physiological processes such as cell signaling, immune responses, tumorigenesis, development, and non-neoplastic disease pathogenesis (Koturbash et al., 2011). Some miRNAs are conserved in both their sequences and expression patterns across a wide range of animals, making them excellent models to better understand how similar processes are controlled in various organisms.

1.3.1 MiRNA biogenesis

MiRNA biogenesis begins with transcription by RNA polymerase II (Pol II), giving rise to a single-stranded RNA molecule called a primary miRNA (pri-miRNA) that is ≥ 1 kb long and has a stem-loop structure (Figure 2). Many pri-miRNAs are 3'polyadenylated and 5'capped, similar to the mRNAs transcribed by the same RNA Pol II enzyme (Lee et al., 2004; Winter et al., 2009). Pri-miRNAs then get processed by the Microprocessor Complex, which consists of the ribonuclease III enzyme, Drosha, and the RNA binding protein, Pasha (DGCR8 in mammals) (Denli et al., 2004; Ha and Kim, 2014). This complex further cleaves the hairpin resulting in the formation of a precursor-miRNA (pre-miRNA) of ~70bp with a 2 nucleotides (nt) long 3' overhang. The pre-miRNA is transported to the cytoplasm by the Exportin-5:RanGTP complex for further processing. This complex can recognize the 2 nt 3' overhang to make transport possible through nuclear pores. Following the translocation of pre-miRNA through the nuclear pore, pre-miRNA is released into the cytosol (O'Brien et al., 2018; Okada et al., 2009).

The cytoplasmic pre-miRNA is further cleaved at the terminal loop by RNase III endonuclease Dicer, and dsRBD Loquacious (Loqs) or TAR RNA-binding protein (TRBP) in humans, consequently producing the mature ~22 nt miRNA duplex (Jiang et al., 2005; Macrae et al., 2006; Saito et al., 2005; Zhang et al., 2004). Pre-miRNA can give rise to abundant mature-miRNAs strands from 5' (left arm) or 3' (right arm).Only one of the mature-miRNA strands

is loaded into an Argonaute (Ago) protein and facilitates the formation of RNA-induced silencing complex (RISC/miRISC). The choice of the 5p or the 3p miRNA complementary strand loaded to RISC is based partly on thermodynamic stability at 5'end. The strand with the lower stability that is loaded to the RISC is known as the "guide strand", and the unloaded strand is called the "passenger strand," which will eventually get degraded by cellular machinery (Broughton et al., 2016; Guo and Lu, 2010; Meijer et al., 2014). Although much progress has been made understanding their biogenesis and biological functions, the mechanisms allowing miRNAs to silence gene expression in animal cells are still under debate.

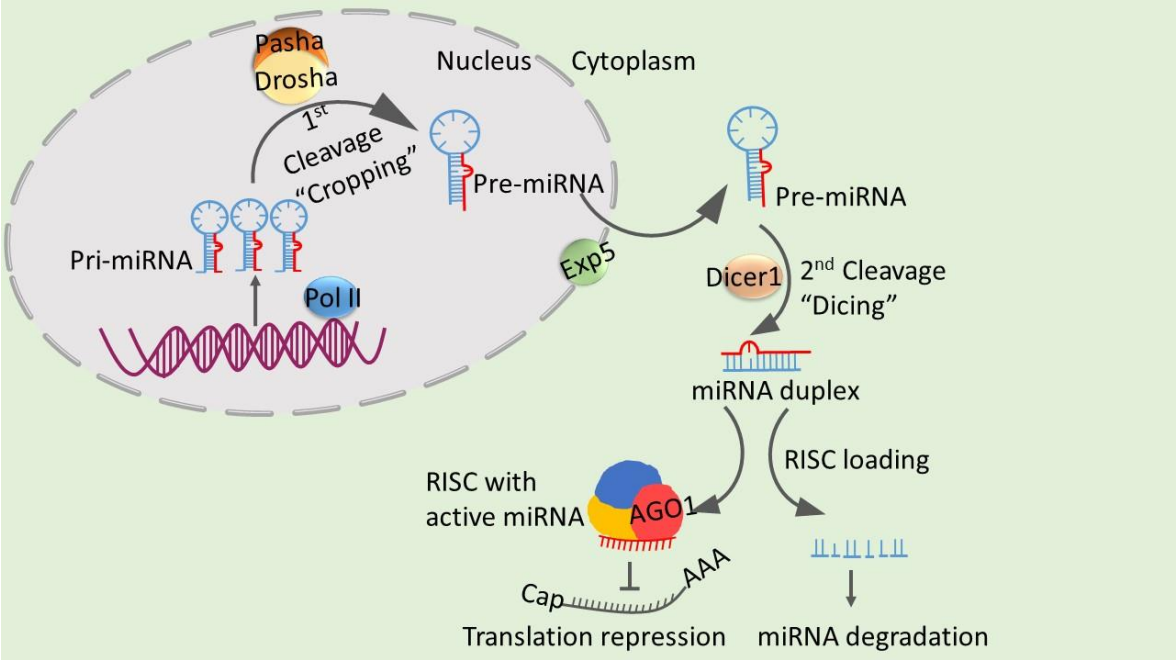

Figure 2. The canonical pathway of miRNA biogenesis

MiRNA biogenesis starts with the generation of pri-miRNA transcript. The microprocessor complex (Drosha and its binding partner Pasha) cleaves the pri-miRNA to pre-miRNA. The pre-miRNA is then exported to the cytoplasm via Exp5, followed by Dicer1 processing to produce a miRNA duplex. Either the 5p or the 3p strand of the miRNA duplex is then loaded to a complex containing Ago1 to form the miRISC, and the other strand gets degraded. MiRISC can bind to target mRNA to induce transitional inhibition.

1.3.2 MiRNA mode of action

MiRNAs can direct the RISC to affect gene expression, mainly via translational repression or mRNA degradation (resulting from mRNA decapping or deadenylation), or a mixture of both. This highly depends on miRNA-target mRNA complementarity. The full miRNA-target mRNA complementarity results in mRNA cleavage in a siRNA-like manner that is mostly observed in plants (Yekta et al., 2004). In a few cases, higher degrees of miRNA-

mRNA complementary can lead to the destabilization of the miRNAs itself (Ameres et al., 2010; Baccarini et al., 2011; Xie et al., 2012). In contrast, animal miRNAs recognize their target mRNAs through partial complementarity, resulting in recruitment of additional effector proteins, which induce translational repression and/or mRNA decay via deadenylation or decapping (Bartel, 2004; Behm-Ansmant et al., 2006; Wu et al., 2006). Not all miRISC targeted mRNA are destined for degradation. MiRISC and targeted mRNA has been reported to be localized in different cellular compartments, such as rough endoplasmic reticulum, early and late endosomes, multivesicular bodies, as well as in stress granules (SG) to regulate miRISC and mRNA concentration over time to promote efficient gene regulation (Barman and Bhattacharyya, 2015; Bose et al., 2017; Gibbings et al., 2009; Kucherenko and Shcherbata, 2018b).

1.3.3 MiRNA target identification and seed sequence

The discovery of the first ever reported miRNA *lin-4* also shed some light on the mechanism of miRNA target identification. The clues came from the observation that *lin-4* has some sequence complementarity at 3'UTR to its target mRNA *lin-14* (Lee et al., 1993; Wightman et al., 1993). Further studies on miRNAs revealed that canonical miRNA-target interactions is based on full complementarity to a 7-8 nt long sequence at 5'region of miRNA, also known as the "seed sequence", together with partial complementarity of the rest of the miRNA to target mRNA (Brennecke et al., 2005; Doench and Sharp, 2004; Kloosterman et al., 2004; Lewis et al., 2003). However, a study in *C. elegans* has shown that both 5', as well as 3' regions of miRNA, are important for stable and specific miRNA target interaction (Broughton et al., 2016). The discovery of the seed sequence has made it possible to develop target prediction algorithms to generate databases to improve the prediction of target mRNAs for a given miRNA and prediction of regulatory miRNAs for a given mRNA (Enright et al., 2003; Kheradpour et al., 2007; Ruby et al., 2007). Many miRNA families are not conserved between plants and animals. Similarly, poorly conserved are their biogenesis, mode of regulation, as well as cellular localization of miRNA processing, suggesting that miRNAs arose independently in plants and animals (Lee et al., 2003; Zhang et al., 2007). Some miRNAs are highly conserved during evolution (Bushati and Cohen, 2007; Liu et al., 2012; Pasquinelli et al., 2000), but their targeted mRNA can differ between species (Chen and Rajewsky, 2007). Even if the mature miRNA is itself not conserved, its seed sequence is

evolutionarily conserved, highlighting the relevance of the seed sequence in target recognition (Brennecke et al., 2005; Lewis et al., 2005; Lewis et al., 2003). Though much is known about their biogenesis, mode of action, and complexity, understanding the functions of individual miRNAs still remains challenging.

1.3.4 MiRNAs role in gene regulation

Due to their peculiar nature of the small size and numerous possibility of target identification via seed sequences, it is no doubt that one miRNA can target several different mRNAs and each mRNA can be targeted by several different miRNAs, generating a complex network of gene expression and regulation. They are known to canalize gene expression, which is contrary to their paradoxical properties of strongly conserved but with not so similar in function or not so conserved but functionally similar. Though they are known to down-regulate their target mRNA in many cases, downregulation of the target gene has been found at a modest level mostly exceeding not more than 50% (Baek et al., 2008; Selbach et al., 2008). The latter study also showed that miRNAs can directly repress translation of many genes contributing to the fine-tuning of protein synthesis from various other genes. They often have the dual function of expression tuning and expression buffering of their target genes (Wu et al., 2009). These two mechanisms are somewhat independent and are achieved by feedforward and feedback regulatory loops. Fine-tuning ensures the precise amounts of target gene expression required for biological processes, which cannot be achieved by transcriptional control alone whereas, expression buffering reduces the variance of highly expressed target gene. There are many ways to achieve the expression-tuning and expression-buffering modes. Expression tuning can be achieved by: 1) directly down-regulating the target gene (Cacchiarelli et al., 2011a; Xiao et al., 2007; Yatsenko and Shcherbata, 2014), 2) a coherent feed-forward loop in which two pathways work coherently to ensure the silencing of the target gene (Hornstein et al., 2005; Makeyev and Maniatis, 2008), and 3) a double-negative feedback loop where a miRNA can down-regulate a target gene that is coupled with second gene, and either one of the genes – but not both – will be expressed due to their target miRNA (Li et al., 2006). Similarly, expression buffering can be achieved through: 1) an incoherent feed-forward loop wherein the expression of one gene is dependent on the expression of a second gene directly or indirectly due to the presence of miRNA. The presence of miRNA is directly proportional to the increase in level of the first gene (O'Donnell et al., 2005), 2) a

negative feedback loop in which both miRNA and its target gene buffer each other's expression (Adams et al., 2018; Martinez et al., 2008; Yatsenko et al., 2014), and 3) an incoherent feedforward loop in which more than one gene can buffer the expression of another gene against the fluctuations in miRNA expression (Choi et al., 2007). Though miRNAs play an important role in buffering and regulating gene expression, they are highly dispensable. Their loss results in very mild or no phenotype in well-controlled laboratory environments (Li and Carthew, 2005; Miska et al., 2007). However, the evolutionary conservation of many miRNAs as well as their functional effectiveness and fast response demonstrate that they are important regulators of spatial and temporal expression patterns of their targeted genes, their downstream targets, and their cofactors.

1.3.5 MiRNAs as biomarkers

MiRNA biogenesis is under tight temporal and spatial control, and deregulation in this process is associated with many human diseases. And many of the miRNA implications have been made to diagnostic and therapeutic application in human diseases. The first identified miRNAs in a human-related disease was the polycistronic miRNA cluster *miR-17~92*. Haploinsufficiency of these miRNAs is responsible for microcephaly, short stature, and digital abnormalities in both humans and mice (de Pontual et al., 2011). The same cluster miRNAs were found to be downstream of an oncogene (*c-Myc*), and upstream of their target gene (*E2F1*), which promotes the cell cycle (O'Donnell et al., 2005). The implication of miRNAs in cancer is emerging, and many miRNAs are known to be altered in cancer patients (Koturbash et al., 2011; Munker and Calin, 2011; Tufekci et al., 2014). Downregulation of *miR-15a/16-1* is associated with multiple myeloma in humans (Li et al., 2015), and *miR-1* and *miR-133a* promote prostate cancer by down-regulating purine nucleoside phosphorylase (PNP) (Kojima et al., 2012). Methylation of the *miR-137* promoter is also associated with derepression of Cyclin-dependent kinase 6 (Cdk6) causing squamous cell carcinoma of head and neck in humans (Langevin et al., 2011). In humans, loss of *miR-137* is also associated with intellectual disability (ID) (Willemsen et al., 2011). MiRNAs are also studied extensively as a biomarker for aging (Dhahbi, 2014). *MiR-34a* was found to be increased reciprocal to the age of the mouse and was directly proportional to the decrease of its target *SIRT1* (Li et al., 2011). The same miRNA in *Drosophila* (*miR-34*) has been reported to cause aging and neurodegeneration (Liu et al., 2012). Many miRNAs are associated with age-related diseases. *MiR-21* is highly expressed in patients with cardiovascular disease (Olivieri et al.,

2012), whereas *miR-433* is associated with Parkinson's disease by negatively regulating fibroblast growth factor 20 (*FGF20*) (Wang et al., 2008).

Many miRNAs also have implication in Muscular Dystrophy. Their expression levels are altered in primary muscular disorders including various kinds of MDs (Eisenberg et al., 2007; Greco et al., 2009). Muscle miRNAs are found to be enriched in the serum of DMD patients; particularly *miR-1, miR-133, and miR-206* have been proposed as diagnostic markers for DMD, as the disease severity correlates with the miRNAs' expression (Cacchiarelli et al., 2011b).

Due to their multiple targeting capacities as well as involvement in multiple biological processes, miRNAs represent promising therapeutic targets, and several pharmaceutical companies are already exploring miRNA in therapeutic development. One such example is the invention by MIRagen Therapeutics of chemically modified structures of *miR-15/195* and *miR-29* that have reached preclinical development in pathologies of metabolic as well as cardiovascular disease (Shah et al., 2016). The same company has three more miRNAs in their drug discovery pipeline, namely Cobomarsen (MRG-106), an inhibitor of *miR-155* for treatment of blood cancer (Phase I, and II clinical trial), a synthetic miRNA mimic of *miR-29b* (MRG-201 in Phase II clinical trial), and *miR-92* (MRG-110) for pathologic fibrosis and heart failure (www.miragen.com).

1.3.6 MiRNAs as stress regulators

Stress can range from prolonged disease conditions to short-term changes in environmental or physiological cellular conditions. To adjust to harsh environments, cells can turn certain pathways on or off to maintain cellular homeostasis. MiRNAs are ideal candidates for stress response regulators as each one can target multiple mRNAs, which can be part of multiple signaling cascades. Under stress conditions, both miRNA and Ago protein are localized to stress granules where mRNAs bound by stalled 40S ribosomes accumulate due to stress-induced repression of translation initiation (Leung and Sharp, 2007). Moreover, miRISCs are detected in many membrane-less structures, *e.g.* ribonucleoprotein (RNP) granules such as stress granules (SG), processing bodies (PBs), GW bodies, and neuronal granules (Kucherenko and Shcherbata, 2018a, b). In flies, miRNAs are known to mediate immediate as well as reversible stress responses to maintain cellular homeostasis (Cicek et al., 2016; Edeleva and Shcherbata, 2013). In many other model organisms, including mice and flies, miRNA knock-outs do not, in most cases, show gross developmental or viability phenotypes,

but the same miRNA mutants can exhibit noticeable phenotypes under stress conditions (Leung and Sharp, 2007, 2010). All these examples lead to a common notion, that miRNAs are profound agents of stress-response pathways. Recently, miRNAs have been implicated as major stress-response factors in many organisms and are known to contribute to disease relevance (Leung and Sharp, 2010; Mendell and Olson, 2012). Yet, signaling systems connecting stress and changes in miRNA expression patterns remain to be discovered.

1.4 Stress and Muscular Dystrophies

MiR-1 has been reported to target Glucose-6-phosphate dehydrogenase (G6PD) to control oxidative stress, and oxidative stress is known to cause progression of DMDs (Cacchiarelli et al., 2010). ER stress is associated with patients with SMA, which is known to cause muscle degeneration similar to MDs (Ng et al., 2015). In flies, it was shown that stresses such as high temperature, low-sugar foods (further sugar starvation), oxidative stress, and aging can cause muscle degeneration in wild-type flies, and this phenotype is accelerated in dystrophic flies (Kucherenko et al., 2011). This indicates that both stress and MDs can act via a common pathway, and dystrophic phenotypes can be recapitulated simply by inducing stress. The same study identified many novel interactors of the DGC that are involved in mechano-signaling and cellular stress response, indicating that the DGC may act as a sensor in mechanical stress-response pathways. Since many miRNAs are deregulated in MDs and they have emerged as diagnostic biomarkers (Chapter 1.3.5), miRNAs can be good candidates for common molecular agents between stress and muscular dystrophies. Hence, it is important to understand the molecular circuits of how stress can modulate levels of miRNAs that contribute to disease pathogenesis.

1.5 MiRNAs profiles in Muscular Dystrophies

In DMD, the Dys-Syn-nNOS pathway is known to regulate the miRNA expression by S-nitrosylation of HDAC2 (Cacchiarelli et al., 2010), and altered miRNAs expression also correlates with the severity of MDs (Chapter 1.3.5). Similarly, miRNAs are also found to regulate the DGC (Cacchiarelli et al., 2011a; De Arcangelis et al., 2010), indicating the important role of miRNAs in balancing the epigenetic network in MDs. In a *mdx* mouse, an animal model of human DMD, *miR-1* and *miR-133* are downregulated in differentiating myoblasts in the absence of *Dys* (Greco et al., 2009; McCarthy and Esser, 2007). *miR-1*, in particular, is evolutionarily conserved and has been shown to act in a positive feedback loop

by modulating epigenetic profiles of muscle genes, e.g. *Mef2* and *Twist*, by targeting HDAC4 (Chen et al., 2006; Sokol and Ambros, 2005). Not only does the DGC regulate miRNAs, but many miRNAs are also found to regulate the DGC. *MiR-222* is known to regulate the Dys-Syn-nNOS pathway by targeting the 3'UTR of β1-Syntrophin (De Arcangelis et al., 2010), while *miR-31* is known to inactivate the Dys-Syn-nNOS pathway by targeting the 3'UTR of *Dys* (Cacchiarelli et al., 2011a). *MiR-206*, which positively regulates muscle differentiation, can target *Utrophin*, a *Dys* homolog in flies and, like *miR-1/133,* is a diagnostic biomarker of MDs (Chapter 1.3.5). All of these studies indicate the important role of miRNAs in MD development. A miRNA microarray screen in *Dg* and *Dys* mutant flies, as well as hyperthermia in dystrophic and wild-type flies revealed groups of miRNAs that were deregulated under differential stress or dystrophy or in both stress and dystrophic conditions (Marrone et al., 2012). Of 110 miRNAs identified in the screen, 65% (28 out of 43) of the miRNAs that are defined in all functional groups were found to be common to more than one group. This study also reported *miR-956, miR-980*, and *miR-252* are regulated via the Dg-Dys-Syn1 dependent pathway. The study also showed tissue-specific expression patterns of all three miRNAs that were either in muscle, brain, or both, indicating the diverse roles of the DGC. The study also highlighted important links of miRNA expression profiles to stress, muscular dystrophy, and DGC signaling. In particular, the third category revealed the miRNAs that do not change normally under stress but are upregulated in dystrophic mutants and the miRNAs that are downregulated as a normal stress response but do not change in dystrophic mutants. Since there are similarities in stress and dystrophy, these miRNAs are good candidates to be involved in regulating the DGC signaling in response to stress. Though this implies flies are an excellent model to determine novel factors that can potentially play a role in the pathogenesis of MDs including miRNAs as potential therapeutic targets, much work is needed to fully understand the molecular mechanism of the DGC-dependent miRNAs to monitor the pathological progression of the disease.

1.6 Architecture of adult *Drosophila* muscle

The DGC provides mechanical stabilization of the muscle sarcolemma by anchoring the ECM to the cytoskeleton. It also provides signal transduction platform between the inner and outer membranes of the muscle cell, and providing a scaffold responsible for the membrane localization of signaling proteins, such as Syn and nNOS. nNOS can nitrosylates the HDACs to regulate gene transcription that includes muscle progenitor cells. Muscle degeneration is

a hallmark of MDs. It can occur due to various reasons, such as physiological and pathological stimuli (*e.g.*, fasting, cachexia) or genetic disorders (*e.g.* inherited or acquired myopathies). Starvation usually results in muscle atrophy, which is loss of muscle mass due to an increase in protein degradation or a decrease in protein synthesis (Piccirillo et al., 2014). Any prolonged disease state is immense stress to the organismal system to withstand the daily requirement of the fully functional active state. Muscles can withstand laborious and continual mechanical stress, and when damaged they can be repaired by the progeny of satellite cells. In response to disease conditions like MDs, muscle fibers are replaced with fat and fibrotic tissues. In the mammalian model, lack of Dys causes the muscle sarcolemma to deteriorate, leading to damage that cannot be easily repaired via response to muscle satellite cells. This results in chronic inflammation, which eventually results in replacement of the muscle fibers by adipose or fibrotic tissues (Porter et al., 2002). Importantly, similar mechanisms can also be seen in flies.

Just like in humans, adult fly muscles are specialized to perform various specific functions, such as flying, jumping, and walking. Fly muscles share structural and functional similarity with vertebrate muscles. Similar to mammals, flies have both oxidative as well as glycolytic muscles. Both the direct and indirect flight muscles are oxidative muscles in flies, whereas leg muscles are glycolytic muscles in flies (Taylor, 2006). Individual muscle groups are made from the same fiber type, but the fiber types can differ for different muscles that are destined for similar functions (Bryantsev et al., 2012; O'Donnell et al., 1989).

One of the distinct and the largest muscle groups in adult *Drosophila* is the indirect flight muscle (IFM). The IFMs are oxidative muscles resembling Type I muscles in mammals that are sensitive to nutrient supply as well as loss of muscle stimulus by nerves or NMJ disorders such as ALS. Adult *Drosophila* has two groups of IFMs, namely DLMs (dorsal-longitudinal muscles) and DVMs (dorsal-ventral muscles) (Figure 3). The IFMs function as a single contractile unit, generating momentum during flight (Dutta et al., 2004). In humans, adult satellite cells allows regeneration of muscle tissue following the injury. Muscle satellite cells are recently discovered in flies, and muscle regeneration upon certain injuries have been reported, there are still more room to explore in muscle regeneration upon genetic disorders in flies (Chaturvedi et al., 2017; Gunage et al., 2017). Fly muscles are also arranged in a stereotyped manner, making them easy to identify and quantify ranges of phenotypes that can be spotted in each individual group. Fly muscles also degenerate in dystrophic as well as in other stress conditions. For this project, DLMs of fly muscles were scored and quantified for muscle degeneration phenotypes.

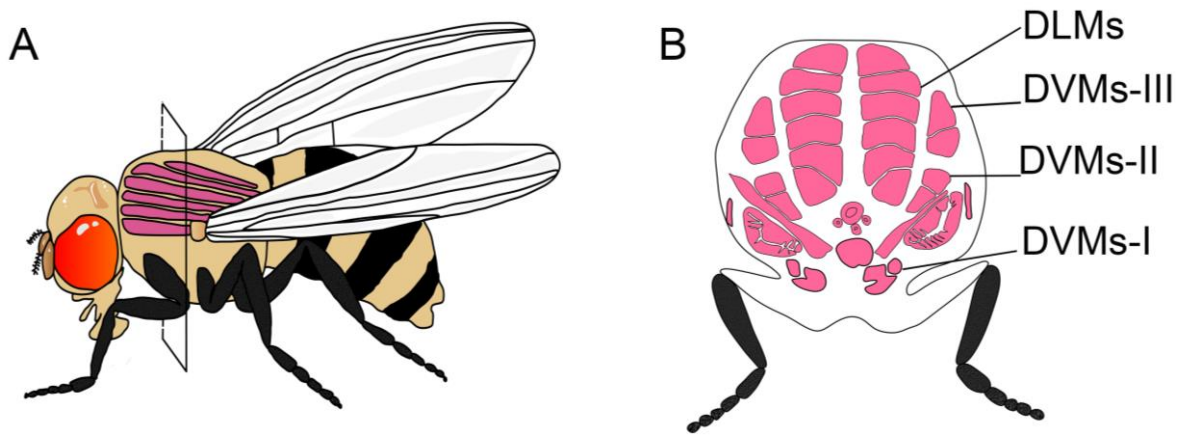

Figure 3. *Drosophila* Indirect Flight Muscles

(A) Schematic representation of a cross-section of indirect flight muscles (IFMs) of *Drosophila melanogaster*. (B) IFMs of fly consists of dorsal longitudinal muscles (DLMs) consisting of twelve fibers in total, and three groups of dorsal-ventral muscles (DVM-I/-II/-III) in the thorax. These muscles function as a single until during flight.

1.7 Sterility and Muscular Dystrophy

Though there is no direct evidence for sterility in MD patients, several DGC components are associated with genes and proteins contributing to infertility in male (Rouillard et al., 2016). Mutation in a gene related to LGMD type 2B in *C.elegans* (*fer-1*) is known to cause sterility (Bashir et al., 1998). Similarly, *Dg* mutant in *C.elegans* (*dgn-1*) are known to be viable, but sterile (Johnson et al., 2006). They show severe disorganization of somatic gonadal epithelium and motor neuron axon guidance defects (Johnson et al., 2006). The DMD-null male mouse is also reported to be sterile (Kudoh et al., 2005). Additionally, some studies indicated that flies lacking POMT expression (required for glycosylation of Dg) are sterile and non-viable at elevated temperatures (Cooley et al., 1988; Ueyama et al., 2010). POMT is a critical enzyme required for glycosylation of *Dg* and is associated with CMD and Walker- Warnurg Syndrome. Studies from flies have shown that glycosylation is a critical step for a mature sperm to fertilize eggs (Perotti et al., 2001). Both *Dg* and *Dys* are found to have stage-specific expressions in Sertoli cells in mammals (Zimmermann et al., 2015). Sertoli cells are somatic cells that form the occluding barrier between two somatic cells to provide a unique environment for germline differentiation in each cyst cells. This soma-germline barrier is also called the Sertoli cell barrier (SCB) or the blood-testis barrier (BTB) (Cheng and Mruk, 2012; Franca et al., 2012). BTB is a selective permeability barrier maintained by tight junction (in mammals) or septate junction in *Drosophila*. The BTB separates the early phases of spermatogenesis. Disruption of BTB in vertebrates is reported

to result in failure in germline differentiation and ultimately leading to sterility (Mazaud-Guittot et al., 2010; Mok et al., 2012). Similarly, in *Drosophila*, knockdown of the soma-specific gene (*chic*) is known to cause sterility due to defective encapsulation (Fairchild et al., 2015). Core septate junction components such as Cora and Nrx-IV are found to localize between the two somatic cells surrounding the germline throughout the spermatogenesis. Knock-down of these components perturbs permeability barrier and gives rise to rudimentary testes (Fairchild et al., 2015). In larval NMJ of *Drosophila* muscle, core septate junction protein Cora and Nrx-IV have been shown to interact with Dg. Dg and Cora reciprocally control each other's concentration at larval NMJs (Bogdanik et al., 2008; Marrone et al., 2011b). In addition, it has been reported that localization of Nrx-IV is also dependent on Dg in follicular epithelium of fly ovaries (Schneider et al., 2006). Overall, the role of the DGC, in particularly Dg, exceeds beyond the nervous and muscle systems. Therefore, it is interesting to investigate roles of the Dg in spermatogenesis to better understand its broad biological and cellular functions.

1.7.1 Spermatogenesis in *Drosophila melanogaster*

Adult *Drosophila* has a pair of testes that are coiled tube-like structures producing sperm throughout the male gametogenesis. Spermatogenesis starts at the apical tip of the testis that contains a pool of stem cells of two separate origins, namely germline stem cells (GSCs) and somatic stem cells (CySCs). Both of these cell types reside in a specialized microenvironment called the stem cell niche. Niche provides architecture and signaling regulation for stem cell maintenance and division. It is composed of the hub (cluster of 10-12 somatic cells), GSCs (a cluster of approximately 8 germline cells), and the CySCs (the number of which approximately match the number of GSCs) (Demarco et al., 2014; Hardy et al., 1979). Hub is a signaling center for both, GSCs and CySCs. Under homeostatic conditions, both GSCs and CySCs divide asymmetrically producing two cells; one attached to the hub that maintains the stem cell characteristics and the other daughter cell that differentiates to give rise to gonialblast (GB) and somatic cyst cells (CySC). The progeny of GSCs give rise to GB and the progeny of CySCs differentiate to somatic cyst cell. Differentiating GBs are encapsulated with two somatic cells and undergoes four rounds of mitotic and two rounds of meiotic division to produce spermatogonia. Spermatogonia then differentiate into spermatocytes that undergo elongation and maturation and eventually form the mature sperm (Figure 4). Proper encapsulation is required for proper germline

differentiation and production of functional gametes. Encapsulation of germline cells by somatic cells also establishes a barrier that is essential for correct germline differentiation (Fairchild et al., 2015). The same study also found that the permeability barrier (BTB) in vertebrates is dependent on septate junction proteins such as NrxIV and Cora. Interestingly, in larval *Drosophila* NMJ, localization of both of these proteins are found to be dependent on Dg (Bogdanik et al., 2008). In fly ovaries, it has been shown that Dg is expressed in both somatic as well as in germline cells (Deng et al., 2003; Yatsenko et al., 2007). Since spermatogenesis is a dynamic developmental process that requires precisely timed transition between several distinct stages, it is important to investigate further the involvement of DGC components and in particular Dg, regulating cellular mechanism relying on *Drosophila* spermatogenesis.

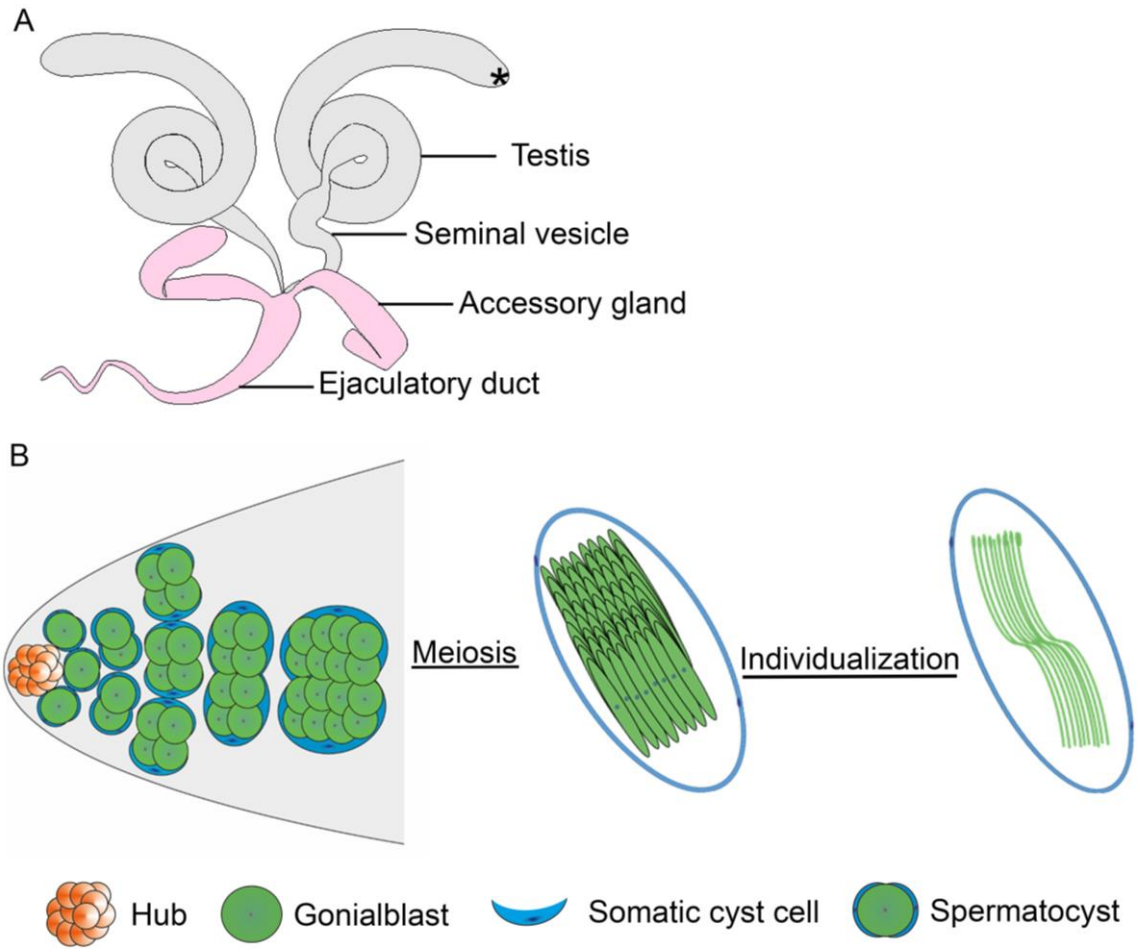

Figure 4. Spermatogenesis in adult *Drosophila melanogaster*

(A) Adult *Drosophila* male gonad consists of a pair of blunt coiled structures called testes, each of which is attached to seminal vesicles and conjoined at a common ejaculatory duct. Spermatogenesis starts at the apical portion of the testes known as a hub and is marked with an asterisk. (B) The apical portion of a testis consists of a hub (marked with asterisk), germline cells (green), and somatic cells (blue). During asymmetric cell division, cells in contact with hub maintain the stem cell characteristics, while the daughter cell differentiates. The differentiating germline cells are called gonialblast, which gets encapsulated with a pair of somatic cells and care called spermatocyst. Within the spermatocyst each gonialblast undergoes 4 rounds of mitotic and two rounds of meiotic division to generate 64 bundles of haploid spermatids. These spermatids go through various steps such as elongation and maturation and finally proceeds to individualization process to make a mature sperm which gets transported to seminal vesicles.

1.8 Aims of the study

The first goal of this project was to identify miRNAs that target the DGC components and influence muscle maintenance. Since most of the MDs' phenotypes can be recapitulated even in wild-type animals under stress conditions, for example, high temperature, starvation and aging, the second goal of this project was to identify miRNAs that act in common pathway shared between stress and MD pathway that controls muscle maintenance and MD development. The final goal of this project was to dissect the role of one identified miRNA targeting DGC components (*miR-137*), and reveal its biological functions contributing to the DGC regulation and pathogenesis of MDs.

2 Materials and Methods

2.1 Fly work

2.1.1 Fly stocks and maintenance

Drosophila melanogaster stocks were raised in standard *Drosophila* food medium with yeast, cornmeal and agar prepared by the fly facility of the MPI for Biophysical Chemistry. All the fly stocks were maintained at well-controlled environment in isolated rooms with a constant humidity of 65%, temperature of 18°C, and 12-12 h daily light-dark cycle. All the experimental analyses were carried out on standard *Drosophila* food media, on standard temperature and humidity condition at 25°C or unless otherwise stated. Food vials were replaced with fresh ones every two days throughout the experiments. Food vials used for the experiments were clear plastic vials of small (28 ml), or medium (68 ml) size (Greiner Bio-One). All the fly strains used for this project were obtained from the Bloomington *Drosophila* Stock Center (BDSC) and are summarized in Table 1.

MiR-137^{ko} fly stock, in particular, was backcrossed to 8 generations in the w^{1118} background and was particularly used in analyses made from Chapter 3.2

Table 1. Fly Stock List

Genotype	BDSC Stock number
w^{1118+}	BL 6326
Oregon-R-C	BL 5
Canton-S	Gift from Patrick O'Farrell lab
w^{1118};*miR-137*^{ko}	BL 58893
w^{1118};*miR-252*^{ko}	BL58901
w^{1118};*KT40 (miR-310*^{ko} *)*	(Tsurudome et al., 2010)
w^{1118},*miR-927*^{KO}	BL 58935
w^{1118};*miR-956*^{ko}	BL 58941
w^{1118};*miR-959-960-961-962*^{ko}	BL 58944
w^{1118};*miR-966*^{ko}	BL 58947
w^{1118},*miR-975-976-977*^{ko}	BL 58954
w^{1118};*miR-1000*^{ko}	BL 58882
w^{1118};*miR-1011*^{ko}	BL 58887
w^{1118};*miR-137*^{Df}	BL 8915

w^{1118},*miR-927*^{Df}	BL 26567
w^{1118};*miR-956*^{Df}	BL 26579
w^{1118};*miR-966*^{Df}	BL 9612
w^{1118};*miR-959-960-961-962-963-964* ^{Df}	BL 7724
w^{1118},*miR-975-976-977* ^{Df}	BL 23171
w^{1118}; *UAS-mir-137*	BL 59881
w^{1118};*UAS-mCherry.miR-137.sponge*	BL 61395
w^{1118};*UAS-DsRed-miR-927*	BL 60599
w^{1118}; *UAS-LUC-miR-966*	BL 41211
w^{1118};*UAS-mCherry.scramble.sponge*	BL 61501
w^{1118};*pUASt-Dg*	(Deng et al., 2003)
w^{1118};*UAS-Dg*^{RNAi}	(Deng et al., 2003)
w^{1118};*Dg*$^{1.10G}$	Unpublished stock (Shcherbata Lab)
w^{1118}, *Mhc-GAL4*	BL 55132
w^{1118};*how*^{24B}*-GAL4*	BL 1767
w^{1118}; *tj-Gal4*	Kyoto 104055

2.1.2 Standard *Drosophila* food media

6.25 g/l agar (Serva)

18 g/l dry yeast (Saf-Instant)

80 g/l corn flour (Zieler & Co)

22 g/l beet syrup (Ferdinand Kreutzer Sabamühle GmbH)

80 g/l malt (Ulmer Spatz)

0.625% propionic acid (Merck)

0.3% nipagin (Sigma)

Note: The food was cooled down to 55°C and then nipagin and propionic acid were added as antifungal and antibacterial agents, respectively.

2.1.3 Temperature and nutritional stress

For temperature stress, flies were kept at 33°C, 48 h post eclosion on standard fly food until desired age. For nutritional stress, *i.e.* sugar starvation and protein starvation, solid food media was prepared using 1% agar-agar (Serva) with 0.3% nipagin (Sigma), and 0.03% propionic acid (Merck). Flies were raised in this medium 48 h post eclosion with a small

quantity of fresh yeast paste prepared from dry yeast and H_2O up to 5 days. Similarly, for protein starvation, fly food was prepared with (apple juice plate) with 3% nipagin (Sigma) and 0.03% propionic acid. Flies were raised in this medium 48 h post eclosion up to 5 days. Both male and female flies were used for these experiments.

2.1.4 Aging & lifespan analysis

Lifespan experiments were carried out at 25°C with 200 male and female flies per genotype. To standardize the age of the experimental flies, parental flies were crossed in plastic cages with apple juice agar plate with fresh yeast paste. After 12 h of egg-laying time, eggs were washed in PBS and transferred from apple agar plates into falcon tubes. Eggs were allowed to sediment. All the supernatant was removed and 10 µl of compact egg/PBS solution was dispensed in medium food vials resulting between 100-150 enclosed flies per vials. Flies were transferred into new food vials after 48 h of post-eclosion. Both female and male flies were sorted into small food vials separately (10 flies/vial). Flies were tipped onto new food three times a week and deaths were scored at the same time. For statistical analysis, P values were calculated using the log-rank survival test.

2.2 Genetic screen of miRNAs

miRNA genetic screen was done by comparing miRNAs loss-of-function along with its over-expression and downregulation using the UAS/Gal4 system in *Drosophila* (Brand and Perrimon, 1993). Muscle-specific Gal4 lines, such as *Mhc-Gal4* and *how*^{24B}*-Gal4* (further *how-Gal4*) were used to drive *UAS-miRNA* line to overexpress miRNAs, *UAS-miRNA-sponge* to downregulated miRNAs, and *pUASt-Dg* was used to overexpress Dg in fly muscles. Progenies of *w*^{1118} virgin females crossed to *Oregon-R* males, and tissue-specific-*Gal4* virgin females crossed to *w*^{1118} males and used as controls. All the crosses were done at standard *Drosophila* conditions (chapter 2.1.1), or unless otherwise stated. For muscle analysis, flies at young (7 day old at 25°C), aged (30 day old at 25°C), temperature stress (5 day at 33°C, 48 h post eclosion), sugar starvation (5 day at sugar starvation, 48 h post eclosion), and protein starvation (30 day on protein starvation at 25°C) were analyzed as mentioned in Chapter2.3. Similarly, for the analysis of the miRNA function in the somatic cell of *Drosophila* testes, *tj-Gal4* was used as early somatic cell-specific driver line and was crossed to *pUASt-Dg*, *UAS-miRNA*, or *UAS-miRNA-sponge* to compare the severity of the phenotypes.

2.3 Muscle Analysis

Adult *Drosophila* muscle tissues were prepared for analysis by placing the flies into collars and fixing them in Carnoy fixative solution (6:3:1 = Ethanol: Chloroform: Acetic Acid) at 4°C overnight. Fly tissues were dehydrated and paraffinized as described by (Kucherenko et al., 2010). Histological sections of 8 µm of indirect flight muscles (IFMs) were prepared using Hyrax M25 (Zeiss) microtome and stained with Hematoxylene and Eosin staining. All the chemicals used for this procedure were obtained from Sigma Aldrich. Muscle analysis was done using a light microscope and the frequency of muscle degeneration was quantified as a ratio of degenerated muscles to the total number of muscles that were analyzed per genotype. The analyzed IFM sections were located at the position 200-250 µm from the posterior of the fly thorax.

2.4 Phenotypic Classification

2.4.1 Muscle Degeneration Phenotypes

The severity of muscle degeneration was categorized into two categories for the simplicity of quantification. Muscles were scored as "strong" muscle degeneration in cases, where all the muscle was deteriorated (absence of fly muscle in the respective area) or substituted with non-muscle tissue. "Moderate" muscle degeneration in cases, where some parts of individual muscle was deteriorated and "mild" muscle degeneration was used as the third category where the muscle showed minor sign of degeneration as punctate-like structures.
Muscle "atrophy" was scored as a separate category for any symptoms of muscles showing loss of muscle integration ranging from the detachment of muscle sarcolemma to low muscle fiber composition.

2.4.2 Septate junction phenotype

In elongated spermatids, septate junctions morphology appear as "H" or "Z" like structure in wild type flies forming the bridge between the two membranes. Both of these shapes were scored as "normal". Any morphological deviation from these shapes, such as a "dot" like structure or an elongated line with no connection to the neighboring cell were scored as "abnormal" septate junction structure. Phenotype was scored beyond 2/3rd from the anterior part of the testes were cells enter meiosis and starts to proceeds through the elongation and the differentiation process to form individual sperms.

2.5 Gene ontology analysis of predicted miRNA targets

Conserved *Drosophila* predicted targets of miRNAs were determined using TargetScan, Release 6.2 (www.targetscan.org). The Generic Gene Ontology (GO) Term Finder tool hosted by the Lewis-Sigler Institute for Integrative Genomics, Princeton University (Boyle et al., 2004) was used to find GO component terms related to predicted targets of each miRNA with a p-value cutoff at 0.01. Visualization was done with the help of Revigo software (Supek et al., 2011) with similarity allowed equal to 0.5

2.6 Immunohistochemistry

Fly testes were dissected in cold phosphate buffered saline (PBS/145 mM NaCl, 7.5 mM Na2HPO4, 2.5 mM NaH2PO4 pH adjusted to 7.4) and fixed using 4% paraformaldehyde (PFA) for 20 min. Samples were then washed 4 times 15 min each with PBT (0.2% Triton^{TM} x-100 (Sigma) in PBS). Fixed tissue was then blocked with PBTB (2 g/l Bovine Serum Albumin (BSA) (AppliChem), 5% Normal Goat Serum (NGS) (Abcam), and 0.5 g/l sodium azide (Sigma)) for 1 h at room temperature (RT). Primary antibodies (Table 2) were then added and incubated overnight at 4°C. Samples were washed again the following day 4 times 15 min each with PBT and were blocked in PBTB for 1 h at RT followed by the addition of secondary antibody solution (Table 2) for 2-3 h at RT. Samples were washed twice in PBT and the procedure was continued with the addition of 10 mg/l DAPI (Sigma) in PBT for 10 min. Samples were washed twice again with PBT and finally, the solution was replaced with mounting medium (70% glycerol (Sigma), 3% n-propylgallate (Sigma) in 1x PBS) and left at 4°C overnight to equilibrate. Finally, the tissues were mounted on whole slides (76X26 mm, Thermo Scientific) and were analyzed with Zeiss LSM700 confocal laser scanning microscope.

Table 2. Antibodies used for immunohistochemistry

Antibody	Dilution	Source	Host
anti-Adducin (Add)	1:50	DSHB	Mouse monoclonal
anti-β-Gal	1:25	DSHB	Mouse monoclonal
anti-PH3	1:10000	Upstate Biotechnology	Rabbit polyclonal
anti-GFP	1:5000	Abcam	Chicken polyclonal
anti-Vasa	1:5000	Gift from Herbert Jäckle MPI-BPC, Göttingen	Rabbit polyclonal

anti-Dystroglycan (Dg)	1:2000	Gift from Hannele Ruohola-Baker UW, Seattle	Rabbit polyclonal
anti-Armadillo (Arm)	1:50	DSHB	Mouse monoclonal
anti-Traffic Jam (Tj)	1:10000	Gift from Dorothea Godt UToronto, Toronto	Guinea pig polyclonal
anti-Eyes Absent (Eya)	1:50	DSHB	Mouse monoclonal
anti-Disc large (Dlg)	1:200	DSHB	Mouse monoclonal
anti-Mega	1:300	Gift from Reinhard Schuh MPI-BPC, Göttingen	Mouse monoclonal
anti-β3 Tubulin (β3tub)	1:2000	Gift from Renate Renkawitz-Pohl PUM, Marburg	Guinea pig polyclonal
anti-Coracle (Cora)	1:25	DSHB	Mouse monoclonal
Alexa 568 anti-mouse	1:500	Invitrogen	Secondary, goat
Alexa 488 anti-rabbit	1:500	Invitrogen	Secondary, goat
Alexa 488 anti-chicken	1:500	Invitrogen	Secondary, goat
Alexa 568 anti-guinea pig	1:500	Invitrogen	Secondary, goat

2.6.1 Permeability assay

Permeability assay was performed as described in (Fairchild et al., 2015). Adult *Drosophila* testes were dissected in Schneider's *Drosophila* Medium (Gibco®) and transferred in medium containing 10 kDa Dextran Dye conjugated to Texas Red® (molecular probes). The final concentration of the dye was 0.2 µg/ml. Images were analyzed with Zeiss LSM700 confocal laser scanning microscope.

2.7 *In situ* hybridization (ISH)

Fly tissues were dissected in cold 1x modified Ephrussi-Beadle Ringer's solution (EBR) (for 10XEBR: 1.3 M NaCl (Merck), 47 mM KCl (Merck), 19 mM CaCl2 (Merck), and 100 mM HEPES (Roth)) and fixed in 4% PFA in PBS. Fixation time varied depending on the type of tissues (see below). Subsequent procedures were followed as described in (Zimmerman et al., 2013). Flies tissue were then dehydrated and stored at -20°C overnight. Next, tissues were rehydrated and permeabilized for 1 h in RT with Proteinase K solution (50 µg/ml Proteinase K (AppliChem) in 50 mM Tris–HCl (VWR) pH 7.5, 50 mM EDTA (Roth))

followed by the post-fixation at 4% PFA in PBT for 30 min at RT. Primary fixation and permeabilization varied between the tissues (Table 2). Samples were then rinsed and pre-hybridized in hybridization buffer (50% formamide (VWR), 25% 20 x SSC, 5 mg/ml Torula yeast RNA (Sigma), and 0.1% Tween 20) for 1 h at 60°C. Hybridization was carried out overnight at 60°C with a 40 nM miRCURY LNA probe (Exiqon; dme-*miR-137-3p* product # 619638-360) in hybridization buffer. Post-hybridization was done for 1 h with three subsequent washes of 20 min with hybridization wash solution (no yeast RNA), 50/50 v/v hybridization wash solution/PBT, and PBT at 62°C. Tissues were then blocked for 1 h in Western Block (Sigma) and anti-digoxigenin (DIG) conjugated with Alkaline Phosphatase that was diluted 1:2000 in the block and incubated with tissues overnight at 4°C. Colorimetric detection was done with 10 µl/ml NBT (Roche) in staining buffer (0.05 M Tris pH 9.5, 0.05 M MgCl2, 0.1 M NaCl, 0.1% Tween 20) for ~30–45 min. Samples were washed 3 more times and let to equilibrate in 80% glycerol in PBS overnight. Finally, tissues were mounted on whole slides (76X26mm, Thermo Scientific), and analysis was done using Zeiss Axiophot microscope.

Table 3. Duration of tissue fixation and permeabilization

Tissue	Primary Fixation	Permeabilization
Testes	1 h	-
Brain	30 min	-
NMJ	5 min	10 min

2.7.1 Fluorescence *in situ* hybridization (FISH)

All the procedures were followed similar to regular ISH up until blocking of the sample in Western Block (Sigma) for 1 h at RT. Samples were then incubated overnight at 4°C in biotin-conjugated anti-DIG antibody (Jackson Immuno Research) diluted in 1:500 in Western Block. Samples were then washed 6 times for 10 min each and incubated 1 h in 1:1000 streptavidin-HRP (TSA kit, PerkinElmer) in the block at RT. For nuclear staining, 1 µg ml^{-1} (final concentration) of DAPI was added during the last wash. Tyramide (TSA kit, PerkinElmer) was diluted in 1:50 and added to the sample and incubated overnight at 4°C in dark. Samples were washed 3 more times and let to equilibrate in mounting medium (70% glycerol (Sigma), 3% n-propylgallate (Sigma) in 1x PBS) overnight at 4°C. Finally, tissues were mounted on whole slides (76x26 mm, Thermo Scientific), and analysis was done using Zeiss LSM700 confocal laser scanning microscope.

2.8 Genomic DNA extraction from fly leg and the whole fly

The middle leg was dissected and then transferred in ice-cold PCR tubes containing squishing buffer (10 mM Tris-HCl, 1mM EDTA, 25 mM NaCl, and 200 µg/ml Proteinase K (AppliChem) with pH adjusted to 8.2). Similarly, the whole fly body was transferred in ice-cold PCR tubes containing squishing buffer and homogenized using the pestle. Genomic DNA was extracted under the following conditions in a thermocycler (Bio-Rad T100^{TM}).

Table 4. Conditions used for genomic DNA extraction

Fly Leg		Whole Fly	
65°C	60 min	37°C	30 min
95 C	10 min	97 C	3 min
4°C	until removal	4°C	15 min high-speed centrifugation (13000 rpm)

2.9 Polymerase chain reaction (PCR)

For genotyping, PCR from extracted DNA was performed by using HotStart Taq *Plus* DNA Polymerase (Qiagen). 0.5 µM of each primer pair were mixed with HotStarTaq *Plus* Master Mix (2x), and 150 ng of template DNA with a final volume of to 20 µl. All the procedures were followed per the manufacturer's instructions. The primer pairs were designed using Primer3: WWW primer tool (http://biotools.umassmed.edu/bioapps/primer3_www.cgi). The amplicons were designed as intron spanning pairs and were ordered from Microsynth unless otherwise stated. Primers are summarized in Table 5.

Table 5. Primers used for qPCR

Gene	Orientation	Sequence	Purpose
Rpl32	Forward	AAGATGACCATCCGCCCAGC	qPCR
Rpl32	Reverse	GTCGATACCCTTGGGCTTGC	qPCR
Dg	Forward	ACTCAAGGACGAGAAGCCGC	qPCR
Dg	Reverse	ATGGTGGTGGCACATAATCG	qPCR
Dys	Forward	GTTGCAGACACTGACCGACG	qPCR
Dys	Reverse	CGAGGGCTCTATGTTGGAGC	qPCR
Syn_1	Forward	GGCATTGAACCAGACGAGGG	qPCR
Syn_1	Reverse	AATCTCAAATACATCGACCC	qPCR
2S	rRNA	TGCTTGGACTACATATGGTTGAGGGTTGTA	qRT-PCR
miR-137-3p	mature-miRNA	UAUUGCUUGAGAAUACACGUAG	qRT-PCR
mini white	Reverse	TTTGTGCGATTGCGGTTTG	PCR
miR-137	Reverse	CCTCAGGCCCGTTTAAATGAGCTGGAA	PCR
Gal4	Forward	GGCTAGAAAGACTGGAACAGCT	PCR
Gal4	Reverse	AGGGCAAGCCATCCGACATG	PCR

pUAST	Forward	AGCAACCAAGTAAATCAACTGC	PCR
pUAST	Reverse	TTAAATCTCTGTAGGTAGTTTGTCC	PCR

2.9.1 Agarose gel electrophoresis

DNA fragments were separated by length by running linear DNA (PCR products) in 1% and 1.5% agarose gel (Sigma) in TAE (40 mM Tris-acetate, 1 mM EDTA with pH adjusted to 8.2). Samples were then mixed with DNA loading dye (6x, New England BioLabs^{R} Inc.) containing bromophenol blue as a visual marker. Gels were post-stained with Midori green advance (Nippon Genetics) and based on the size of the PCR product, Hyper Ladder 50 bp and 100 bp (New England Bio Labs) were used to determine DNA size.

2.10 RNA extractions and cDNA synthesis

Total RNA was extracted from the whole body of 5 male flies or 50 testes per genotype by homogenizing in 200 µl Trizol reagent (Ambion). Further procedures were followed as per the manufacturer's protocol. Quantification of total RNA concentration was done using the Nano Drop (ND-1000 Spectrophotometer, Peqlab Biotechnologie GmbH). Total cDNA was reverse transcribed using random primers with High Capacity Reverse Transcriptase (Applied Biosystems) with 1.5 µg of total RNA template in a 20 µl reaction with following conditions at thermocycler (Bio-Rad T100^{TM}).

2.11 Quantitative PCR (qPCR)

Fast SYBR Green reagents in Step One Plus Real-Time PCR System (Applied Biosystems) was used according to the manufacturer's instructions to perform qPCR. Each reaction was set up with forward and reverse primer of 300 nM concentrations and 100 ng cDNA as template in the 15 µl total reaction volume. Amplification was done using StepOne Plus thermocycler (Applied Biosystems). C_T values were acquired from StepOne Software (Applied Biosystems), and technical replicate average C_T values of respective genes were normalized to the endogenous control (housekeeping gene, *Rpl32*) to achieve ΔC_T value. qPCR data were validated using the $\Delta\Delta C_T$ method that was achieved by subtraction of ΔC_T value of each genotype to the control genotype. Relative expression of the gene of interest was calculated using the formula: $2^{-\Delta\Delta CT}$. For statistics, two-tailed Student's t-test was used for the calculation of p values.

2.11.1 Quantitative miRNA expression analysis

TaqMan® microRNA assays (Applied Biosystems) were used to determine miRNA levels. 2S rRNA was used as an endogenous control for this procedure. Reverse transcription was done as described in chapter 2.9, and amplification was done using StepOne Plus thermocycler (Applied Biosystems). Subsequent procedures were carried out as per the manufacturer's protocol. The assay involved reverse transcribing the mature miRNA of interest in a reaction and subsequently detecting the quantity via PCR coupled with fluorescence-labeled oligonucleotide probes.10 ng of total RNA was used for 20 µl reaction volume, and 1.33 µl of resulting reaction was loaded for the qPCR. The amplicons were ordered from Thermo Fisher Scientific and are summarized in Table.5. The calculation of the relative miRNA expression levels and statistics were done using the respective C_T values as described in chapter 2.10.

2.12 Transfection of *Drosophila* cell lines (S2R+ cell lines)

Drosophila S2R+ cells (DGRC) were cultivated in Schneider's *Drosophila* medium (Gibco®) with 10% heat-inactivated fetal bovine serum (FBS, GE healthcare) and 100 units/ml penicillin and 100 µg/ml streptomycin (Gibco®) in 25 cm^2 culture flasks in the 6 ml medium at 25ºC. Cells were split into 96 wells plate (polystyrene black plate, costar) and incubated overnight to achieve confluency of 60-70%. Transfection mixes were prepared using Effectene® transfection reagent (Qiagen) as per manufacturer's protocol. Following amounts of the reporter and constructs were added on the transfection mixes: 50 ng of empty *psiCHECK™-2* or 50 ng of *psiCHECK™-2-Dg*-3'UTR plasmid fragments (Yatsenko et al., 2014) containing miRNA binding sites, 25 ng of *act*-Gal4, and 50ng of the *pUAST-miRNA* plasmid (Gift from Eric Lai). Transfection mix without reporter constructs was used as background control.

2.13 Luciferase reporter assay

To measure firefly and renilla luciferase activity, the Dual-Glo® luciferase assay kit (Promega) was used approximately 72 h of post-transfection. All the procedures were followed as per the manufacturer's instructions. Luciferase activity was measured as luminescence using Wallac 1420 luminometer (PerkinElmer). To calculate relative downregulation of reporter luciferase values, signals by miRNAs, raw readouts of *Renilla* to *Firefly* luciferase values were measured. Next, background values (transfection with empty *psiCHECK*^{TM}-2 with no reporter construct) were subtracted from the respective values. Obtained values were then normalized to empty *psiCHECK*^{TM}*-2* to the values of *psiCHECK*^{TM}*-2-Dg-3'UTR* in presence of miRNAs.

All transfections were done in triplicates. Data observed from triplicates were used to determine an average downregulation and standard deviation of the data. Student's two-tailed t-test was used for the statistical analysis.

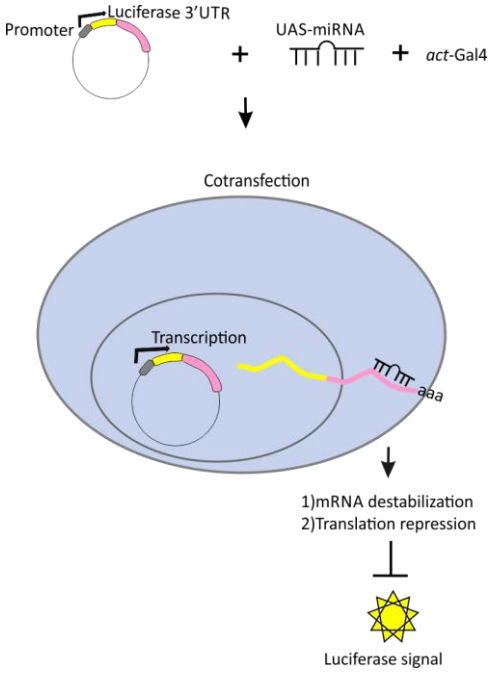

Figure 5. Schematic representation of luciferase assay

S2R+ cells were transfected with *psiCHECK*^{TM}-2 with or without *Dg*-3'UTR fragments together with *act*-Gal4, as well as, *pUAST-miRNA* plasmids. When all three constructs are transfected, miRNA will bind to the *Dg*-3'UTR resulting in mRNA destabilization or translation repression of reporter gene can be detected as no to less luciferase signal. *pUAST-miRNA* plasmids transfected with *psiCHECK*^{TM}*-2-Dg*-3'UTR that doesn't have predicted binding site, or with empty *psiCHECK*^{TM}-2 will have no effect on transcription of the luciferase reporter. Hence, resulting in normal or high luciferase signal as compared to the miRNA inhibition.

2.14 Bacterial transformation

Respective *psiCHECK*^{TM}-2 vectors together with *pUAST-miRNA* plasmids were transformed into chemically competent bacteria (DH5α *Escherichia coli* cells, Invitrogen) following the manufacturer's protocol. Cells were heat shocked at 42°C for 45 sec followed by incubation on ice for 2 min. Transformed bacteria were then incubated in SOC medium at 37°C for 1 h with a slow shake of 100 rpm in an incubator shaker (Infors AG) and plated on Lysogeny Broth (LB, Invitrogen) agar plate containing 100 µg/ml ampicillin. Plates were incubated overnight at 37°C. The following day, a single colony was picked using sterile pipette tip and dropped into liquid LB medium with ampicillin at 250 rpm in an incubator shaker (Infors AG) for overnight culture, and were subjected for midi-preparation the next day.

2.15 Midi-preparation of plasmid DNA

Bacterial cultures were harvested by centrifuging at 6000x *g* for 15 min at 4°C. To obtain high purity DNA, Plasmid *Plus* Midi Kit (Qiagen) was used according to the manufacturer's protocol. The purified DNA was eluted in 200 µl of EB buffer (Plasmid *Plus* Midi Kit). For quality control, total DNA concentration was measured using the Nano Drop (ND-1000 Spectrophotometer, Peqlab Biotechnologie GmbH).

2.16 Image processing and quantification

Somatic cell quantification and digital processing of all the microscope images were done using ImageJ-win64 or Adobe Photoshop. Schematic illustrations were done using CorelDRAW X6, and Microsoft PowerPoint. All the heatmaps were drawn using R program version 3.2.3.

2.17 Bioinformatical analyses

To find human homologs of the proteins, STRING v10 database (Szklarczyk et al., 2015) with a medium confidence score (0.4) and prediction methods that included neighborhood, gene fusion, co-occurrence, co-expression, experiments, databases, and text mining were used. To assign molecular function and involvement in biological processes of genes, FB2018_05 release FlyBase was applied. To search for the human disease association the http://www.flyrnai.org (Hu et al., 2011) and http://www.genecards.org were used.

3 Results

3.1 Screen of miRNAs that are predicted to target the DGC

3.1.1 The DGC components are predicted to be targeted by multiple miRNAs

A single gene can be targeted by multiple miRNAs, at the same time, a single miRNA can target multiple genes. Such genes can be positive or negative regulators of the same pathways. To investigate miRNAs that can potentially play a role in MD pathogenesis by targeting the DGC components, we selected miRNAs based on whether or not they are predicted to target the core DGC components.

In *Drosophila* model of MD, Dg have been shown to be localized postsynaptically at the NMJ and are required for appropriate homeostatic control of neurotransmitter release and proper localization of Cora and Nrx-IV (Bogdanik et al., 2008). It has also been reported that in the absence of Dg, GluR are improperly localized causing insufficient muscle response (Marrone et al., 2011b). Importantly, mutation in any of these components are also associated with phenotypes similar to MD. Therefore, core components of the DGC as well as the proteins known to interact with Dg were taken together to extract miRNAs that are predicted to target the extended DGC components. Such components consists of multiple protein, among which are Dg, Dys, Syn1/2, nNOS, Scg, Nrx-IV, Cora, Yki, GluR, Lan A/B, Arm, Hts, and Mei-P26 (Chapter 1.1, Figure 1). Several target-prediction tools were utilized to find miRNAs that can target the DGC, namely TargetScan, Release 6.2 (www.targetscan.org), miRBase, Release 20 (www.mirbase.org), and Diana Tools (http://diana.imis.athena-innovation.gr/DianaTools/index.php). This search yielded a group of 72 miRNAs, both conserved and non-conserved, that are predicted to target the transcripts of DGC components (Figure 6).

Interestingly, among these miRNAs, around 20% (17 out of 72) are known to be DGC- or stress-dependent (Marrone et al., 2012), indicating that they can play an integral role in stress response and in MD pathogenesis. Many of these miRNAs can target more than one component of the DGC; however, we were not able to alienate a single group of miRNAs targeting common components of the DGC. Previously it has been shown that miRNAs often regulate multiple components of the same signaling pathway to assure quick and robust response to changes in external conditions and in internal cellular environment (Cicek et al.,

2016; Yatsenko and Shcherbata, 2014). Since Dg is an integral membrane receptor linking the ECM to the actin-based cytoskeleton and is required for correct localization of the majority of the DGC components, we decided to study miRNAs that can target *Dg* and any three other components of the complex. As a result, a much narrower miRNA group was formed which possibly would ensure the dynamic, efficient, and fast control over the DGC pathway activity (Figure 7A).

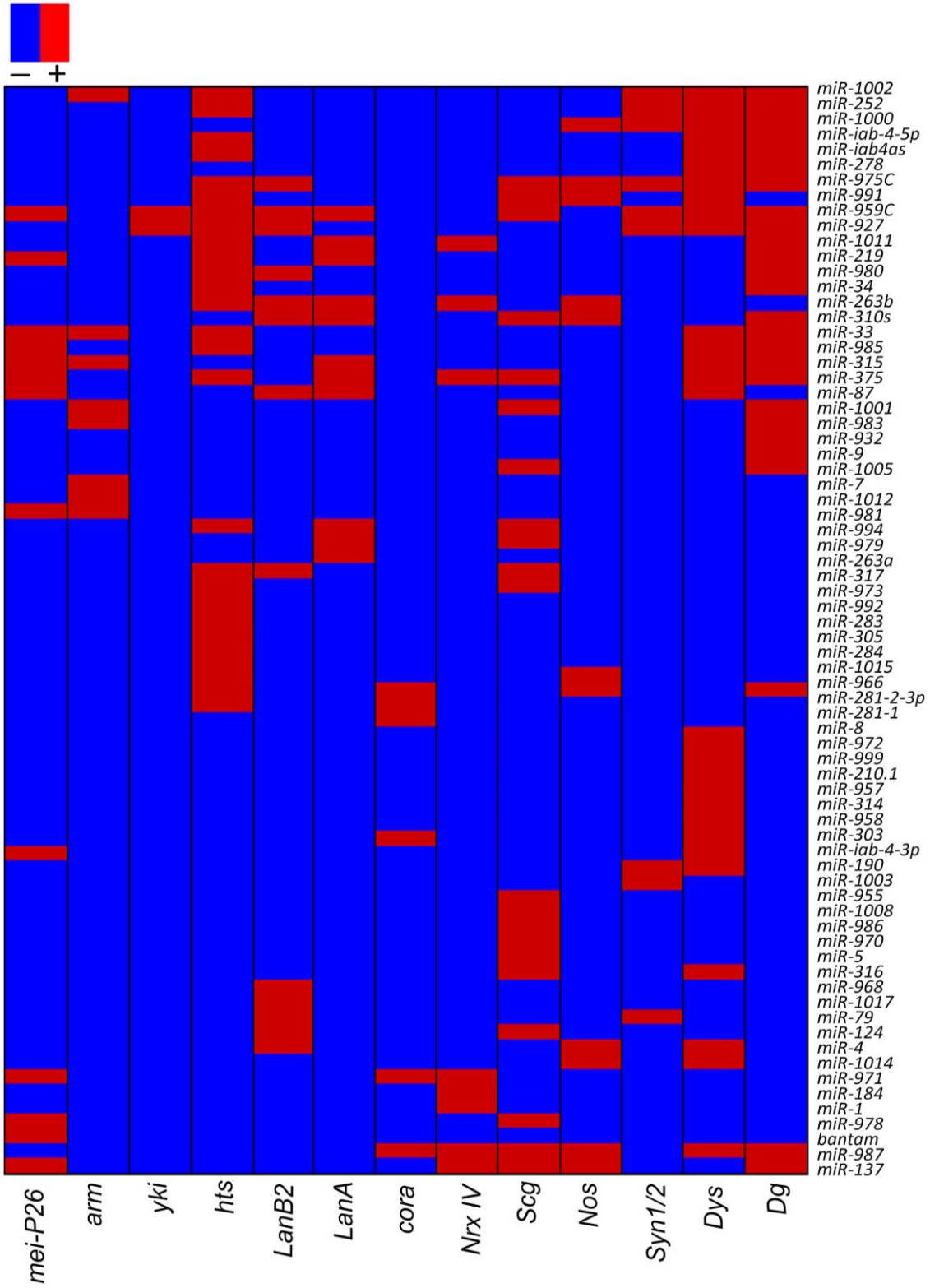

Figure 6. Multiple miRNAs are predicted to target the DGC components

MiRNAs that are predicted to target any component of the DGC, identified using the online tools TargetScan, miRBase, and DIANA/microT-CDS, are grouped in the heatmap based on their ability to target DGC components. Red indicates a predicted target and blue indicates no target. In total, 72 miRNAs are predicted to target any one of the DGC components.

3.1.2 MiRNA mutants have deregulated mRNA levels of *Dg*, *Dys*, and *Syn1*

To validate that the miRNAs from this group (Figure 7A) can indeed be involved in regulation of the DGC complex, mRNA levels of the major DGC components were tested in some miRNA mutants. Since the Dg-Dys-Syn1 signaling pathway has been shown to be regulated by miRNAs (Marrone et al., 2012; Yatsenko et al., 2014), we tested the mRNA levels of these three major DGC components via qRT-PCR in ten miRNA mutants. These miRNAs were selected based on the availability of the loss-of-function mutants at the time of the screen and are highlighted with black arrow (Figure 7A). RNA was extracted from the whole body of 1-week old male flies and were normalized to control. *MiR-956* is not predicted to target the DGC and therefore, was used as a negative control. Most of the miRNA mutants revealed deregulated mRNA levels of the DGC components. Since this group of miRNA has been selected firstly, by their ability to target *Dg*, we analyzed *Dg* levels in these mutants. *MiR-137*, *miR-252, miR-959C, miR-966*, and *miR-1000* had *Dg* mRNA levels upregulated by more than three folds, suggesting that *Dg* can be their direct target. Some miRNAs such as *miR-966* showed upregulated mRNA levels of all three components with approximately 2.5-5 fold increase relative to the control. In addition to *Dg* and *Dys* levels were also upregulated in most of these mutants. Such miRNAs were *miR-137, miR-252, miR-310s*, and *miR-966* even though, *Dys* was predicted to be a direct target only for *miR-252*, the increase in *Dys* level in these miRNA mutants can be explained because it has been previously shown that *Dys* stability depends on the levels of *Dg* (Bogdanik et al., 2008; Marrone et al., 2012). Since miRNA mutants have *Dg* levels increased possibly due to direct targeting of *Dg*, *Dys* levels would be upregulated. Analysis of *miR-310s* mutants showed approximately 2.5 fold increase in mRNA levels of *Syn1* relative to control, suggesting that *miR-310s* can target *Syn1* as predicted (Figure 7B). Though *miR-927* and *miR-975C* are predicted to target all three components, the loss of *miR-927* and *miR-975C* had no influence in the expression levels of *Dg*, *Dys,* or *Syn1*. Intriguingly, some of the miRNA mutants had deregulated levels of the DGC components that they are not predicted to target. Since DGC components are known to have compensatory effects on each other levels of expressions, the more rigorous screen is required to find out the miRNAs that could directly target DGC components or indirectly via targeting other factors, leading to MD development. This preliminary screen identified

miRNAs that have abnormal expression levels of major DGC components and could be involved in maintenance of muscle health via regulation of the DGC.

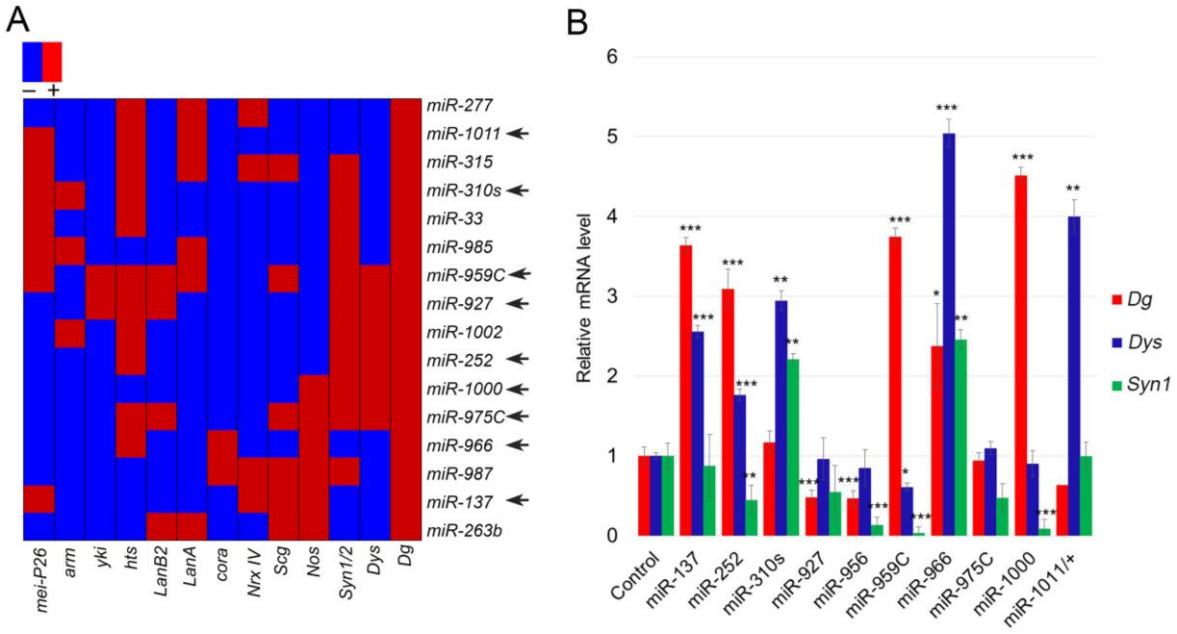

Figure 7. Candidate miRNA mutants have deregulated mRNA levels of the DGC components

(A) Clustering of miRNAs targeting *Dg* as well as any three other components of the DGC results in 16 different miRNAs. Red indicates predicted target and blue indicates no target. The black arrow indicates the availability of loss-of-function miRNA mutants at the time of the screen. (B) qRT- PCR performed on 1-week old male flies revealed altered mRNA levels of *Dg, Dys*, and *Syn1* shown in red, blue and green bars, respectively. Relative mRNA levels of miRNA mutant flies were normalized to the control flies (*Canton- S/OR*). *MiR-137* and *miR-252* mutants have an increase in mRNA levels of *Dg* and *Dys,* while *miR-310s* mutants have an increase in mRNA levels of *Dys* and *Syn1*. Loss of *miR-959C* and *miR-1000* influence *Dg* level only and *miR-966* mutants show an increase in mRNA levels of all three components of the DGC. Error bars represent AVE±SD, and statistical significance was determined by two-tailed Student's t-test (*P<0.05, **P<0.01, ***P<0.001). See also Supplementary Table 1.

3.1.3 Loss of miRNA causes muscle degeneration phenotypes

Among ten candidate miRNAs, the expression levels of six miRNAs (*miR-137, miR-252, miR-310s, miR-959C, miR-927,* and *miR-975C*) have been shown to be downregulated in hyperthermia-stressed wild type and/or in dystrophic flies. To study their potential roles in MD development, we decided to test whether the loss of these miRNAs can affect muscle architecture in normal and in stress conditions. We analyzed muscle integrity in miRNA mutants kept at the following conditions: young (7 day old at 25°C), aged (30 day old at 25°C), temperature stress (5 day at 33°C), sugar starvation (5 day at 25°C), and protein

starvation (30 day at 25°C). As expected, most of the miRNA mutants showed progressive muscle degeneration phenotypes (Figure 8). Muscle degeneration phenotypes were quantified as mild, moderate, and strong degeneration as shown in quantification panel (Figure 8A). miRNA mutants, such as *miR-959C* and *miR-1000* showed an increase in muscle degeneration phenotypes as early as in young age (approximately 15% and 17.5% of muscle degeneration as compared to 5% in control flies), indicating these miRNAs can be already involved in muscle formation during developmental stages. Most miRNA mutants, such as *miR-137, miR-310s, miR-959C, miR-966*, and *miR-975* were sensitive to more than one type of stress. Interestingly, only *miR-137* mutants were responsive to all stress conditions with more than five times increase in the frequency of muscle degeneration at temperature stress, sugar starvation, protein starvation, and aging, when compared to the young non-stressed animals (Figure 8B). We also noticed that wild type flies itself were sensitive to stress and aging, as they showed stress- and age-dependent muscle degeneration compared to the young age, albeit at the lower than miRNA mutants frequency. Stress- and age-dependent muscle degeneration in wild type flies have also been reported before (Kucherenko et al., 2011). *MiR-927* and *miR-959C* mutants were more responsive to protein starvation with an average muscle degeneration of 20-30% compared to 4-15% in young flies of the same genotype. A similar case was observed for *miR-966* with 15% of muscle degeneration compared to 4% in young flies.

MiR-959C and *miR-975C* though had stress-dependent muscle degeneration, these mutants were dropped to follow up further, since these miRNAs are in a complex of more than three different miRNAs, each with unique seed sequence and to follow up these miRNAs, an individual miRNA mutants must be generated. *MiR-1000* and *miR-1011* were not followed up due to the low survival rate, indicating that their role is broader than just muscle maintenance in animals.

Interestingly, loss of muscle degeneration phenotype during stress or aging was also noted in some miRNA mutants when compared to them at young age. Such miRNAs were *miR-310s, miR-966, miR-975C, miR-1000,* and *miR-1011*. This can be due to the fact that animals with severe phenotype could be dying and the animals that survived would have normal muscles. Contrarily, the expression of these miRNAs could have a negative effect on muscle maintenance and their loss could have a protective role, which would be interesting to study in greater detail in the future. Based on the severity of the muscle phenotypes and stress response, only *miR-137, miR-927,* and *miR-966* were followed further to dissect their roles in MDs and DGC signaling.

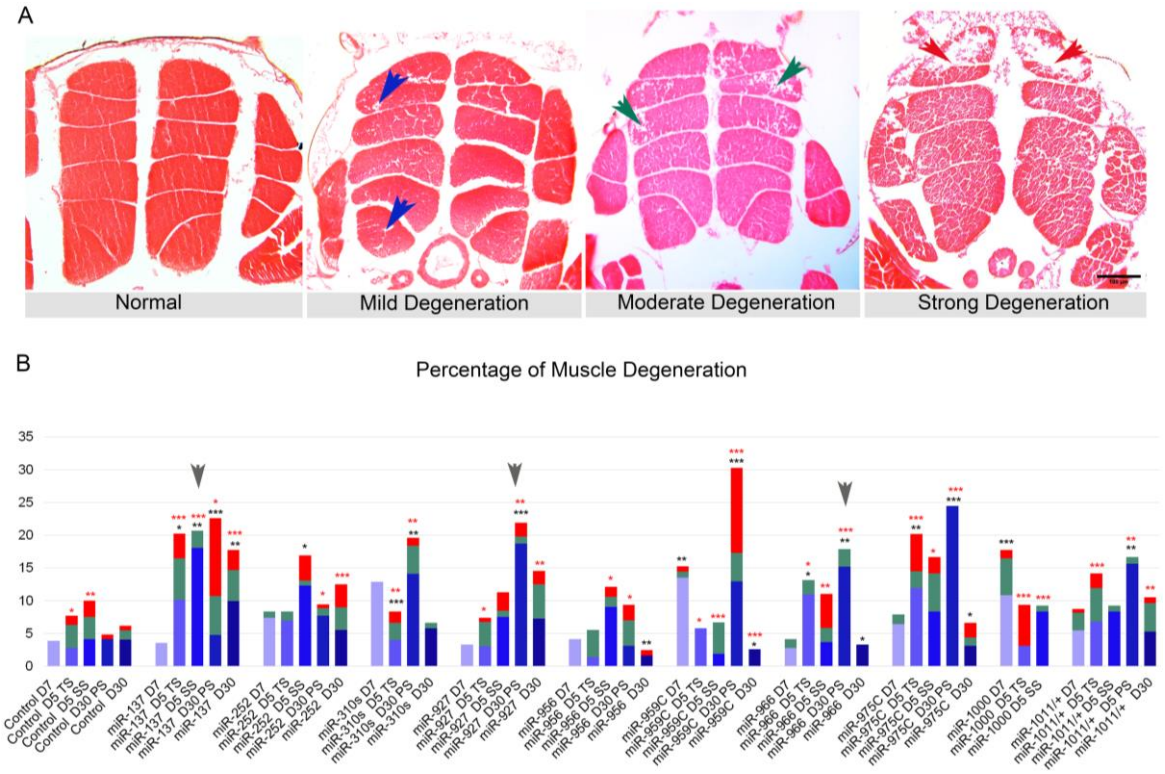

Figure 8. MiRNA mutants show muscle degeneration phenotype that is enhanced upon stress

(A) Representative images of muscle degeneration phenotype in IFMs of adult *Drosophila*. Blue, green and red arrows show mild, moderate and strong muscle degeneration. (B) A bar graph showing muscle degeneration due to miRNA loss at young, temperature stress, sugar starvation, protein starvation, and aging. Muscle degeneration mainly starts as early as in young flies and the phenotypes are accelerated upon stress even in control flies (Canton-*S/OR*). *MiR-137*, *miR-927,* and *miR-966* were responsive to most stress conditions (grey arrows on bar graph). *MiR-1000* mutants have the least tolerance for the temperature stress and sugar starvation and had a low survival rate in general, while *miR-959C* responded only to the protein starvation. Statistical significance was determined by χ^2test with Yate's correction (*P<0.05, **P<0.01, ***P<0.001 when compared to control flies at same condition), (*P<0.05, **P<0.01, ***P<0.001 when compared to the same genotype at a young age). Protein starvation was compared to the aged flies. D7= young, 7 day old, TS= temperature stress, SS= sugar starvation, PS= protein starvation, and D30= aging, 30 day old. Scale bar 100 µm. See also Supplementary Table 3.

3.2 Validation of muscle degeneration due to miRNA loss

The progression of muscle degeneration phenotypes upon stress, due to miRNA loss was further followed up in greater detail for three miRNAs (*miR-137*, *miR-927,* and *miR-966*). The experiment was done in three independent biological replicates and the appearance of MD phenotypes was quantified in miRNA mutants as mild and strong muscle degeneration (Figure 9A).

Additionally, muscle atrophy was scored in these animals at normal and different stress conditions. Muscle atrophy, in general, is described as a loss of muscle mass that is driven by an increase in protein degradation or a decrease in protein synthesis. It is an integral feature of systemic diseases including cancer, cachexia, cardiac failure, AIDS, and sepsis. Loss of muscle mass due to aging, also known as sarcopenia is often associated with muscle disuse, fasting (starvation), extrinsic changes in innervation, stem cell function, and endocrine regulation of muscle homeostasis (Demontis et al., 2013). Since most miRNA mutants were responsive to various stresses, including aging, muscle atrophy was also studied in miRNA mutants to dissect miRNA involvement in muscle maintenance.

The frequency of muscle degeneration and muscle atrophy in miRNA mutants kept at normal and different stress conditions, such as young, temperature stress, sugar starvation, and aging were normalized to the frequency of muscle degeneration and atrophy of young control animals. Muscle degeneration phenotypes were scored as mild and strong muscle degeneration as shown with blue and red arrows, respectively and muscle atrophy was scored as shown in green arrows (Figure 9A). As observed before, all animals, miRNA mutants and control were sensitive to stress and develop muscle degeneration and muscle atrophy in response to unfavorable conditions. However, the severity of stress-dependent muscle maintenance defects was different in different mutants. Interestingly, even change in genetic background in controls resulted in different frequencies of muscle degeneration, implying that in general, the muscle tissue is extremely sensitive to stress. For example in Figure 8, heterozygous *Canton-S/OR* were used as control and the frequency of muscle degeneration was never higher than 10%, while in this experiment (Figure 9), we used w^{1118} mutants crossed to wildtype *OR* as control. This resulted in the dramatic increase in muscle degeneration phenotypes. A similar observation was made on *miR-137* mutants that were back-crossed in the w^{1118} genetic background for 8 generations.

Upon stress and aging, controls themselves showed approximately 1.5-2.5 fold increase in the incidence of muscle degeneration relative to young non-stressed animals. *MiR-137* mutants had approximately 2 fold increase in muscle degeneration already at young age when compared to control flies of the same age. This phenotype was even more enhanced upon temperature stress and aging. Similarly, *miR-966* mutants showed muscle degeneration phenotypes as early as in young age (1.5 fold higher than control) and the phenotype was enhanced upon aging (3.5 fold compared to 2.5 fold in control). However, *miR-927* and *miR-966* mutants did not show temperature stress or sugar starvation response (Supplementary

Table 4). *MiR-927* mutants were responsive only to aging with approximately 4 fold increase in muscle degeneration compared to control flies (Figure 9B).

A comparison of muscle atrophy showed that upon various stresses control flies had an increase in the frequency of muscle atrophy when compared to young non-stressed animals (approximately 2.5-4 fold increase). Young miRNA mutants had muscle atrophy already at 7 day, the frequency of which was approximately three times higher than in control. In addition, miRNA mutants showed loss of muscle integrity in response to sugar starvation and during aging, and the frequency of atrophic muscle appearance was six times higher than in young controls. This tendency of being extremely sensitive to aging was also observed in *miR-927* and *miR-966* mutants that also showed 6-fold increase in the frequency of atrophic muscle appearance in comparison to young controls (Supplementary Table 4). The frequency of muscle atrophy was observed in higher rate compared to the frequency of muscle degeneration. *MiR-927* and *miR-966* mutants did not show any differences in muscle degeneration phenotypes during temperature stress and sugar starvation, while an increase in 3-4 fold difference of atrophic muscles was observed compared to young control. Since *miR-137* mutants showed an increase in muscle degeneration and muscle atrophy phenotypes already in young animals and these phenotypes were significantly progressing during aging, it indicates that this miRNA can be an especially good candidate to study further in order to elucidate the common mechanisms between MD and age-dependent muscle loss.

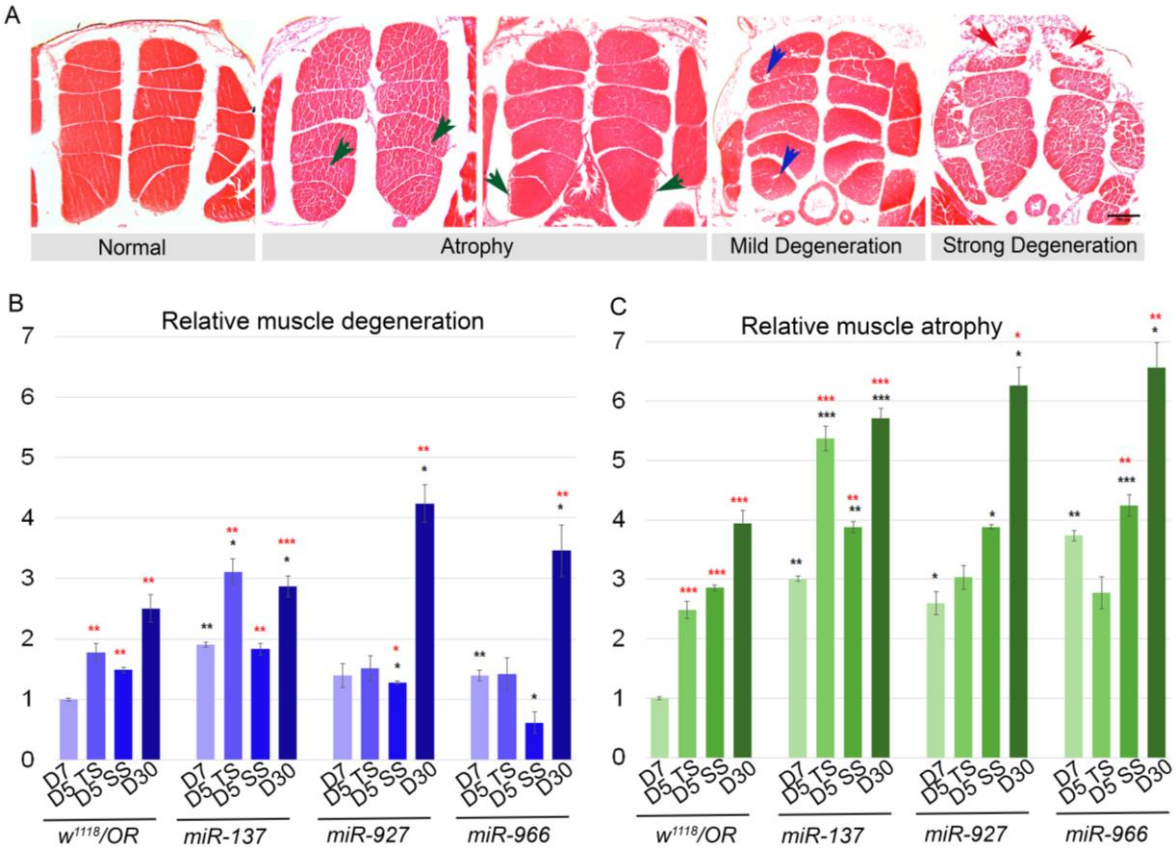

Figure 9. Loss of miRNA affects muscle maintenance

(A) Representative images of muscle degeneration and atrophic muscle phenotypes in adult *Drosophila* IFMs. Blue and the red arrows represent mild and strong muscle degeneration, while the green arrows represent muscle atrophy. (B) A bar graph representing relative muscle degeneration and (C) relative muscle atrophy in different stresses compared to young control flies (w^{1118}/*OR*). Stress enhances muscle degeneration and atrophy even in wild type flies. Control and *miR-137* mutants were responsive to all stresses when compared to young age (significance shown by red stars). In general, *miR-137* mutants had ~2 times more muscle degeneration in young and sugar starvation and ~3 times more muscle degeneration in temperature stress and aging compared to young controls. Similarly, an increase in muscle atrophy by ~3-5.5 fold was observed in *miR-137* mutants when compared to young controls. Values are obtained from the averages of 3 biological replicates. Error bars represent AVE±SEM and statistical significance was determined by two-tailed Student's t-test. *P<0.05, **P<0.01, ***P<0.001 represent comparisons to control at the same condition, while *P<0.05, **P<0.01, ***P<0.001 represent comparisons within the same genotype at a young age. D7= young, 7 day old, TS= temperature stress, SS= sugar starvation, and D30= aging, 30 day old. Scale bar 100 µm. See also Supplementary Table 4.

3.3 Conserved predicted targets of miRNAs are associated with multiple biological functions

To verify whether *miR-137, miR-927*, and *miR-966* have muscle-related target genes to have function in muscle maintenance, we combined their putative conserved targets by TargetScan, release 6.2 (www.targetscan.org) to predict their possible biological roles related to muscle maintenance. Individual lists of predicted targets of all three miRNAs were processed separately in Generic Gene Ontology term finder tool (Boyle et al., 2004). *MiR-137* having the largest number of conserved targets (252 targets in total), which were found to be involved in the processes associated with multiple biological terms including synapse, neuromuscular junction, neuron, voltage-gated potassium complex, as well as transporter complex. Majority of *miR-137* target genes were found to be associated with functions related to cell periphery and plasma membrane protein complex (Figure 10A). *MiR-927* and *miR-966* having 120 and 30 conserved targets, respectively, which were found to be involved in processes related to the cell periphery and cell membrane function (Figure 10B-C). Interestingly, among many genes that share similar associations, Dg is well known for its role in all of these processes that are coined for these miRNA predicted targets.

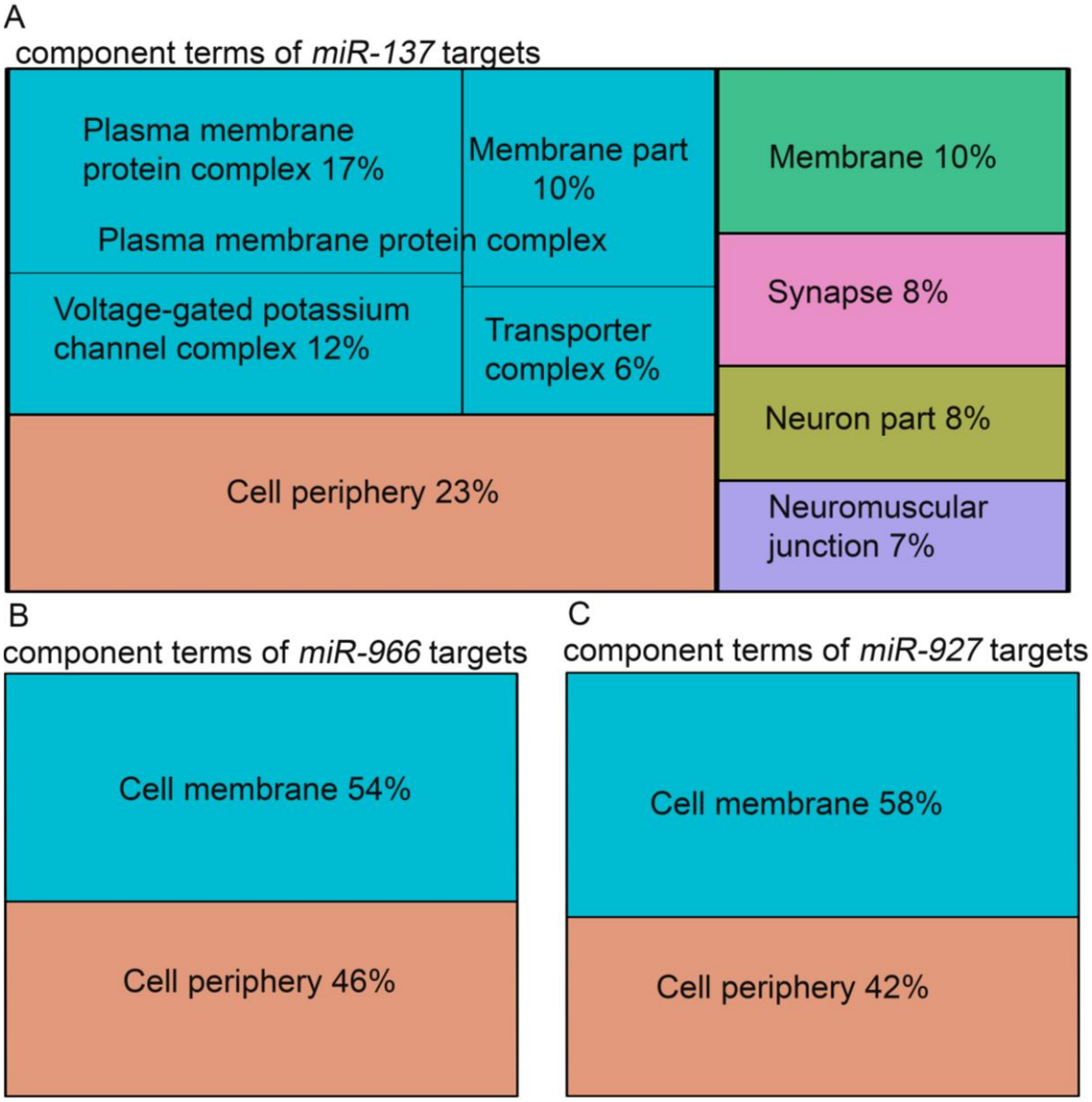

Figure 10. GO term for component processes for each miRNA targets

(A) Putative *miR-137* targets are involved in plasma membrane protein complex, cell periphery or voltage-gated potassium channel complex and in neuronal functions related to the synapse and neuromuscular junction. (B-C) Putative targets of both *miR-927* and *miR-966* are involved in the cell membrane- and cell periphery-related functions.

3.4 Ectopic expression of candidate miRNA affects muscle maintenance

Our previous data showed that muscle integrity upon miRNA loss was severely compromised, indicating these miRNAs are required for normal muscle functions. The GO component terms further indicated that these miRNAs are required in majority of the functions related to the cell membrane and cell periphery related processes. In IFMs of *Drosophila*, Dg has been shown to be localized in muscle membrane (sarcolemma) and loss of Dg cause muscle degeneration and the phenotype is accelerated upon stress (Kucherenko et al., 2011). The study further identified genes that interact with the DGC components and shared functional similarity in the development of MDs. To further elucidate miRNAs affecting muscle maintenance by targeting muscle-specific target genes, we over-expressed our candidate miRNAs in muscle and scored for the muscle degeneration and atrophy phenotypes similar to its loss-of-function.

Over-expression of miRNAs in muscle was achieved by the UAS/Gal4 system. Two muscle-specific-Gal4 lines were chosen to overexpress candidate miRNAs, one that drives the expression in adult muscle only and one that is active throughout the development: *Mhc-Gal4* and *how-Gal4*, respectively. Male flies of *UAS-miRNA* lines with virgin females of *Mhc-Gal4* lines were crossed and the IFMs of progenies were analyzed. *Mhc-Gal4* resides in X-chromosome; therefore, only females were analyzed for this experiment to reduce the dosage compensation effect on muscles. Using these two driver lines, we over-expressed *miR-137, miR-927*, and *miR-966* in muscles. Over-expression of *miR-137* and *miR-927* during development caused lethality at various developmental stages of flies (Supplementary Table 4). Ectopic expression of *miR-137* with *Mhc-Gal4* was semi-lethal and few escapers that were analyzed showed severe muscle degeneration and muscle loss, appearing as the complete absence of individual muscle (Figure 11). Over-expression of *miR-927* and *miR-966* in adult muscle were not lethal for flies, however, the muscle integrity was severely compromised (Figure 12). On average, over-expression of *miR-927* and *miR-966* in adult muscle showed an increase in muscle degeneration (35-85% and 22-60%) compared to control flies (10-40%) at young, temperature stress, sugar starvation, and aging (Figure 12A). Ectopic expression of *miR-966* using *how-Gal4* resulted in 22-65% cases of average muscle degeneration at young and various stresses compared to 10-40% cases observed in controls. In general, *miR-966* over-expression with *how-Gal4* ensued in much milder phenotype compared to *Mhc-Gal4*.

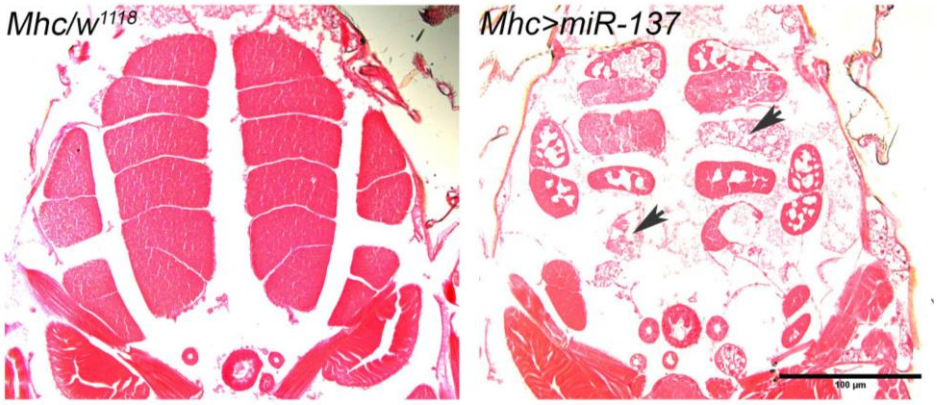

Figure 11. Over-expression of *miR-137* results in strong muscle degeneration and muscle loss

Ectopic expression of *miR-137* in adult fly muscle is semi-lethal to flies and few escapers that were analyzed show severe muscle degeneration or complete absence of an individual muscle (black arrow) as compared to control flies of genotype *Mhc>w*^{1118}, indicating level of *miR-137* in adult muscle must be maintained at the proper level. Scale bar 100 µm. See also Supplementary Table 4.

Over-expression of miRNAs also showed muscle atrophy phenotype. Over-expression of *miR-927* and *miR-966* in adult muscle caused a significant increase in muscle atrophy (70-90% and 28-74% cases of atrophic muscles) compared to control (10-50% cases of atrophic muscle) (Figure 12B). Over-expression of *miR-966* during developmental stage resulted in relatively milder phenotype compared to over-expression during adult stage similar to the observation on muscle degeneration phenotypes (21-63% atrophic muscle when over-expressed during development compared to 70-90% in adult over-expression). Together with the muscle degeneration and muscle atrophy phenotypes observed upon over-expression of *miR-966*, it was concluded that *miR-966* is required more for adult muscles maintenance. Similar to muscle degeneration, flies of all genotypes were sensitive to aging, indicating aging in general affects muscle maintenance. Altogether the data show that over-expression of identified miRNAs in our screen specifically in the muscle tissue resulted in severe phenotypes, indicating all of these candidate miRNAs can control at least one or more targets that are required for muscle maintenance and development.

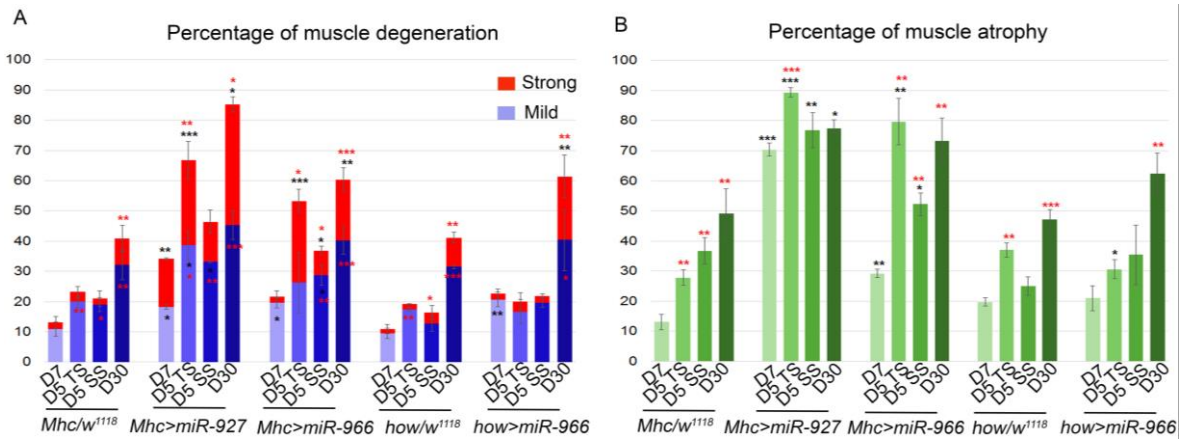

Figure 12. Over-expression of candidate miRNAs affects muscle maintenance

Bar graphs showing muscle degeneration (A) and muscle atrophy (B) phenotypes in adult IMFs. Over-expression of *miR-927* in adult muscle caused 35-85% of degenerated muscle and 70-90% of atrophic muscle, while over-expression of *miR-966* caused 20-60% of degenerated muscle and 20-80% atrophic muscle. Over-expression of *miR-966* was more detrimental to flies at adult stage compared to over-expression during developmental stage. Values are obtained from the averages of 3 biological replicates. Error bars represent AVE±SEM and statistical significance was determined by two-tailed Student's t-test. *P<0.05, **P<0.01, ***P<0.001 represent comparisons to control at the same condition, while *P<0.05, **P<0.01, ***P<0.001 represent comparisons within the same genotype at a young age. D7= young, 7 day old, TS= temperature stress, SS= sugar starvation, and D30= aging, 30 day old. See also Supplementary Table 4.

3.5 Candidate miRNAs target *Dg-3' UTR in vitro*

In order to validate that miRNAs identified in our screen (*miR-137, miR-927*, and *miR-966*) can indeed regulate *Dg* by targeting its 3'UTR, *Drosophila* S2 cell-based luciferase reporter assay was carried out. According to FlyBase, a database for *Drosophila* gene and genome (http://flybase.org/), *Dg* transcript has two different *3'UTRs*: the long 3'UTR is 2102 bp long (Figure 10A) and the short 3'UTR is 1609 bp long. About 60% of *Dg* transcripts had been shown to contain long 3'UTR (Yatsenko et al., 2014). To study all miRNA based regulation possibilities, the long 3'UTR was divided into four smaller fragments (S1-S4). This made cell culture analyses easier and made it accessible to study individually selected miRNAs based on the predicted position of the miRNA binding sites.

MiR-927 is predicted to have a binding site on long *Dg-3'UTR*, while both *miR-137* and *miR-966* have predicted binding sites on short *Dg-3'UTR*. Importantly, *miR-137* and *miR-927* are predicted to have multiple binding sites in *Dg-3'UTR* (highlighted with marron box and blue box, Figure 13A), while *miR-966* is predicted to have only one binding site (highlighted with yellow box). To test if all three miRNAs can target *Dg in vitro*, plasmid containing sequence

that include individual miRNA predicted binding sites were transfected in S2R+ cell lines. S3 fragment of *Dg-3'UTR* did not contain any predicted binding sites for these three miRNAs; therefore, S3 fragment was used as a negative control and was transfected with the empty *psiCHECK^{TM}-2* vector. In addition, *miR-956* was chosen as a negative control as it is not predicted to have any binding sites on *Dg 3'UTR*. Both renilla and firefly luminescence light signals encoded by the constructed plasmid transcripts with and without miRNA binding sites were measured. The relative signal intensity values showed the significant downregulation of corresponding *Dg* transcripts by all three miRNAs (*miR-137, miR-927*, and *miR-966*), indicating that *Dg* can be targeted by all these miRNAs *in vitro* (Figure 10B). As a negetive control, *miR-956* that is not predicted to have any binding sites on *Dg-3'UTR* was used. It failed to downregulate the luciferase signal, supporting in silico predictions for miRNA binding sites.

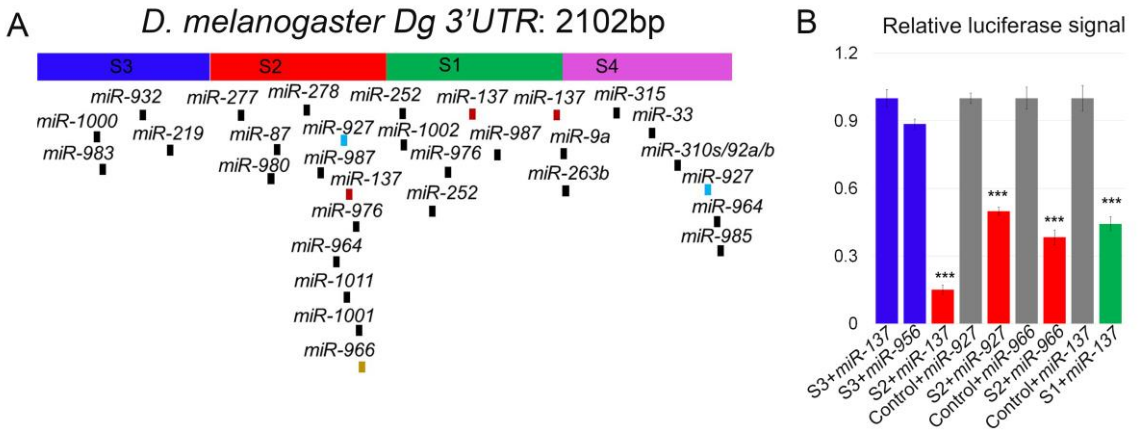

Figure 13. Selected miRNAs can target *Dg in vitro*

(A) Predicted miRNA binding sites in *Dg 3'UTR*, which is subdivided into four regions corresponding to constructs used in the luciferase assay (S1-S4). Out of all the miRNAs that are predicted to target *Dg*, *miR-137* is predicted to have 3 binding sites (highlighted in marron), *miR-927* has 2 binding sites (highlighted in light blue), and *miR-966 has* 1 binding site (highlighted in yellow) in *Dg 3'UTR*. (B) To calculate relative downregulation by miRNAs, a reporter luciferase values were calculated from raw readouts of *Renilla* to *Firefly* luciferase values. The background control values (transfection with empty *psiCHECK^{TM}*-2 with no reporter construct) were subtracted from respective readouts. Obtained values were then normalized to empty *psiCHECK^{TM}-2* to the values of *psiCHECK^{TM}-2-Dg-3'UTR* (S1-S4) in the presence of miRNAs. Error bars represent AVE±SEM, and statistical significance was determined by two-tailed Student's t-test (*P<0.05, **P<0.01, ***P<0.001). See also Supplementary Table 5.

3.6 Downregulation of Dg affects muscle maintenance

The precise level of Dg has been implicated in many neuronal and muscular dysfunctions (Yatsenko et al., 2014; Yatsenko and Shcherbata, 2014). Our *in vitro* data demonstrated that all three miRNAs (*miR-137*, *miR-927*, and *miR-966*) can target *Dg 3'UTR* and the analysis of GO component terms of conserved targets further suggests their involvement in processes related to the cell membrane and cell periphery.We have also shown that over-expression of miRNAs resulted more severe phenotype compared to their loss, indicating these miRNA can regulate muscle-specific genes. Altogether, we hypothesized that the precision of Dg expression in adult muscle especially in repsonse to stress is maintained by these miRNAs. The previous study has shown that complete loss of *Dg* causes muscle degeneration and this phenomenon is enhanced upon stress conditions (Kucherenko et al., 2011). However, phenotypes caused by downregulation of a gene often results in milder phenotypes than its complete loss. Therefore, to further verify the role of Dg in muscle maintenance, we downregulated Dg specifically in adult muscle and scored for muscle degeneration and muscle atrophy phenotypes in young and aged flies as described in chapter 3.1.3.

Downregulation of Dg in adult muscle caused muscle degeneration and muscle atrophy already in young flies and the phenotype was enhanced during aging (Figure 14A). IMFs analyzed in young and aged flies of *Mhc>Dg*^{RNAi} genotype had approximately 1.5-2 times increase in muscle degeneration when compared to the control genotype (*Mhc/OR*). Similar increase in muscle atrophy was observed in young and aged flies upon downregulation of Dg. As observed before, both genotypes were sensitive to aging and showed an increase in muscle degeneration and atrophy phenotypes (Figure 12B). Overall, this result further concluded that downregulation of Dg is causing muscle degeneration similar to its loss of function and also affects muscle maintenance. Both phenotypes progress in an age-dependent manner.

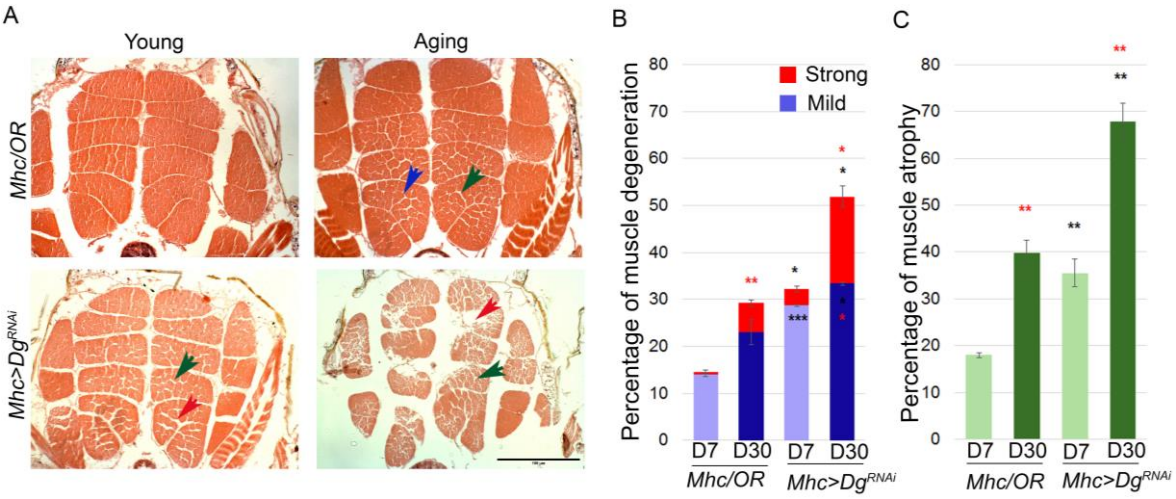

Figure 14. Downregulation of Dg shows age-dependent loss of muscle integrity

(A) IMFs of adult *Drosophila* showing mild and strong muscle degeneration phenotypes (indicated by blue and red arrows) and muscle atrophy phenotype (indicated by green arrows) in control (*Mhc/OR*) and *Mhc>Dg*^{RNAi} flies. Bar graphs showing the frequency of muscle degeneration (B) and muscle atrophy (C). On average, 1.5-2 times increase in muscle degeneration and muscle atrophy was observed upon downregulation of Dg in young and aged animals compared to control. Both genotypes show age-dependent muscle maintenance phenotypes with an average of two fold increase as compared to young animals. Values are obtained from the averages of 3 biological replicates. Error bars represent AVE±SEM and statistical significance was determined by two-tailed Student's t-test. *P<0.05, **P<0.01, ***P<0.001 represents comparisons to control at the same condition, while *P<0.05, **P<0.01, ***P<0.001 represent comparisons within the same genotype at a young age. D7= young, 7 day old, TS= temperature stress, SS= sugar starvation, and D30= aging, 30 day old. Scale bar 100 µm. See also Supplementary Table 4.

3.7 Dissecting biological roles of *miR-137*

MiR-137 was further followed up to decipher its role in MDs with various reasons: 1) *miR-137* mutants had an increase in *Dg* and *Dys* mRNA levels, 2) the severity of muscle maintenance phenotypes were ameliorated in *miR-137* mutants as well as upon its over-expression compared to *miR-927* and *miR-966*, indicating *miR-137* is a better candidate to have role in regulating muscle-specific genes, 3) *miRNA-137* mutants were responsive to various stresses, indicating it is required to address negative effects of stress, 4) it can target Dg *in vitro,* and 5) *miR-137* is predicted to have multiple functions including neuronal, cell membrane and cell periphery related biological processes, for which the precision of Dg expression has been shown to essential.

3.7.1 *MiR-137* is conserved among higher eukaryotes

MiR-137 is well conserved among animal kingdom (Figure 15). *Drosophila miR-137* is predicted to have 252 conserved targets (TargetScanFly, Release 6.2), among which dystroglycan and sarcoglycan are common predicted targets in higher eukaryotes, including humans, mouse, zebrafish, and worms, which implies that *miR-137* can share similar functions in these organisms. Besides *Dg*, *mei-P26*, N-methyl-D-aspartate (*NMDA*) receptor (*NMdar2*), dopamine receptor (*D2R*), and γ-aminobutyric acid (GABA) receptor (*GABA-B-R3*) are among other verified targets (*in vitro*) of *miR-137* in flies (Herranz et al., 2010; Kong et al., 2015).

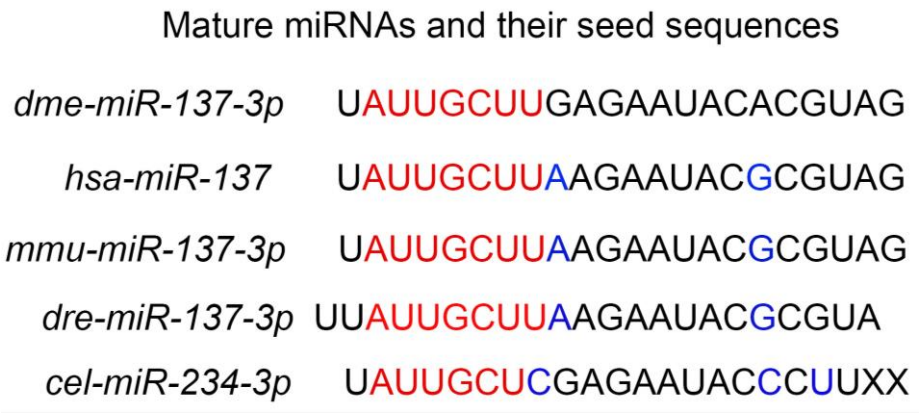

Figure 15. *MiR-137* has conserved seed as well as mature miRNA sequences

The mature *Drosophila* miRNA together with its human, mouse, zebrafish, and worm orthologues shows the conservation of the seed sequence and the mature miRNA sequence among different animal species.

3.7.2 *MiR-137* is expressed in larval muscle, brain, and testis

MiRNAs are known for expression tuning and expression buffering of their target mRNAs. In *Drosophila*, it has been shown previously that *miR-310s* buffers the expression of Dg in in larval brain and influence the proper formation of nervous tissue (Yatsenko et al., 2014). Similarly, it has been reported that precise level of Dg to form myotendious junction (MTJs) in fly embryo is regulated by *miR-9a* (Yatsenko and Shcherbata, 2014). Studies have shown that Dg is virtually expressed in all tissues, indicating its function is much more diverse and complex in the whole organism. Therefore, we further investigated the biological roles of *miR-137* and characterized its function in relation to diverse phenotypes observed in MD and dystroglycanopathies.

First, we analyzed its expression patterns in different tissues. *In situ* hybridization as well as fluorescence *in situ* hybridization (FISH) was performed using *miR-137-3p* LNA probe. Abdominal segments A3-A5 of muscle 5, 6, and 7 were analyzed to check the *miR-137* expression in larval muscle. FISH showed that *miR-137* is expressed in larval muscle and its expression was concentrated more at the edge of the muscle wall, possibly at the NMJ (Figure 16 A-A'). In the *miR-137^{ko}* mutants, used as a negative control, no expression pattern in muscle was observed, verifying the specificity of LNA probe (Figure 16 B-B').

In situ hybridization showed the expression of *miR-137* in nervous system. It is expressed in several cell types presumably in type I/II neuroblasts, Kenyon cells of the mushroom body, abdominal neuromeres, and dorsal cell bodies of the larval brain (Figure 16C). The expression pattern in the larval brain suggests that *miR-137* also could have a role in neuronal processes. *MiR-137* expression was also detected in the apical portion of the adult fly testis (Figure 16E-E'). The apex of adult fly testes is composed of a pool of germline as well as somatic cells surrounding the hub. Cells next to the hub are stem cells in nature, while the cells away from the hub are differentiating gonialblast encapsulated with two somatic cells. Since *miR-137* LNA probe was concentrated only on a subset of the cells in the apex and appeared as dots (Figure 16E'), it was assumed that *miR-137* is possibly expressed in early somatic cells of fly testes. The expression patterns of *miR-137* further suggest the involvement of *miR-137* in the neuronal, cell membrane and cell periphery related processes as coined by GO component terms of its predicted mRNA targets.

The role of Dg has been well studied in larval NMJs and brain. It will be interesting to study further the relationship between *miR-137* and Dg and their shared function not only in the muscle, but also in the nervous system and in spermatogenesis.

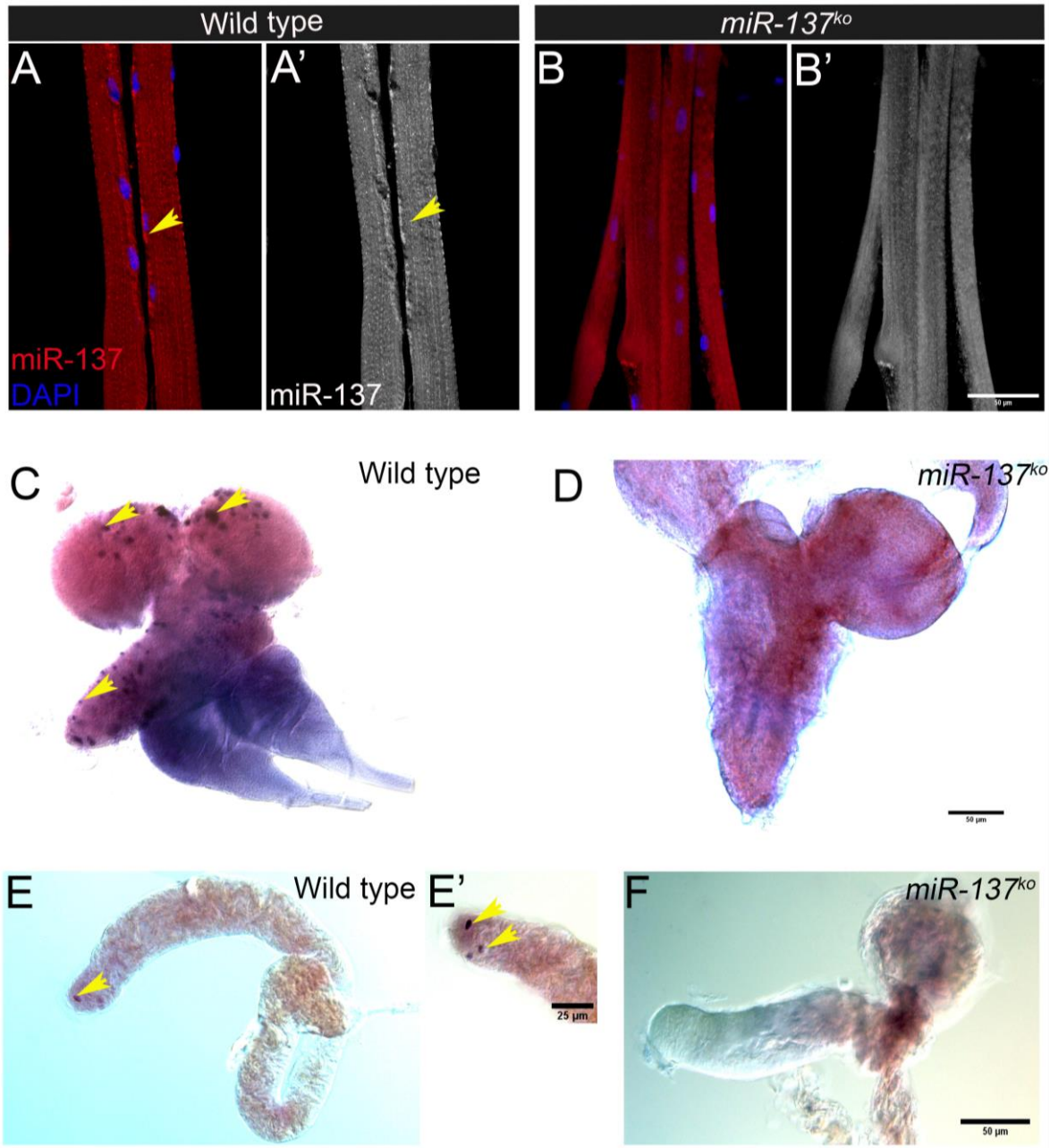

Figure 16. *MiR-137* expression patterns

In situ hybridization (ISH) and Fluorescence *in situ* hybridization (FISH) in wild type flies using LNA probe for mature *miR-137* shows that *miR-137* is expressed in larval muscle and brain as well as in adult testis (indicated by yellow arrows) (A-C-E). FISH shows that *miR-137* is expressed in larval muscle; in particular in neuromuscular junctions (NMJs). Calorimetric reaction of *miR-137* LNA probe shows expression of *miR-137* in L3 larval brain (C) presumably in type I/II neuroblasts, Kenyon cells of the mushroom body, abdominal neuromeres, and dorsal cell bodies as well as in adult fly testes (E-E'), particularly, in early somatic cells at the apex of the testis. Contrary, the absence of fluorescence as well as calorimetric signal was noted in *miR-137* mutants (B-D-F). Scale bar 50 µm.

3.7.3 *MiR-137* affects muscle maintenance

3.7.3.1 Downregulation of *miR-137* is more detrimental for adult muscle maintenance

To confirm the specificity of role of *miR-137* in adult muscles to maintain its integrity during adulthood and in response to stress, we down-regulated *miR-137* in fly muscle. Muscle degeneration, as well as muscle atrophy phenotype, was scored as described in Figure 9A. Down-regulation of *miR-137* was achieved using *UAS-miR-137^{sponge}*. Sponge contains multiple miRNA binding sites with central bulges to stably sequester the miRNA *in vivo*. For most miRNAs, sponge had been shown to produce accurate but milder version of loss-of-function phenotype (Cohen, 2009).

Downregulation of *miR-137* resulted in phenotypes similar to its loss-of-function. This further favored that *miR-137* is important for muscle maintenance. *Mhc-Gal4>miR-137^{sponge}* flies showed 1.5-3 times increase in incidence of muscle degeneration and 3-5 times increases in incidence of muscle atrophy under young and stress conditions. Similar comparison was made on *how>miR-137^{sponge}* flies. The calculated phenotype showed about 1.5 times increase in incidence of muscle degeneration and about 2 times increase in muscle atrophy compared to controls. It was also noted that down-regulation of *miR-137* during developmental stage resulted in relatively milder phenotype compared to its downregulation in adult muscle, indicating *miR-137* contributes to muscle maintenance during adult stage. Over-expression of Dg in adult muscle was relatively milder compared to downregulation of *miR-137*. The calculated phenotype showed about 1.5-2 times increase in muscle degeneration and muscle atrophy compared to controls (Figure 17). However, over-expression of Dg during development using *how-Gal4* driver was semi-lethal and few escapers that were analyzed showed fused muscle phenotype (Supplementary Figure 1) rather than the muscle degeneration or atrophy phenotypes, indicating over-expression of Dg during developmental stage does not cause MD development. Overall, it was concluded that both over-expression and downregulation of *miR-137* is detrimental for muscle maintenance, indicating *miR-137* is required for muscle maintenance. Similarly, both loss-of-function and downregulation, as well as over-expression of Dg, are detrimental to flies, indicating, the precise level of Dg needs to be maintained for healthy musculature.

The experiment further showed that phenotypes caused in adult muscle due to downregulation of *miR-137* can be partially rescued by Dg over-expression.

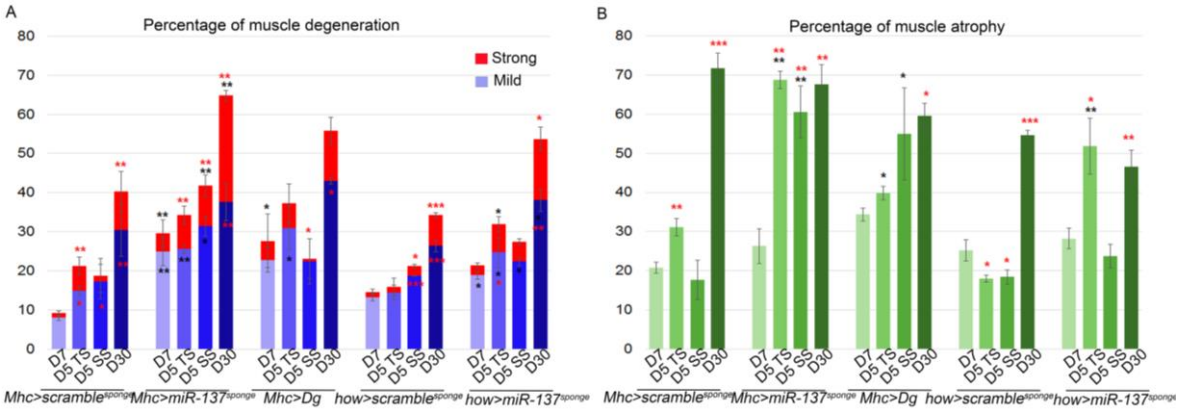

Figure 17. *MiRNA-137* regulates Dg levels for muscle maintenance

Bar graphs showing frequency of muscle degeneration (A) and muscle atrophy (B) in IFMs of *Drosophila*. Downregulation of *miR-137* specifically in muscle leads to muscle degeneration as well as muscle atrophy phenotype. Both phenotypes were more severe as compared to over-expression of Dg in muscle. Downregulation of *miR-137* using *Mhc-Gal4* also resulted in an increase in muscle and atrophy phenotypes as compared to the control indicating, *miR-137* is required for regulation of genes expressed in muscles. Values are obtained from the averages of 3 biological replicates. Error bars represent AVE±SEM and statistical significance was determined by two-tailed Student's t-test. *P<0.05, **P<0.01, ***P<0.001 represents comparison to control at the same condition, while *P<0.05, **P<0.01, ***P<0.001 represents comparison within the same genotype at a young age. D7= young, 7 day old, TS= temperature stress, SS= sugar starvation, and D30= aging, 30 day old. See also Supplementary Table 4.

3.7.3.2 Downregulation of *Dg* in *miR-137* loss-of-function mutants rescues the muscle maintenance phenotypes

To further verify that Dg level must be regulated in adult muscle to maintain healthy musculature, we analyzed *miR-137* heterozygous mutants (*miR-137$^{ko/Df}$*) that have reduced level of Dg by one copy. *MiR-137* resides on the second chromosome, 16 kbs away from *Dg* genomic locus (http://flybase.org/). The deficiency line available at BDSC (*Df (2R) ED2457*) referred as *miR-137^{Df}* apart from removing *miR-137*, also has genomic locus of *Dg* deleted (Figure 18). The *miR-137^{ko}* line, however, only affects *miR-137* locus and replaces with *mini-white* gene (Chen et al., 2014). Hence, *miR-137$^{ko/Df}$* lines have one *Dg* copy loss compared to homozygous *miR-137^{ko}* lines that have both *Dg* copies intact. Therefore, I analyzed and compared muscle maintenance phenotypes in *miR-137^{ko}* and *miR-137$^{ko/Df}$* to further pinpoint that Dg is regulated by *miR-137*.

As expected, *miR-137$^{ko/Df}$* flies had a much milder phenotype compared to *miR-137^{ko}* lines. The calculated phenotype include average muscle degeneration of 12-35% in control at young and stress conditions, while *miR-137^{ko}* flies had up to 35-55% of muscle degeneration.

This phenotype was relatively reduced in *miR-137*$^{ko/Df}$ lines with an average frequency of muscle degeneration ranging 30-45%. The effect of muscle maintenance upon reduced level of *Dg* was not visible in young flies, however upon stress the phenotypes were relatively milder in *miR-137*$^{ko/Df}$ compared to *miR-137*^{ko} lines (35-55% in *miR-137*^{ko} compared to 30-45% (Figure 19A). The severity of the phenotypes in *miR-137*$^{ko/Df}$ were statistically lower than *miR-137*^{ko} flies under stress conditions, indicating a partial rescue of muscle maintenance phenotype due to one copy loss of *Dg*. Interestingly, downregulation of Dg by one copy in *miR-137* loss-of-function background could not rescue muscle atrophy phenotype suggesting that other than *Dg*, more *miR-137* dependent targets could be involved in regulation of muscle size upon stress (Figure 19B).

qRT-PCR on thoraces of young flies further revealed 2-3 times increase in *Dg* mRNA levels in *miR-137*$^{ko/Df}$ and *miR-137*^{ko} lines compared to control. The level of Dg in *miR-137*$^{ko/Df}$ was relatively lower as compared to *miR-137*^{ko} (Figure 19C). Overall, this experiment indicates that that *Dg* is a *bona fide* target *miR-137* in muscles.

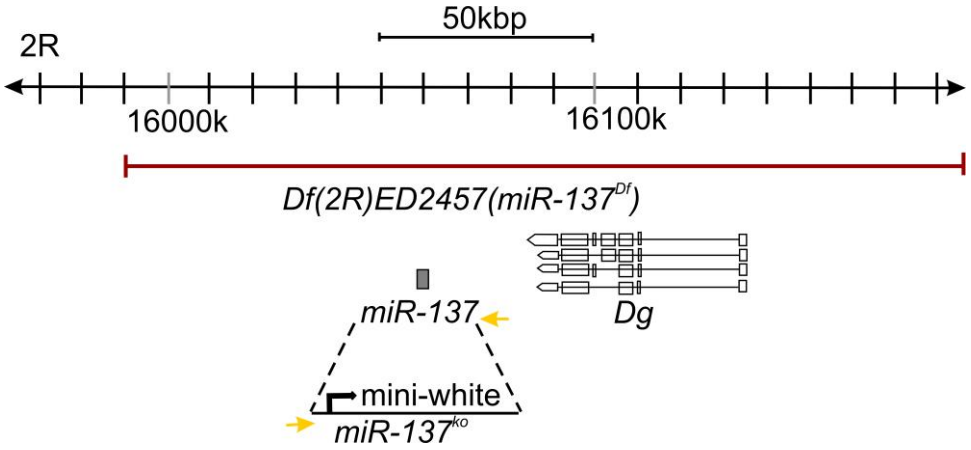

Figure 18. Genomic locus of *miR-137*

MiR-137 is located on the minus strand of chromosome 2R, and the *miR-137*^{ko} line was made using *pRMCE* (recombinase-mediated casette exchange), which replaces *miR-137* with *mini-white* gene. *MiR-137*^{Df} genomic locus *Df(2R)ED2457,* available from BDSC, uncovers a large genomic region including *miR-137* and *Dg*. For use in all phenotypic analyses, the *miR-137*^{ko} line was backcrossed in the w^{1118} background for 8 generations, and the final stocks were verified using primers that detect *mini-white* and the *miR-137* locus (yellow arrows).

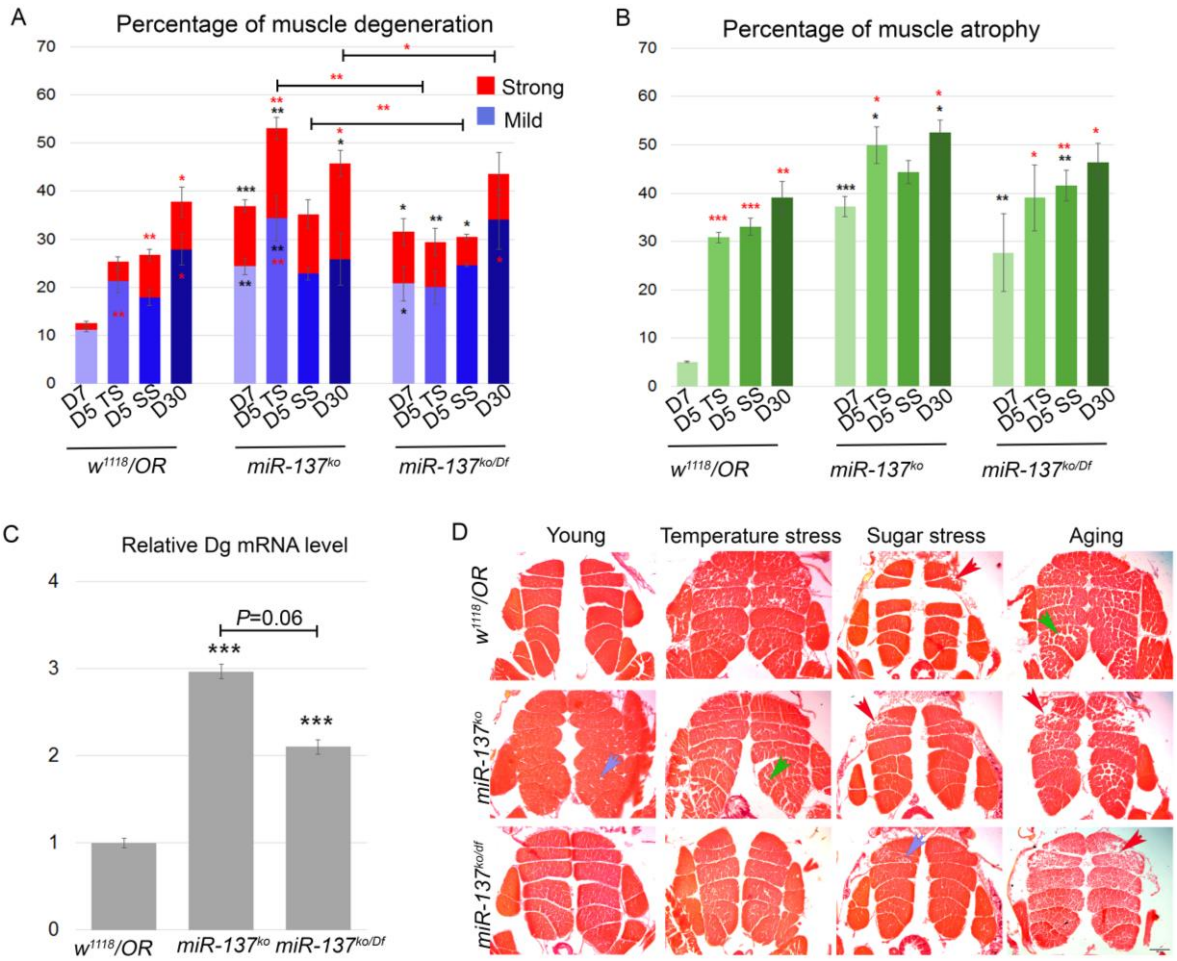

Figure 19. *Dg* is a bona fide target of *miR-137* in muscle

A bar graph showing muscle degeneration (A) muscle degeneration and (B) muscle atrophy phenotypes in *miR-137* mutants and control. *MiR-137*$^{ko/Df}$ lines can rescue muscle degeneration as well as muscle atrophy phenotypes of *miR-137*^{ko}. (C) qRT-PCR shows that the mRNA level of *Dg* is significantly increased in *miR-137*^{ko} and *miR-137*$^{ko/Df}$ lines. No significant difference is detected between the homozygous and trans-heterozygous knockout lines. (D) Representative images of IMFs of control, *miR-137*^{ko}, and *miR-137*$^{ko/Df}$ lines showing mild and strong muscle degenerations (blue and red arrows, respectively) as well as, muscle atrophy (green arrows) phenotypes in young, temperature stress, sugar starvation, and aging conditions. Values are obtained from the averages of three biological replicates. Error bars represent AVE±SEM and statistical significance was determined by two-tailed Student's t-test. *P<0.05, **P<0.01, ***P<0.001 represents comparison to control at the same condition, while *P<0.05, **P<0.01, ***P<0.001 represents comparison within the same genotype at a young age. D7= young, 7 day old, TS= temperature stress, SS= sugar starvation, and D30= aging, 30 day old. See also Supplementary Table 4.

3.7.4 *MiR-137* mutants have perturbed spermatogenesis

3.7.4.1 *MiR-137* affects early somatic cell numbers in adult fly testis

The somatic cells of testes provide essential support to the germline and have been implicated in proper spermatogenesis. Due to the expression pattern of *miR-137*, presumptively detected in early somatic cells of the adult testis (Figure 16), we investigated whether the loss of *miR-137* causes defective spermatogenesis. Adult testes of 8-12 day old flies were dissected and stained with an early somatic cell marker Traffic jam (Tj) as well as a late somatic cell marker Eyes absent (Eya). We found that control animals maintain constant early somatic cell population (56.3 ± 2.0) and a late somatic cell population (84.0 ± 1.2) per testis, whereas *miR-137* mutants have significantly more early somatic cells (82.2 ± 1.5) and nearly the same number of late somatic cells (80.4 ± 0.5) per testis (Figure 20C). Both Tj and Eya can be visualized in 4-8 cell stage spermatocysts. However, quantification of cells co-stained with both anti-Tj and anti-Eya antibodies revealed statistically insignificant population of early somatic cells (6.4 ± 0.5 compared to 11.1 ± 2.0) between the control and *miR-137* mutants, respectively. The visible differences were seen in a total somatic cell population in *miR-137* mutants (151.6 ± 0.1) compared to control (134.2 ± 2.9). The total increase in somatic cells was therefore solely due to an increase in early somatic cell numbers, while late somatic cell numbers do not change (Figure 20B-B'). Therefore, for further analysis, only early somatic cells, found at the apical region approximately 145 μm away from the hub, were counted. The increase in the early somatic cell population can be due to either an increase in proliferation or a delay in differentiation. Among somatic cells, only CySCs proliferate in wild type testes. Therefore, we stained control and mutant testes with the mitotic marker Phospho-Histone H3 (PH3). Proliferating somatic cells were found only near the hub therefore, no obvious difference in increase in proliferation in *miR-137* mutant testes was concluded (data not shown). We further stained the control and mutant testes with spectrosome and fusome marker, Adducin (Add) to mark mitotically active cells and found increase in differentiating germline, further supporting our latter hypothesis of delayed differentiation (Supplementary Figure 2).

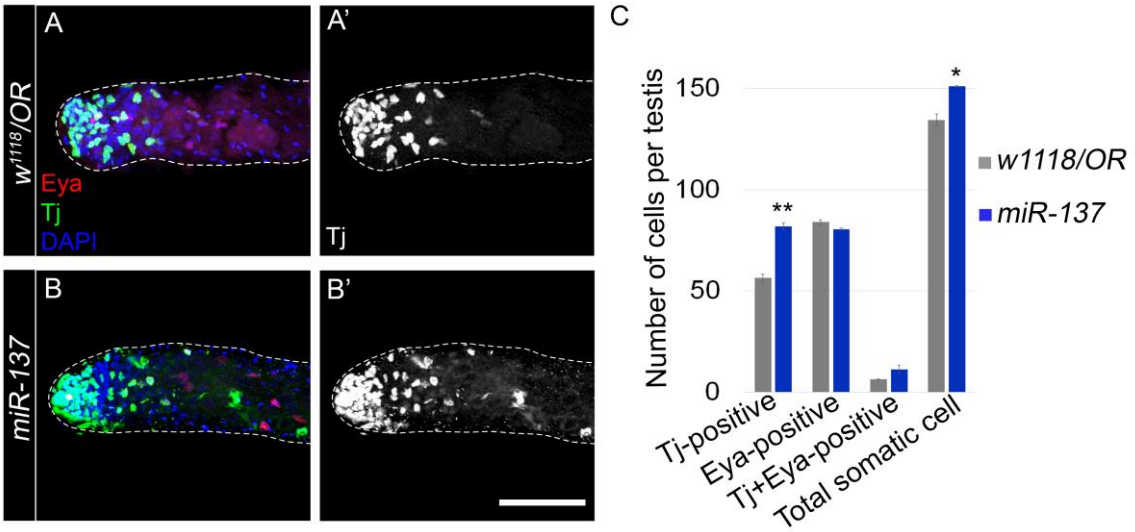

Figure 20. *MiR-137^{ko}* mutants have an increase in somatic cell population

Representative images of the apex of control testis (A) and *miR-137* testis (B) stained with early and late somatic cell markers Tj and Eya. In *miR-137* mutants, higher number of early somatic cells are visibly concentrated at the apex (B') compared to control (A'). (C) Quantification of the somatic cell population in control and *miR-137* showing an increase in an early somatic cell population in *miR-137* resulting in a total increase in somatic cell count. No significant difference was observed in somatic cell numbers co-stained with anti-Tj and anti-Eya. Values are obtained from an average of 3 biological replicates. Error bars represent AVE±SEM and statistical significance was determined by two-tailed Student's t-test. *P<0.05, **P<0.01, ***P<0.001 Scale bar 50 µm. See also Supplementary Table 7.

Studies from the *Drosophila* ovary have shown that Dg is required to maintain epithelial-cell polarity (Schneider et al., 2006) and is expressed in both germline and soma (Deng et al., 2003). In adult fly testes, Dg is also expressed in germline and soma (Figure 21). To further investigate the role of Dg in adult fly testes and to verify a *miR-137-Dg* interaction, we quantified the early somatic cell population in *miR-137^{ko}* (68.6 ± 2.9) and *miR-137$^{ko/Df}$* (36.7 ± 2.9) flies. Furthermore, downregulation of *miR-137* specifically in early somatic cells by crossing *tj-Gal4* with *UAS-miR-137^{sponge}* causes an increase in the number of early somatic cells (70.9 ± 4.5), similar to the *miR-137^{ko}* phenotype. In addition, we also compared the downregulation of *miR-137* with the over-expression of *Dg* in early somatic cells and found that upon over-expression of Dg, the early somatic counts were statistically irrelevant to controls (42.2 ± 1.5 and 52.9 ± 2.1, respectively). *tj-Gal4* lines used in this experiments were reported to be hypomorphic allele of *tj*, therefore, we suspected that the increased in early somatic cell counts in our controls (*tj/w^{1118}*) is due to the reported mutation in the region of *tj* transcription (Panchal et al., 2017). Further, we also over-expressed *miR-137* and scored

for early somatic cell numbers and found no subsequent increase (50.2 ± 0.9) compared to controls. Similar quantification was also analyzed in lines that had downregulation of *miR-137* in early somatic cells along with one copy loss of Dg in the background ($Dg^{1.10G}$::*tj>UAS-miR-137*^{sponge}) and found no increase in Tj-positive cell counts (39.1 ± 2.5) (Figure 21). From this experiment we concluded that *miR-137* regulates *Dg* to maintain early somatic cell population in fly testes, further indicating *Dg* is a relative target in testes.

We further verified the rescue of phenotype upon derepression of Dg in *miR-137*^{ko} by qRT-PCR. RNA was extracted from 25-30 pairs of fly testes and normalized to control. We found increase in *Dg* mRNA levels in *miR-137*^{ko} *testes* (4 fold increase) compared to *miR-137*$^{ko/Df}$ (1.5 fold increase) relative to control, indicating the rescue of phenotype in *miR-137*$^{ko/Df}$ was due to repression of *Dg* level. Consistent with these results, we found an increase in *Dg* mRNA level (2.5 fold) in *tj>UAS-miR-137*^{sponge} mutants. When we remove one copy of *Dg* in this genetic background, we have only 1.5 fold increase in *Dg* levels. Our data suggest that *miR-137* can efficiently regulate *Dg* level in testes. Consistent with our *in vitro* data, we propose that *miR-137* is required to regulate Dg level to maintain early somatic cell numbers.

A recent study has shown that knockdown of the soma-specific gene *chic* results in an increase in early somatic cell number and causes defective encapsulation of spermatocysts (Fairchild et al., 2015). We were further interested to know whether an increase in early somatic cell number leads to delayed differentiation that affects spermatogenesis in *miR-137* mutant testes.

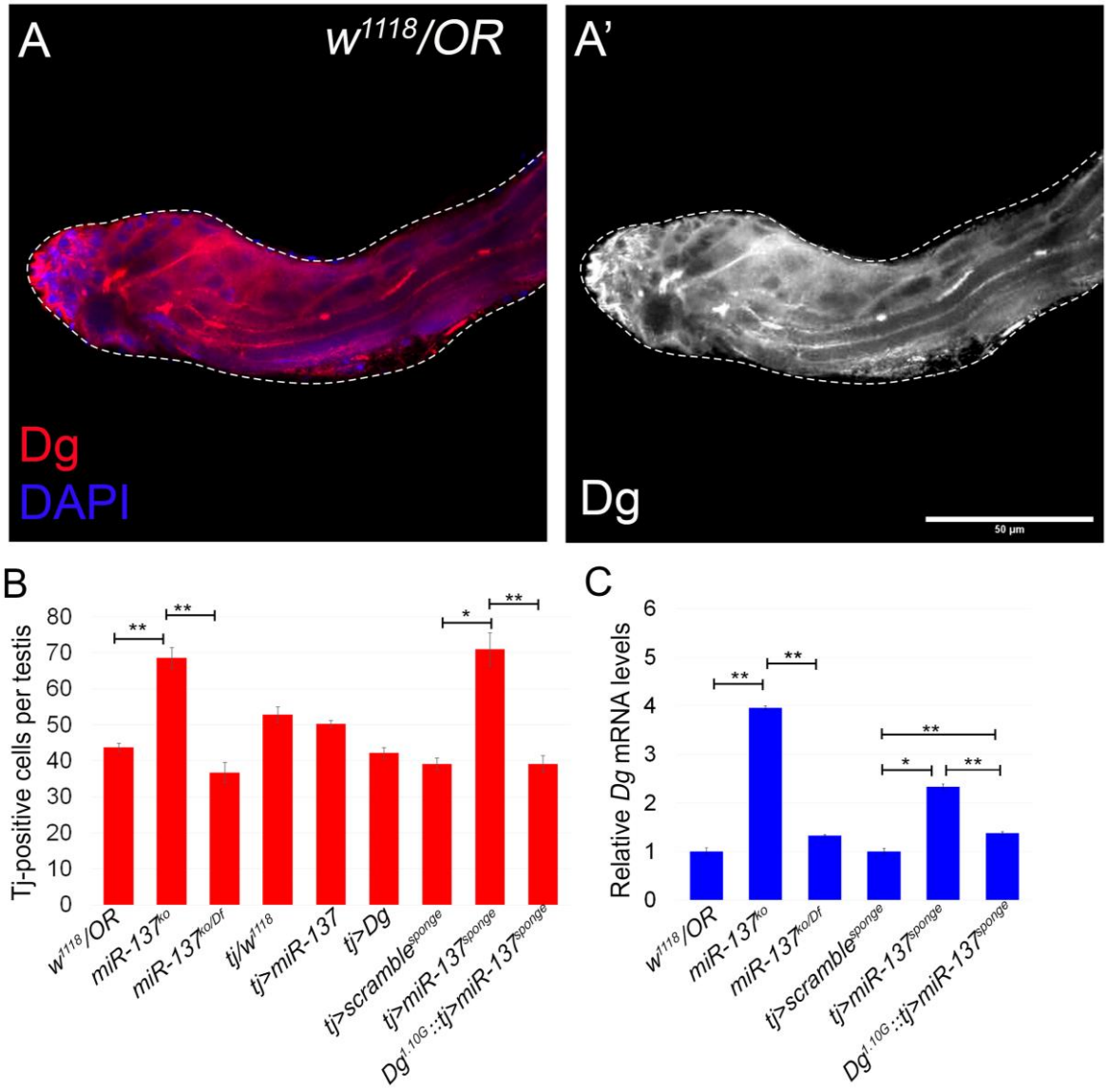

Figure 21. The early somatic cell population is maintained by downregulating Dg in *miR-137* mutants

(A) Dg staining in the apex of the control fly (w^{1118}/OR) testis showing Dg is expressed in both soma and germline. (B) Quantification of the early somatic cell population in the apex of the adult fly testis shows an increase in early somatic cell numbers in *miR-137*^{ko} which was rescued in *miR-137*$^{ko/Df}$. No significant differences in early somatic cell population is detected upon over-expression of *Dg* as well as *miR-137*. However, downregulation *miR-137* in early somatic cells phenocopied the loss of function phenotype which is further rescued when one copy loss of Dg is maintained in the background. (C) A bar graph showing *Dg* mRNA levels in testes. Almost 4 fold increase in *Dg* mRNA level in *miR-137*^{ko}, which is reduced to 1.5 fold in *miR-137*$^{ko/Df}$. Similar observations are made with 2.5 fold increase upon down regulation of *miR-137* compared to 1.5 fold increase when one copy loss of *Dg* is maintained in the background. Values are obtained from averages of 2 biological replicates. Error bars represent AVE±SEM and statistical significance was determined by two-tailed Student's t-test. *P<0.05, **P<0.01, ***P<0.001 Scale bar 50 µm. See also Supplementary Table 8.

3.7.5 *MiR-137* is essential to maintain permeability barrier

Proper gametogenesis requires continuous interaction between soma and germline. Soma encapsulates germline ensuring cell integrity, supply with nutrients and signaling cues required for proper differentiation. Isolation of germline is maintained via a permeability barrier that is formed by soma. Previous research has reported that alteration in somatic cell differentiation perturbed this barrier. Since *miR-137* mutants have a higher number of early somatic cells and possibly abnormal differentiation (Figure 20), we were interested to know whether this affects the permeability barrier during spermatogenesis. Therefore, we performed a permeability assay with 10 kDa Dextran dye. Permeability assay is a non-invasive assay that asses isolated germline from the outer environment surrounding somatic cells (Fairchild et al., 2015). After incubating the dissected testis in dye for 30 min, we found that in control testis, dye was trapped around the barrier surrounding the 8- to 16-cell cyst, while in *miR-137* mutants majority of the testes that were analyzed had dye detected inside the germline indicating defective blood-testis barrier (BTB). Almost 90% of the analyzed testes were found to have defective BTB while only 28% of defective BTB was scored in control flies (Figure 22B).

Our previous data suggests that *Dg* is a *bona fide* target of *miR-137*. To further investigate, whether *miR-137-Dg* interaction is also required to maintain BTB, we performed the permeability assay in both $miR\text{-}137^{ko/Df}$ and *Dg* mutant allele ($Dg^{1.10G}$). We found that not only $Dg^{1.10G}$ has the perturbed BTB phenotype (86% defective BTB compared to control) but this phenotype was rescued in $miR\text{-}137^{ko/Df}$ flies (38% of defective BTB similar to 30% in control). Downregulation of *miR-137* in early somatic cell causes defective BTB (70%) similar to over-expression of Dg. However, no effect was noted on BTB upon over-expression of *miR-137*. Consistent to our previous data, it further indicated that *miR-137* repressed *Dg* to maintain BTB. To further verify our rescue due to *miR-137-Dg* interaction, first, we analyzed over-expression of *miR-137* in early somatic cells with homozygous $miR\text{-}137^{ko}$ background. Second, we analyzed downregulation of *miR-137* in early somatic cells with a heterozygous $Dg^{1.10G}$ allele in the background. In both cases, we observed an intact BTB, similar to controls. This is consistent with the results of the rescue experiments that demonstrates that downregulation of Dg in males that have *miR-137* levels reduced specifically in early somatic cells, fully rescues the frequencies of the defective BTB phenotype. This further indicates, *miR-137* is required in early somatic cells to maintain the BTB; in particular, *miR-137* is required to maintain the adequate level of ECM receptor *Dg*

in early somatic cells to maintain proper formation of cellular junction, possibly septate junctions (SJs).

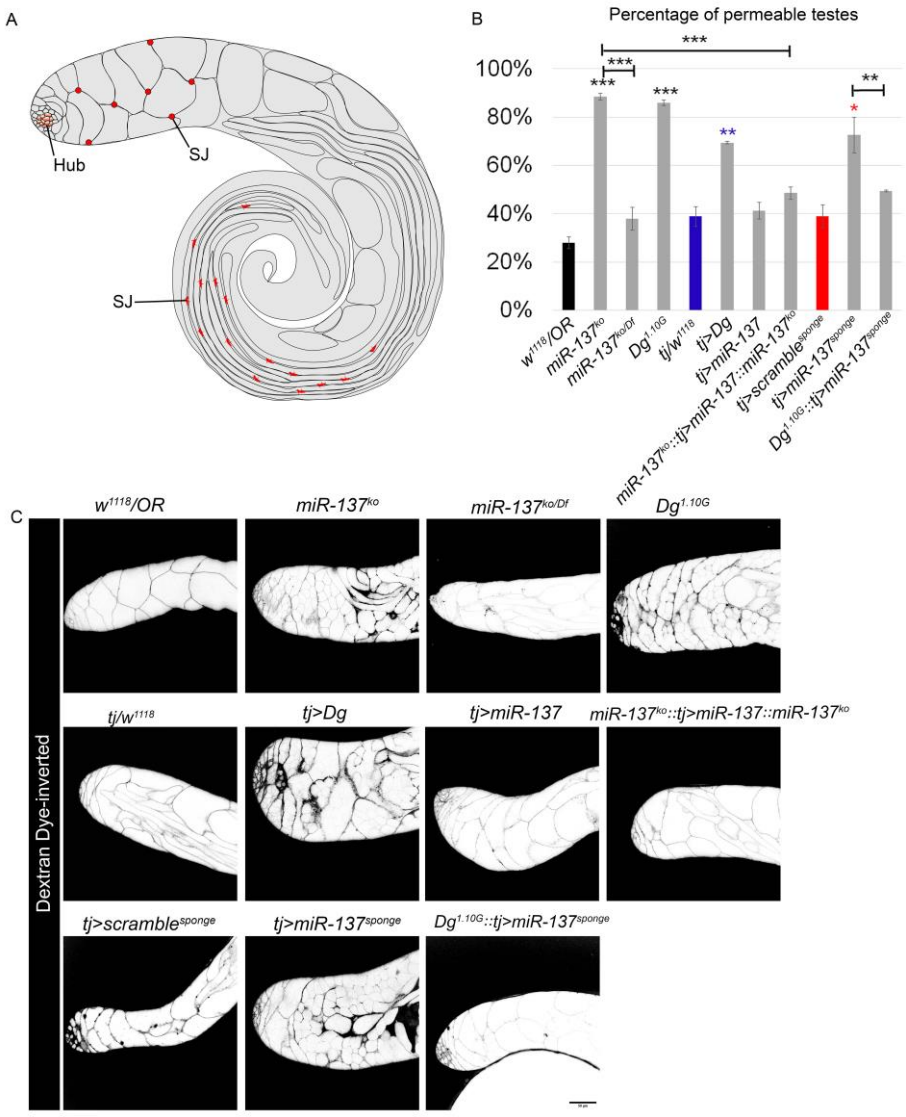

Figure 22. Permeability barrier is maintained by *miR-137*

(A) Schematic of differentiating gonialblasts encapsulated with two somatic cells forming spermatocyst in adult testes. The septate junction (SJ) are formed between two somatic cyst cells within the same cyst shown red in both early cyst cells (8- to 16-cell cyst) and in elongated spermatids. (B) Quantification of BTB phenotype in fly testes. $Dg^{1.10G}$, as well as over-expression of Dg, shows perturbed BTB. *MiR-137* loss-of-function and its downregulation in early somatic cells also have perturbed BTB which is rescued upon *miR-137* overexpression in the homozygous $miR\text{-}137^{ko}$ background, similar to $Dg^{1.10G}$:: $tj>miR\text{-}137^{sponge}$, indicating downregulation of Dg level partially rescues the BTB phenotype. (C) Representative images of permeability assays showing loss of BTB in $miR\text{-}137^{ko}$, $Dg^{1.10G}$, *tj>Dg*, and *tj>miR*-137^{sponge}. Values are obtained from averages of 3 biological replicates. Error bars represent AVE±SEM and statistical significance was determined by two-tailed Student's t-test. *P<0.05, **P<0.01, ***P<0.001 Scale bar 50 µm. See also Supplementary Table 9.

3.7.6 *MiR-137* mutants have abnormal septate junction (SJ) morphology

The major septate junction (SJ) proteins, such as Nrx-IV, Cora and Dlg have been well characterized in establishing the permeability barrier (also known as blood-brain barrier *i.e.* BBB) in invertebrate brain (Hindle and Bainton, 2014). Studies have also shown that these proteins are localized around spermatocysts and knockdown of SJ proteins also leads to perturbed permeability barrier in fly testes (Fairchild et al., 2015). To further investigate the cause of an increase in perturbed permeability barrier in early spermatocysts in *miR-137* mutants, we further stained the adult fly testis with antibodies for SJ marker: anti-Dlg and anti-Mega and analyzed their morphology. In elongated spermatids, SJ proteins maintain the bridge between the two somatic cells appearing "H" or "Z" like structure (Figure 23 A-A', pointed by yellow arrows). When this morphology is compromised, the immune staining appeared more like a "dot" or a "dashed line" (Figure 23 A-A', pointed by white arrows). In *miR-137* mutants, we found that approximately 50% of SJ had abnormal morphology compared to 20% in control. A similar case had been observed upon downregulation of *miR-137* in early somatic cells compared to the control with an average of 45% abnormal SJ compared to 15% in controls (Figure 23B). Further quantification on flies with genotypes: *tj>miR-137* and $miR137^{ko/Df}$ showed a decrease in number of abnormal SJ morphology (18% and 30%, respectively) compared to 50% of abnormal SJ in $miR137^{ko}$. Importantly, no significant change was observed in average number of SJ counted per testis in all animals (Supplementary Table 10), which suggests that the occurrence of SJ formation is normal in *miR-137* mutants, while the morphology of their SJs is abnormal. Statistical analysis was not performed on *tj>miR-137* and $miR137^{ko/Df}$ due to lack of biological replicates.

Altogether our data indicates that loss of *miR-137* can cause increase in early somatic cell numbers leading to defective SJ formation and defective BTB. Since our data also show that miR-137 is required for regulation of Dg levels in somatic cells in testis, it would be interesting to study further, if interaction between *miR-137* and *Dg* is also necessary for proper SJ morphology.

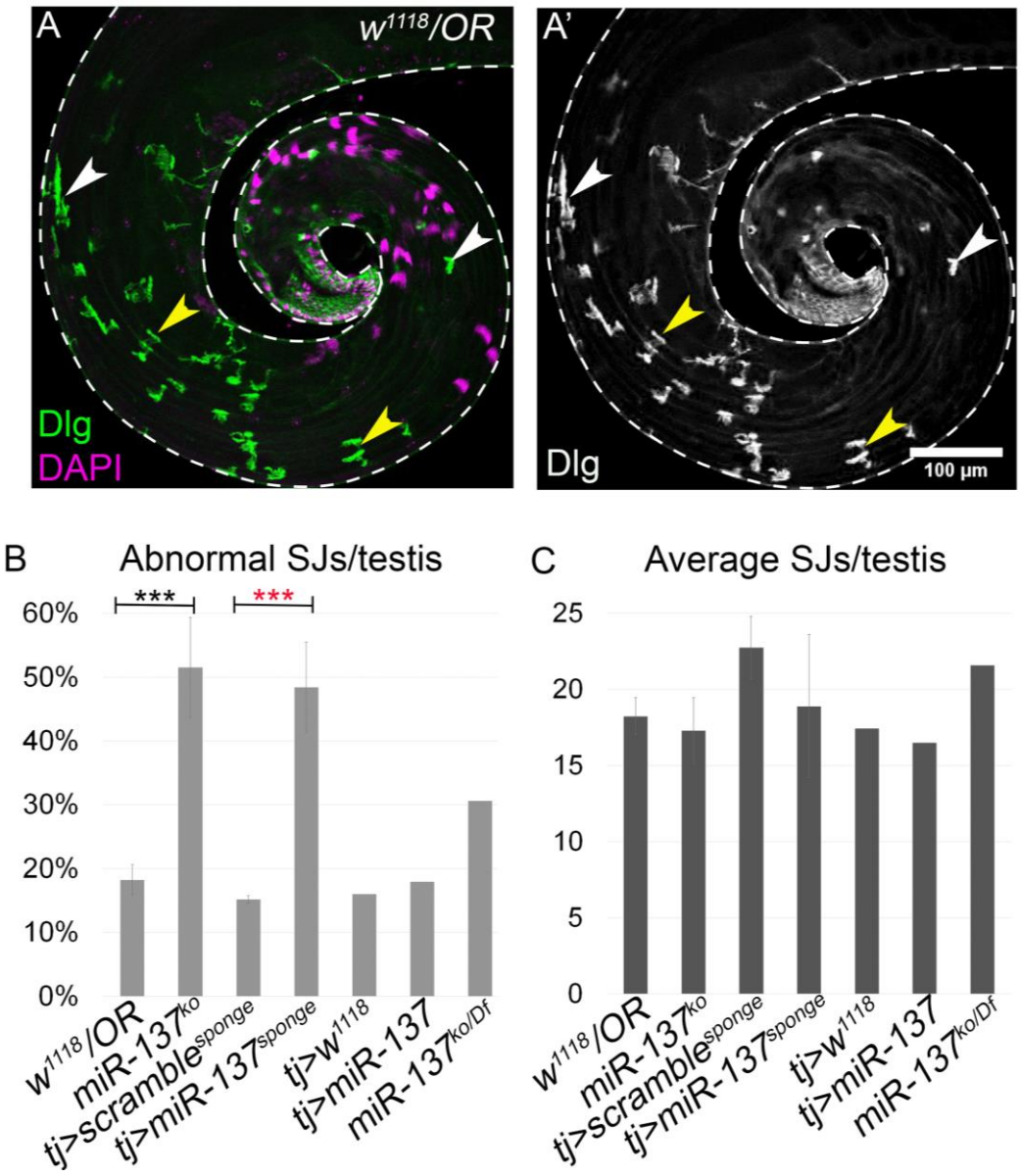

Figure 23. ***MiR-137*** **mutants have defective septate junction phenotype**

(A) Septate junction protein Dlg staining in adult control (*w1118/OR*) testis showing a normal septate junction morphology in elongated spermatids (yellow arrowheads) and abnormal septate junction morphology (white arrowheads). (B) Quantification of abnormal septate junction morphology and (C) quantification of the average number of SJ count per testis. About 50% of the septate junction in *miR-137* have abnormal morphology and no significant difference on the average numbers of SJ present in elongated spermatids per testis is found. Black star represents values obtained from averages of two biological replicates. Error bars represent AVE±SEM and statistical significance was determined by two-tailed Student's t-test. *P<0.05, **P<0.01, ***P<0.001. Red star represents statistical significance determined by χ^2test with Yate's correction (*P<0.05, **P<0.01, ***P<0.001). Scale bar 100µm. See also Supplementary Table 10.

4 Discussion

MDs are a group of diseases having diverse phenotypes related to neuronal and muscular systems in humans. MDs are genetically linked to the DGC and various animal models for the DGC have contributed significantly to understanding the variability of phenotypes in MDs, however, questions regarding the pathogenesis still remain unanswered.

The DGC involves a major transmembrane protein Dg that connects ECM to cytoskeleton accounting for the flexibility and durability of the plasma membrane providing signal transduction platform to many signaling molecules like Syn and nNOS. Hypoglycosylation of Dg is involved in various forms of dystroglycanopathies, CMD, and LGMD. In flies, studies have shown that loss of Dg cause muscle degeneration and the phenotype is enhanced upon stress (Kucherenko et al., 2011). Similarly, flies with Dg mutation are shown to have a low survival rate, delayed in development, altered metabolism, decrease mobility and age-dependent muscle degeneration (Shcherbata et al., 2007). Reduced level of metabolic rate is also linked to miRNA expression (Biggar and Storey, 2011). MiRNAs are also implicated in the stabilization of diverse biological processes and to contribute to the consequences of normal development and physiological conditions and disease in different animals systems (Ebert and Sharp, 2012). MiRNAs having the ability to target multiple genes at once can regulate a complex network of genes influencing signaling required to maintain proper cellular homeostasis. Similarly, any imbalance in cellular homeostasis caused by stress or disease state can further influence miRNAs expression. Therefore, gene expression and miRNA levels are reciprocally regulated. The expression of miRNAs profile has been shown to be altered in Duchenne muscular dystrophy. The expression of certain miRNAs (*miR-1, miR-133*, and *miR-206*) have been shown to correlate with severity of the diseases and was proposed as diagnostic markers for DMD (Cacchiarelli et al., 2011b). In flies, Dg-Dys-Syn1 signaling has been reported to regulate miRNA profile (Marrone et al., 2012). Importantly, the study also showed that a similar level of miRNA profiles was altered upon stress in wild type animals indicating stress and MD share a common regulatory pathway to overcome negative effect in animal health. This study further reports the role of miRNAs in DGC signaling and their contribution to MDs and its pathogenesis in greater detail.

4.1 MiRNAs are required for muscle maintenance

In this study, we have shown that the absence of miRNAs that are predicted to target multiple components of the DGC (Dg plus any three other components) affects muscle maintenance in flies. Dg was chosen as a baseline targeting component while grouping these miRNAs as Dg is associated with multiple pathways. Besides Dg-Dys-Syn1 pathway , it has been reported that Dg interacts with Hippo-signaling pathway component Yap to prevent cardiomyocyte proliferation (Morikawa et al., 2017). Inhibition of ubiquitinates ligase Trim32 has been shown to enhance plakoglobin binding to affect muscle atrophy (Cohen et al., 2014) and we further postulated that it can interact with Dg similar to plakoglobin to promote muscle maintenance. Therefore, miRNAs targeting the DGC importantly, Dg can influence more likely muscle maintenance phenotype associated with MDs. Further, Dg is required for correct localization of many other proteins such as Nrx-IV, Cora and GluRs mutations of which are also associated with MD-like phenotypes.

miRNAs are known to mediate stress response in animals to maintain cellular homeostasis. The expression of many of the miRNAs predicted to target the DGC components have been reported to be deregulated under hyperthermia stress in wild-type animals and/or in absence of Dg or Dys (Marrone et al., 2012). A prolong disease state can display immense stress for organismal health. Therefore, it was interesting to investigate miRNAs regulating a common pathway between stress and MD to decipher MD-related pathogenesis. This study, in particular, determines that in absence of *miR-137, miR-927,* and *miR-966* the muscle integrity in animals was severely compromised. This study further validates various stresses and aging can affect muscle degeneration even in control flies. Further, we were able to show that besides muscle degeneration, muscle atrophy is also increased in control animals during different stress conditions such as temperature stress, sugar starvation, and aging. All miRNA mutants were responsive to stress similar to control animals, indicating long term stress *i.e.* aging is more detrimental than a short term stresses such as hyperthermia stress and nutrition amelioration. Muscle atrophy was affected more than muscle degeneration in all genotypes in both stress and aging. This further highlights the importance of muscle maintenance in aging or in a prolonged disease state such as cancer that leads to cachexia. Not only miRNA loss was found to affect muscle integrity, but downregulation of Dg was also detrimental for healthy musculature. Previous studies have shown loss of Dg and Dys cause muscle degeneration and the phenotype is accelerated upon stress (Kucherenko et al., 2011). We further showed that upon downregulation of Dg specifically in adult muscle,

cause muscle degeneration and atrophy in flies. Muscle atrophy was more detrimental as the frequency of muscle atrophy was higher than the frequency of muscle degeneration compared to control indicating, a proper level of Dg is required to maintain a healthy musculature in young and aged animals. Apart from its role in muscle maintenance, number of studies have reported that precise level of Dg is required to maintain energy homeostasis, establishment of NMJ, photoreceptor differentiation, and cellular polarity (Bogdanik et al., 2008; Marrone et al., 2011a; Shcherbata et al., 2007; Yatsenko et al., 2009). In flies, *miR-9a* and *miR-310s* had been shown previously to serve as a regulatory molecule to maintain the proper level of Dg to canalize myotendinous junction formation and to buffer MD related type II lissencephaly phenotype. *miR-137, miR-927*, and *miR-966* can further play a similar role in maintaining Dg levels in muscle to protect animals from stress- or age-related muscular dysfunction.

qRT-PCR on *miR-137*and *miR-966* mutants showed upregulated mRNA levels of either, *Dys* and/or *Syn1* even though they were not the predicted to target these genes while *miR-927* mutants had either no change in mRNA levels or showed downregulation of *Dg, Dys*, and *Syn1* even though it is predicted to target all three components. There can be a number of reasons following this discrepancy: 1) many miRNAs can have a tissue or sex-specific expression; since qRT-PCR was performed on the whole body of the organism, tissue-specific miRNA expression can be easily masked when normalized to whole body of control genotype. In the future, tissue-specific qRT-PCR could resolve this issue to validate the prediction based miRNA targeting *in vivo*. 2) The DGC signaling had been shown to have compensatory effects (Cote et al., 2002; Gao and McNally, 2015; Hughes et al., 2018), the fluctuation of mRNA levels between its predicted and non predicted targets could simply be the mimic of compensatory mechanisms of the DGC components.

MiR-137 and *miR-966* mutants showed muscle degeneration as early as young age indicating, these miRNAs are required in muscle during development. The severity of muscle degeneration upon aging was more prominent for *miR-966* mutants compared to temperature stress and sugar starvation. This further indicated that *miR-966* is required to maintain healthy muscle in aging. *MiR-966* is also reported to be enriched in hemolymph in old flies (Dhahbi et al., 2016). We have also shown from lifespan analysis that *miR-966* mutants, in general, had a higher survival rate compared to control (Supplementary Figure 3). Altogether, these findings further suggest that loss of *miR-966* can be more responsive to physiological changes related to aging. Muscle atrophy was also observed in all miRNA

mutants at a young age. This further indicates that all three miRNAs are required during developmental stage to maintain muscle integrity.

Muscle degeneration phenotype can be caused by muscles as well as neuronal defects. GO component term analyzed on conserved predicted mRNA targets of all three candidate miRNAs implied that these miRNA can be involved in the cell membrane and cell periphery related processes. *MiR-137* having the most predicted targets, in addition, can be associated with neuronal processes like synapse and NMJs. GO terms for predicted miRNAs targets are in agreement with Dg functions. Luciferase reporter assay further confirmed that all three miRNAs *miR-137, miR-927*, and *miR-966* can downregulate *Dg in vitro.* Therefore, an *in vivo* screen on miRNAs gain-of-function was performed to further confirm all three selected miRNAs can downregulate Dg and/or any other muscle-specific target genes. As expected, over-expression of miRNAs gave stronger phenotypes as compared to their loss-of-function mutants. Over-expression of *miR-137* was the most severe in flies as its over-expression during developmental stage cause embryonic lethality, while over-expression in adult muscle resulted in strong muscle degeneration or complete absence of individual muscle. The experiment further confirmed that *miR-927* is required more during developing muscle as over-expression of *miR-927* with *how-Gal4* was lethal during the embryonic stage. Though the severity of phenotype can also depend on the strength of the *UAS-miR*-lines used, we observed that over-expression of *miR-966* in adult muscle resulted in more severe phenotype compared to developing muscle. Over-expression in developing muscle also affected the muscle maintenance at young age but the effect of aging was prominent in flies. This further indicates, *miR-966* can regulate age-dependent gene expression to maintain healthy muscles in animals. Many muscle-specific miRNAs (myomiRs) have been proposed as biomarkers for pathological and physiological muscle processes. myomiRs such as *miR-1, miR-133, miR-206, miR-208,* and *miR-499* have been proposed as a diagnostic marker for DMD (Cacchiarelli et al., 2011b; Jeanson-Leh et al., 2014; Li et al., 2014). This study further suggests, *miR-137, miR-927,* and *miR-966* can act as a regulatory molecule to regulate Dg level in respons to stress to maintain healthy muscle in flies.

4.2 *MiR-137* is required cell autonomously for muscle maintenance

This study further deciphers the role of newly emerged *miR-137* in MD development. *MiR-137* is highly conserved miRNA. Not only the seed sequence of *miR-137* is conserved, but the mature miRNA itself is conserved from flies to humans. It is also predicted to target *Dg* and *Scg*, the major transmembrane components of the DGC in all higher eukaryotes. We further confirmed that *Dg* is the direct target of *miR-137 in vitro*. *MiR-137* is a stress-dependent miRNAs as its expression was downregulated upon hyperthermia stress in wild-type flies (Marrone et al., 2012). *Dg* mutants are known to have preference for low temperature (18°C) (Takeuchi et al., 2009), and in microarray screen, *miR-137* level remain unchanged in dystrophic flies at hyperthermia stress suggesting; 1) temperature fluctuation alone can cause a decreased level of *miR-137* in wild type flies and this downregulation relies on the DGC and 2) *Dg* mutants already have deregulated *miR-137* and temperature stress doesn't affect its level on the DGC mutants. Compared to all the candidate miRNA mutants in our screen, the severity of phenotypes was observed higher in *miR-137* mutants at young and stress conditions, indicating it is required during developmental stage as well as for normal stress response. This was further confirmed by phenotypes observed upon downregulation of *miR-137* during developing and adult muscle. Regardless of the activity of the drivers used (*Mhc-Gal4* and *how-Gal4*), muscle maintenance was severely compromised. Though the severity of phenotypes was observed stronger upon its downregulation in adult muscle compared to developing muscle, it was also noted that upon stress, the phenotypes were accelerated by more than two-fold when compared to young animals. This further confirmed, in adult muscle, *miR-137* is required to address the negative effect of stress. The over-expression of *miR-137* caused stronger phenotype leading to lethality and complete absence of muscle. Therefore, the study also confirms that *miR-137* levels must be maintained to have proper muscle function. Besides muscle maintenance phenotype, *miR-137* mutant flies have climbing defects and increased variance in zygotic PGCs (Chen et al., 2014). In addition, they have a low survival rate (Supplementary Figure 2) and are developmentally delayed (data not shown). *miR-137* is enriched in adult brain in mammals (He and Hannon, 2004) and is studied extensively in many retrospect involving schizophrenia, intellectual disability, neurodegeneration disorders such as Parkinson's Disease, synaptic development and dendritic arborization, and cancer profiling (Kong et al., 2015; Langevin et al., 2011; Ma et al., 2018; Munker and Calin, 2011; Olde Loohuis et al.,

2012; Silber et al., 2008; Smrt et al., 2010; Verma et al., 2015; Willemsen et al., 2011). In *Drosophila*, we were able to show its expression in neuronal and muscle tissues as well as in early somatic cell of adult fly testes. The previous study has also detected its expression in the adult fly thorax (Fulga et al., 2015). It will be interesting to further investigate the neuronal involvement of *miR-137* to further explore its function in MDs or in other neurological disorders.

4.3 *MiR-137* is required to maintain a precise level of Dg in adult muscle

We have shown that the level of Dg in adult muscle affects muscle integrity in age-dependent manner. To investigate if this effect can be ameliorated by over-expression of Dg in adult muscle, over-expression of Dg in adult muscle was analyzed at young, aged, and stressed animals. Surprisingly, it was found that not only its downregulation affects muscle maintenance, its over-expression also had a negative effect on normal muscle function. Muscle degeneration was seen in flies already at a young age, while muscle atrophy was not affected. This further indicated that over-expression of Dg is protective for flies to reduce atrophy upon aging. However, during temperature stress and sugar starvation, flies had more incidence of muscle degeneration and atrophy compared to control flies, indicating flies with over-expression of Dg can respond differently to different stress conditions. This study further implied that a proper level of Dg is required to maintain healthy adult muscle; therefore, it is interesting to investigate further how levels of Dg can affect muscle integrity in general.

To further investigate whether *miR-137* can regulate Dg level in muscle, *miR-137* mutants with one copy loss of *Dg* in the background were further analyzed. If *Dg* is a direct target in muscle, the level of Dg in $miR\text{-}137^{ko/Df}$ should be normalized to endogenous level, hence, the severity of phenotype should be reduced in $miR\text{-}137^{ko/Df}$ lines compared to $miR\text{-}137^{ko}$ lines. Analysis of IMFs of flies showed that in general, $miR\text{-}137^{ko/Df}$ flies had stronger phenotype compared to control, however, this was reduced almost by two times when compared to $miR\text{-}137^{ko}$. Our data suggests that *miR-137* regulates Dg levels and affects adult muscle maintenance. The difference in severity of phenotype was not visible in flies at a young age further suggesting a precise level of Dg is more important to overcome muscle loss upon stress. qRT-PCR performed on adult fly thoraces further confirmed relatively low *Dg* mRNA levels on $miR\text{-}137^{ko/Df}$ lines compared to $miR\text{-}137^{ko}$. Therefore, only partial rescue of muscle

maintenance phenotype was observed during various stresses upon one copy loss of *Dg* in *miR-137* mutants. At normal condition, over-expression, as well as loss of Dg, posed a negative effect on muscles. A similar case was observed upon *miR-137* over-expression and loss-of-function. The down-regulation of *miR-137* was not as severe as over-expression of Dg and over-expression of *miR-137* was more severe than phenotypes reported for Dg loss-of-function at ambient condition. Taken together, we propose that *miR-137* can target more muscle-specific genes other than *Dg* and influence MD development. Based on the prediction tool and qRT-PCR on miRNA mutants showed that *miR-137* can further target Dys, Scg, NOS, Nrx-IV, and Mei-P26 as DGC components. It will be interesting to investigate in future how *miR-137* can affect the expression of the DGC components to contribute to MD development.

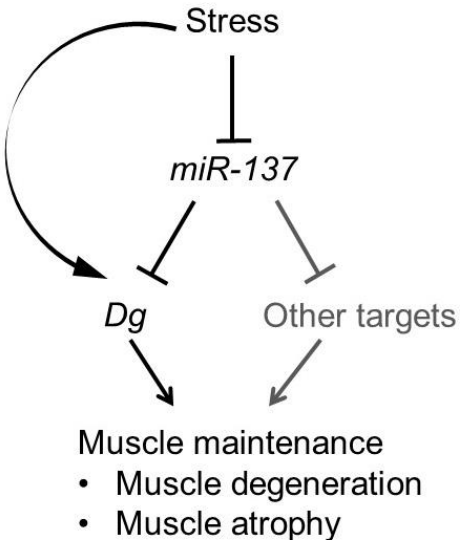

Figure 24. Mode of action of *miR-137* in muscle

During stress, *miR-137* is downregulated upon which its target mRNAs in muscle, including *Dg,* are upregulated. This affects muscle maintenance such as muscle degeneration and muscle atrophy. Stress itself induces Dg expression that can further affect muscle maintenance.

4.4 *MiR-137* is required in somatic cells to maintain permeability barrier

This project further identifies the role of *miR-137* in *Drosophila* spermatogenesis. The *in situ* hybridization in wild type testis suggested that *miR-137* is possibly expressed in early somatic cells. Analysis of *miR-137* mutant testes further showed an abnormal number of early somatic cell population at the apex of the testis (stained with anti-Tj) compared to control flies. We also observed similar phenotype upon *miR-137* knock-down in early somatic cells. Our analysis showed that in male gametogenesis, *miR-137* is required specifically in somatic cells. This was further supported by the total rescue of abnormal early somatic cell counts upon over-expression of *miR-137* in early somatic cells. The latter experiment also suggests that the endogenous level of *miR-137* can efficiently downregulate its target gene specifically in soma. The expansion of Tj-positive cells can be either due to an increase in proliferation or delayed in differentiation. However, we did not observe an abnormal number of CySCs stained with anti-PH3 (mitotic cell marker) in control and mutant testes. Further staining with anti-Add (spectrosome and fusome marker) showed an increase in differentiating germline cells in mutant testes supporting our latter hypothesis of delayed differentiation in *miR-137* mutants. Though both the possibilities are not conclusive from our experiments, further staining with Edu together with anti-Zfh1 (a marker for CySCs and its early daughter cells) or staining with cell cycle marker like anti-Cyclin can further shed lights to the pinpoint increase in somatic proliferation or differentiation process.

We have shown from our data from fly muscle that *Dg* is a relative target of *miR-137*. We have further shown that Dg is also expressed in germline and soma in fly testis. To further investigate whether the interaction between *miR-137-Dg* is also required to establish cellular homeostasis during male gametogenesis, we analyzed the effect on early somatic cell numbers on $miR\text{-}137^{ko/Df}$ lines first. We did not find abnormal early somatic cell numbers in $miR\text{-}137^{ko/Df}$ testes. The reduced level of Dg in $miR\text{-}137^{ko}$ lines fully rescued the abnormal somatic cell number phenotype. A similar observation was made on genetic rescue achieved by downregulating *miR-137* with one copy loss of Dg in the background ($Dg^{1.10G}$::*tj*>$miR\text{-}137^{sponge}$). A significant difference in early somatic cells population as observed in genetic rescue compared to down-regulation of *miR-137* further supports the idea that *miR-137* is required in early somatic cells in adult fly testis and regulates the Dg level in order to maintain proper spermatogenesis. Therefore, in testis, Dg is the relative target of *miR-137*.

4.5 Dg levels must be regulated to maintain the permeability barrier

In male gametogenesis, somatic cells are required to encapsulate differentiating germlines and maintain a barrier around them. Each spermatocyst (germline enveloped with two somatic cells) is connected with neighboring spermatocysts by their outer somatic membrane maintaining a closed barrier between inner-membrane of the somatic cell and the germline. This barrier is also known as the permeability or blood-testis barrier (BTB). Genes required in somatic cells in *Drosophila* testis have been shown to have an important function in spermatogenesis (Fairchild et al., 2017). Knockdown of the soma-specific gene (*chic*) has been shown to regulate cell proliferation and affect the permeability barrier (Fairchild et al., 2015). Consistent with this study, we also found that *miR-137* mutants have perturbed BTB and this phenotype was rescued upon one copy loss of *Dg* in *miR-137* mutants. Our data further verified the increase in early somatic cells can cause perturbed BTB. Interestingly, both loss and over-expression of Dg caused perturbed BTB. Knock-down of *miR-137* in early somatic cell recapitulated the BTB phenotype of Dg over-expression in early somatic cells and this phenotype was rescued upon downregulation of *miR-137* with one copy loss of Dg in the background as well as with over-expression of *miR-137* in homozygous *miR-137^{ko}* background (*miR-137^{ko}*::*tj*>*miR-137*::*miR-137^{ko}*). Taken together, these results show that *miR-137* is required to regulate Dg level in soma to maintain permeability barrier. This study further claims the scope of perturbed BTB as a MD related phenotype and miRNAs are required to regulate the level of the DGC components in *Drosophila* spermatogenesis.

4.6 *MiR-137* acts in soma to regulate Dg in septate junctions

Studies have shown that the permeability barrier is dependent on the function of septate junction proteins. Septate junction (SJ) proteins like Cora and Nrx-IV have been shown to be concentrated at the sites of contact between two somatic cells that encapsulates the germline (Fairchild et al., 2015). The study also reported that knock-down of these components cause the BTB phenotype. Recent progression made on understanding *Drosophila* spermatogenesis also showed that loss of Dg cause mislocalization of SJ proteins Cora and Nrx-IV resulting in perturbed BTB (unpublished data). The study also showed that downregulation of Dg in soma, as well as germline, caused perturbed BTB, indicating Dg is required in both soma and germlines to maintain BTB. Our study further showed that over-expression of Dg in somatic cells and its loss caused perturbed BTB. And this phenotype

was recovered upon reducing the level of *Dg* in *miR-137*^{ko} flies. The observed phenotype of perturbed BTB was rescued not only in *miR-137*$^{ko/Df}$ lines but also in *miR-137*^{ko}::*tj>miR-137*::*miR-137*^{ko} and *Dg*$^{1.10G}$::*tj>miR-137*^{sponge} lines that have reduced the level of *Dg* compared to *miR-137*^{ko}. Our qRT-PCR data further showed that *Dg* mRNA levels in these genetic backgrounds varied vastly. Complete loss of *miR-137* and its downregulation on early somatic cells caused an increase in *Dg* mRNA levels which was reduced by two-fold in *miR-137*$^{ko/Df}$ and one copy loss of *Dg* in *tj>miR-137*^{sponge}. This further concluded that *miR-137* regulates *Dg* level in soma and maintains the BTB.

Many SJ related proteins and genes that are required in soma are predicted targets of *miR-137*. Such protein includes Nrx-IV, Dlg, and Chic. It will be further interesting to study how *miR-137* influence the expression and their possible interaction with *Dg* to maintain spermatogenesis in Drosophila testis.

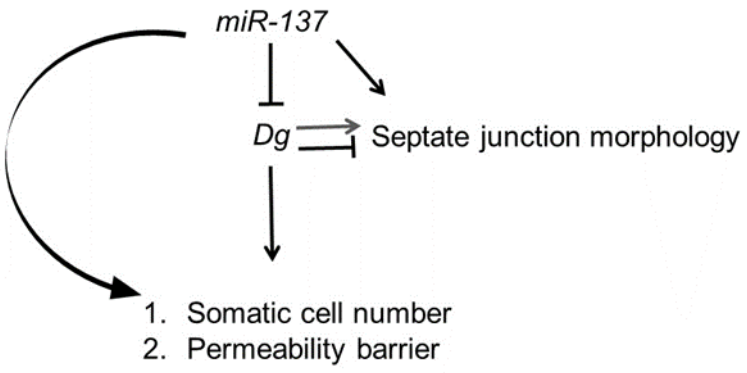

Figure 25. Mode of action of *miR-137* in testis

Loss of *miR-137* caused upregulation of *Dg* that increases somatic cell population and affect BTB. *miR-137* also affects septate junction morphology and it has been shown that upon Dg loss core components of septate junction protein are mislocalized. The possible interaction of *miR-137* and *Dg* to maintain septate junction morphology is yet to be defined (grey arrow).

5 Conclusions

During this study, we identified a set of miRNAs that regulate muscle maintenance upon various stresses. Furthermore, our study demonstrates a novel role for miRNAs *miR-137, miR-927* and *miR-966* in regulation of major DGC components including Dg. We propose that these miRNA can be involved in fine-tuning of DGC signaling and MD development.

In this study, a highly conserved *miR-137* was found to target *Dg 3'UTR* and regulate its levels specifically in muscles and in testicular soma. Deregulation of *miR-137* and Dg expression lead to stress dependent muscle degeneration and atrophy. Therefore, we propose that *miR-137* potentially can be used as a biomarker and a candidate for MD therapeutics.

Moreover, we found that *miR-137* is required for proper blood-testis barrier (BTB) establishment which also requires proper levels of the ECM receptor Dg. Since, MDs in general, have multiple phenotypic characteristics in patients which show abnormalities not only in muscle but other systems, this study further implies that perturbed spermatogenesis could be a novel MD-related phenotype.

6 References

Adams, M.E., Odom, G.L., Kim, M.J., Chamberlain, J.S., and Froehner, S.C. (2018). Syntrophin binds directly to multiple spectrin-like repeats in dystrophin and mediates binding of nNOS to repeats 16-17. Human molecular genetics *27*, 2978-2985.

Ameres, S.L., Horwich, M.D., Hung, J.H., Xu, J., Ghildiyal, M., Weng, Z., and Zamore, P.D. (2010). Target RNA-directed trimming and tailing of small silencing RNAs. Science (New York, NY) *328*, 1534-1539.

Astrea, G., Romano, A., Angelini, C., Antozzi, C.G., Barresi, R., Battini, R., Battisti, C., Bertini, E., Bruno, C., Cassandrini, D.*, et al.* (2018). Broad phenotypic spectrum and genotype-phenotype correlations in GMPPB-related dystroglycanopathies: an Italian cross-sectional study. Orphanet journal of rare diseases *13*, 170.

Baccarini, A., Chauhan, H., Gardner, T.J., Jayaprakash, A.D., Sachidanandam, R., and Brown, B.D. (2011). Kinetic analysis reveals the fate of a microRNA following target regulation in mammalian cells. Current biology : CB *21*, 369-376.

Baek, D., Villen, J., Shin, C., Camargo, F.D., Gygi, S.P., and Bartel, D.P. (2008). The impact of microRNAs on protein output. Nature *455*, 64-71.

Balci, B., Uyanik, G., Dincer, P., Gross, C., Willer, T., Talim, B., Haliloglu, G., Kale, G., Hehr, U., Winkler, J.*, et al.* (2005). An autosomal recessive limb girdle muscular dystrophy (LGMD2) with mild mental retardation is allelic to Walker-Warburg syndrome (WWS) caused by a mutation in the POMT1 gene. Neuromuscular disorders : NMD *15*, 271-275.

Barman, B., and Bhattacharyya, S.N. (2015). mRNA Targeting to Endoplasmic Reticulum Precedes Ago Protein Interaction and MicroRNA (miRNA)-mediated Translation Repression in Mammalian Cells. The Journal of biological chemistry *290*, 24650-24656.

Bartel, D.P. (2004). MicroRNAs: genomics, biogenesis, mechanism, and function. Cell *116*, 281-297.

Bashir, R., Britton, S., Strachan, T., Keers, S., Vafiadaki, E., Lako, M., Richard, I., Marchand, S., Bourg, N., Argov, Z.*, et al.* (1998). A gene related to Caenorhabditis elegans spermatogenesis factor fer-1 is mutated in limb-girdle muscular dystrophy type 2B. Nature genetics *20*, 37-42.

Bazzini, A.A., Lee, M.T., and Giraldez, A.J. (2012). Ribosome profiling shows that miR-430 reduces translation before causing mRNA decay in zebrafish. Science (New York, NY) *336*, 233-237.

Behm-Ansmant, I., Rehwinkel, J., Doerks, T., Stark, A., Bork, P., and Izaurralde, E. (2006). mRNA degradation by miRNAs and GW182 requires both CCR4:NOT deadenylase and DCP1:DCP2 decapping complexes. Genes & development *20*, 1885-1898.

Bhat, H.F., Adams, M.E., and Khanday, F.A. (2013). Syntrophin proteins as Santa Claus: role(s) in cell signal transduction. Cellular and molecular life sciences : CMLS *70*, 2533-2554.

Biggar, K.K., and Storey, K.B. (2011). The emerging roles of microRNAs in the molecular responses of metabolic rate depression. Journal of molecular cell biology *3*, 167-175.

Bogdanik, L., Framery, B., Frolich, A., Franco, B., Mornet, D., Bockaert, J., Sigrist, S.J., Grau, Y., and Parmentier, M.L. (2008). Muscle dystroglycan organizes the postsynapse and regulates presynaptic neurotransmitter release at the Drosophila neuromuscular junction. PloS one *3*, e2084.

Bonnemann, C.G., Wang, C.H., Quijano-Roy, S., Deconinck, N., Bertini, E., Ferreiro, A., Muntoni, F., Sewry, C., Beroud, C., Mathews, K.D.*, et al.* (2014). Diagnostic approach to the congenital muscular dystrophies. Neuromuscular disorders : NMD *24*, 289-311.

Bose, M., Barman, B., Goswami, A., and Bhattacharyya, S.N. (2017). Spatiotemporal Uncoupling of MicroRNA-Mediated Translational Repression and Target RNA Degradation Controls MicroRNP Recycling in Mammalian Cells. Molecular and cellular biology *37*.

Boyle, E.I., Weng, S., Gollub, J., Jin, H., Botstein, D., Cherry, J.M., and Sherlock, G. (2004). GO::TermFinder--open source software for accessing Gene Ontology information and finding significantly enriched Gene Ontology terms associated with a list of genes. Bioinformatics (Oxford, England) *20*, 3710-3715.

Brand, A.H., and Perrimon, N. (1993). Targeted gene expression as a means of altering cell fates and generating dominant phenotypes. Development (Cambridge, England) *118*, 401-415.

Brennecke, J., Stark, A., Russell, R.B., and Cohen, S.M. (2005). Principles of microRNA-target recognition. PLoS biology *3*, e85.

Broughton, J.P., Lovci, M.T., Huang, J.L., Yeo, G.W., and Pasquinelli, A.E. (2016). Pairing beyond the Seed Supports MicroRNA Targeting Specificity. Molecular cell *64*, 320-333.

Brown, S.C., and Winder, S.J. (2017). 220th ENMC workshop: Dystroglycan and the dystroglycanopathies Naarden, The Netherlands, 27-29 May 2016. Neuromuscular disorders : NMD *27*, 387-395.

Bryantsev, A.L., Duong, S., Brunetti, T.M., Chechenova, M.B., Lovato, T.L., Nelson, C., Shaw, E., Uhl, J.D., Gebelein, B., and Cripps, R.M. (2012). Extradenticle and homothorax control adult muscle fiber identity in Drosophila. Developmental cell *23*, 664-673.

Bushati, N., and Cohen, S.M. (2007). microRNA functions. Annual review of cell and developmental biology *23*, 175-205.

Cacchiarelli, D., Incitti, T., Martone, J., Cesana, M., Cazzella, V., Santini, T., Sthandier, O., and Bozzoni, I. (2011a). miR-31 modulates dystrophin expression: new implications for Duchenne muscular dystrophy therapy. EMBO reports *12*, 136-141.

Cacchiarelli, D., Legnini, I., Martone, J., Cazzella, V., D'Amico, A., Bertini, E., and Bozzoni, I. (2011b). miRNAs as serum biomarkers for Duchenne muscular dystrophy. EMBO molecular medicine *3*, 258-265.

Cacchiarelli, D., Martone, J., Girardi, E., Cesana, M., Incitti, T., Morlando, M., Nicoletti, C., Santini, T., Sthandier, O., Barberi, L.*, et al.* (2010). MicroRNAs involved in molecular circuitries relevant for the Duchenne muscular dystrophy pathogenesis are controlled by the dystrophin/nNOS pathway. Cell metabolism *12*, 341-351.

Chaturvedi, D., Reichert, H., Gunage, R.D., and VijayRaghavan, K. (2017). Identification and functional characterization of muscle satellite cells in Drosophila. eLife *6*.

Chen, J.F., Mandel, E.M., Thomson, J.M., Wu, Q., Callis, T.E., Hammond, S.M., Conlon, F.L., and Wang, D.Z. (2006). The role of microRNA-1 and microRNA-133 in skeletal muscle proliferation and differentiation. Nature genetics *38*, 228-233.

Chen, K., and Rajewsky, N. (2007). The evolution of gene regulation by transcription factors and microRNAs. Nature reviews Genetics *8*, 93-103.

Chen, Y.W., Song, S., Weng, R., Verma, P., Kugler, J.M., Buescher, M., Rouam, S., and Cohen, S.M. (2014). Systematic study of Drosophila microRNA functions using a collection of targeted knockout mutations. Developmental cell *31*, 784-800.

Cheng, C.Y., and Mruk, D.D. (2012). The blood-testis barrier and its implications for male contraception. Pharmacological reviews *64*, 16-64.

Choi, W.Y., Giraldez, A.J., and Schier, A.F. (2007). Target protectors reveal dampening and balancing of Nodal agonist and antagonist by miR-430. Science (New York, NY) *318*, 271-274.

Cicek, I.O., Karaca, S., Brankatschk, M., Eaton, S., Urlaub, H., and Shcherbata, H.R. (2016). Hedgehog Signaling Strength Is Orchestrated by the mir-310 Cluster of MicroRNAs in Response to Diet. Genetics *202*, 1167-1183.

Cohen, S., Lee, D., Zhai, B., Gygi, S.P., and Goldberg, A.L. (2014). Trim32 reduces PI3K-Akt-FoxO signaling in muscle atrophy by promoting plakoglobin-PI3K dissociation. The Journal of cell biology *204*, 747-758.

Cohen, S.M. (2009). Use of microRNA sponges to explore tissue-specific microRNA functions in vivo. Nature methods *6*, 873-874.

Cohn, R.D. (2005). Dystroglycan: important player in skeletal muscle and beyond. Neuromuscular disorders : NMD *15*, 207-217.

Cooley, L., Kelley, R., and Spradling, A. (1988). Insertional mutagenesis of the Drosophila genome with single P elements. Science (New York, NY) *239*, 1121-1128.

Cote, P.D., Moukhles, H., and Carbonetto, S. (2002). Dystroglycan is not required for localization of dystrophin, syntrophin, and neuronal nitric-oxide synthase at the sarcolemma but regulates integrin alpha 7B expression and caveolin-3 distribution. The Journal of biological chemistry *277*, 4672-4679.

De Arcangelis, V., Serra, F., Cogoni, C., Vivarelli, E., Monaco, L., and Naro, F. (2010). beta1-syntrophin modulation by miR-222 in mdx mice. PloS one *5*.

de Pontual, L., Yao, E., Callier, P., Faivre, L., Drouin, V., Cariou, S., Van Haeringen, A., Genevieve, D., Goldenberg, A., Oufadem, M.*, et al.* (2011). Germline deletion of the miR-17 approximately 92 cluster causes skeletal and growth defects in humans. Nature genetics *43*, 1026-1030.

Demarco, R.S., Eikenes, A.H., Haglund, K., and Jones, D.L. (2014). Investigating spermatogenesis in Drosophila melanogaster. Methods (San Diego, Calif) *68*, 218-227.

Demontis, F., Piccirillo, R., Goldberg, A.L., and Perrimon, N. (2013). Mechanisms of skeletal muscle aging: insights from Drosophila and mammalian models. Disease models & mechanisms *6*, 1339-1352.

Deng, W.M., Schneider, M., Frock, R., Castillejo-Lopez, C., Gaman, E.A., Baumgartner, S., and Ruohola-Baker, H. (2003). Dystroglycan is required for polarizing the epithelial cells and the oocyte in Drosophila. Development (Cambridge, England) *130*, 173-184.

Denli, A.M., Tops, B.B., Plasterk, R.H., Ketting, R.F., and Hannon, G.J. (2004). Processing of primary microRNAs by the Microprocessor complex. Nature *432*, 231-235.

Dhahbi, J.M. (2014). Circulating small noncoding RNAs as biomarkers of aging. Ageing research reviews *17*, 86-98.

Dhahbi, J.M., Atamna, H., Li, R., Yamakawa, A., Guerrero, N., Lam, H.T., Mote, P., and Spindler, S.R. (2016). MicroRNAs Circulate in the Hemolymph of Drosophila and Accumulate Relative to Tissue microRNAs in an Age-Dependent Manner. Genomics insights *9*, 29-39.

Djuranovic, S., Nahvi, A., and Green, R. (2012). miRNA-mediated gene silencing by translational repression followed by mRNA deadenylation and decay. Science (New York, NY) *336*, 237-240.

Doench, J.G., and Sharp, P.A. (2004). Specificity of microRNA target selection in translational repression. Genes & development *18*, 504-511.

Durbeej, M., and Campbell, K.P. (2002). Muscular dystrophies involving the dystrophin-glycoprotein complex: an overview of current mouse models. Current opinion in genetics & development *12*, 349-361.

Dutta, D., Anant, S., Ruiz-Gomez, M., Bate, M., and VijayRaghavan, K. (2004). Founder myoblasts and fibre number during adult myogenesis in Drosophila. Development (Cambridge, England) *131*, 3761-3772.

Ebert, M.S., and Sharp, P.A. (2012). Roles for microRNAs in conferring robustness to biological processes. Cell *149*, 515-524.

Edeleva, E.V., and Shcherbata, H.R. (2013). Stress-induced ECM alteration modulates cellular microRNAs that feedback to readjust the extracellular environment and cell behavior. Frontiers in genetics *4*, 305.

Eisenberg, I., Eran, A., Nishino, I., Moggio, M., Lamperti, C., Amato, A.A., Lidov, H.G., Kang, P.B., North, K.N., Mitrani-Rosenbaum, S., *et al.* (2007). Distinctive patterns of microRNA expression in primary muscular disorders. Proceedings of the National Academy of Sciences of the United States of America *104*, 17016-17021.

Enright, A.J., John, B., Gaul, U., Tuschl, T., Sander, C., and Marks, D.S. (2003). MicroRNA targets in Drosophila. Genome biology *5*, R1.

Ervasti, J.M., and Campbell, K.P. (1993). Dystrophin-associated glycoproteins: their possible roles in the pathogenesis of Duchenne muscular dystrophy. Molecular and cell biology of human diseases series *3*, 139-166.

Fairchild, M.J., Islam, F., and Tanentzapf, G. (2017). Identification of genetic networks that act in the somatic cells of the testis to mediate the developmental program of spermatogenesis. PLoS genetics *13*, e1007026.

Fairchild, M.J., Smendziuk, C.M., and Tanentzapf, G. (2015). A somatic permeability barrier around the germline is essential for Drosophila spermatogenesis. Development (Cambridge, England) *142*, 268-281.

Franca, L.R., Auharek, S.A., Hess, R.A., Dufour, J.M., and Hinton, B.T. (2012). Blood-tissue barriers: morphofunctional and immunological aspects of the blood-testis and blood-epididymal barriers. Advances in experimental medicine and biology *763*, 237-259.

Frosk, P., Weiler, T., Nylen, E., Sudha, T., Greenberg, C.R., Morgan, K., Fujiwara, T.M., and Wrogemann, K. (2002). Limb-girdle muscular dystrophy type 2H associated with mutation in TRIM32, a putative E3-ubiquitin-ligase gene. American journal of human genetics *70*, 663-672.

Fulga, T.A., McNeill, E.M., Binari, R., Yelick, J., Blanche, A., Booker, M., Steinkraus, B.R., Schnall-Levin, M., Zhao, Y., DeLuca, T., *et al.* (2015). A transgenic resource for conditional competitive inhibition of conserved Drosophila microRNAs. Nature communications *6*, 7279.

Gao, Q.Q., and McNally, E.M. (2015). The Dystrophin Complex: Structure, Function, and Implications for Therapy. Comprehensive Physiology *5*, 1223-1239.

Gibbings, D.J., Ciaudo, C., Erhardt, M., and Voinnet, O. (2009). Multivesicular bodies associate with components of miRNA effector complexes and modulate miRNA activity. Nature cell biology *11*, 1143-1149.

Grady, R.M., Zhou, H., Cunningham, J.M., Henry, M.D., Campbell, K.P., and Sanes, J.R. (2000). Maturation and maintenance of the neuromuscular synapse: genetic evidence for roles of the dystrophin--glycoprotein complex. Neuron *25*, 279-293.

Greco, S., De Simone, M., Colussi, C., Zaccagnini, G., Fasanaro, P., Pescatori, M., Cardani, R., Perbellini, R., Isaia, E., Sale, P., *et al.* (2009). Common micro-RNA signature in skeletal muscle damage and regeneration induced by Duchenne muscular dystrophy and acute ischemia. FASEB journal : official publication of the Federation of American Societies for Experimental Biology *23*, 3335-3346.

Greener, M.J., and Roberts, R.G. (2000). Conservation of components of the dystrophin complex in Drosophila. FEBS letters *482*, 13-18.

Grimson, A., Srivastava, M., Fahey, B., Woodcroft, B.J., Chiang, H.R., King, N., Degnan, B.M., Rokhsar, D.S., and Bartel, D.P. (2008). Early origins and evolution of microRNAs and Piwi-interacting RNAs in animals. Nature *455*, 1193-1197.

Gunage, R.D., Dhanyasi, N., Reichert, H., and VijayRaghavan, K. (2017). Drosophila adult muscle development and regeneration. Seminars in cell & developmental biology *72*, 56-66.
Guo, H., Ingolia, N.T., Weissman, J.S., and Bartel, D.P. (2010). Mammalian microRNAs predominantly act to decrease target mRNA levels. Nature *466*, 835-840.

Guo, L., and Lu, Z. (2010). The Fate of miRNA* Strand through Evolutionary Analysis: Implication for Degradation As Merely Carrier Strand or Potential Regulatory Molecule? PloS one *5*.

Ha, M., and Kim, V.N. (2014). Regulation of microRNA biogenesis. Nature reviews Molecular cell biology *15*, 509-524.

Hardy, R.W., Tokuyasu, K.T., Lindsley, D.L., and Garavito, M. (1979). The germinal proliferation center in the testis of Drosophila melanogaster. Journal of ultrastructure research *69*, 180-190.

He, L., and Hannon, G.J. (2004). MicroRNAs: small RNAs with a big role in gene regulation. Nature reviews Genetics *5*, 522-531.

Heimberg, A.M., Sempere, L.F., Moy, V.N., Donoghue, P.C., and Peterson, K.J. (2008). MicroRNAs and the advent of vertebrate morphological complexity. Proceedings of the National Academy of Sciences of the United States of America *105*, 2946-2950.

Herranz, H., Hong, X., Perez, L., Ferreira, A., Olivieri, D., Cohen, S.M., and Milan, M. (2010). The miRNA machinery targets Mei-P26 and regulates Myc protein levels in the Drosophila wing. The EMBO journal *29*, 1688-1698.

Hindle, S.J., and Bainton, R.J. (2014). Barrier mechanisms in the Drosophila blood-brain barrier. Frontiers in neuroscience *8*, 414.

Hoffman, E.P., Brown, R.H., Jr., and Kunkel, L.M. (1987). Dystrophin: the protein product of the Duchenne muscular dystrophy locus. Cell *51*, 919-928.

Hornstein, E., Mansfield, J.H., Yekta, S., Hu, J.K., Harfe, B.D., McManus, M.T., Baskerville, S., Bartel, D.P., and Tabin, C.J. (2005). The microRNA miR-196 acts upstream of Hoxb8 and Shh in limb development. Nature *438*, 671-674.

Hu, Y., Flockhart, I., Vinayagam, A., Bergwitz, C., Berger, B., Perrimon, N., and Mohr, S.E. (2011). An integrative approach to ortholog prediction for disease-focused and other functional studies. BMC bioinformatics *12*, 357.

Hughes, D.C., Marcotte, G.R., Baehr, L.M., West, D.W.D., Marshall, A.G., Ebert, S.M., Davidyan, A., Adams, C.M., Bodine, S.C., and Baar, K. (2018). Alterations in the muscle

force transfer apparatus in aged rats during unloading and reloading: impact of microRNA-31. The Journal of physiology *596*, 2883-2900.

Jeanson-Leh, L., Lameth, J., Krimi, S., Buisset, J., Amor, F., Le Guiner, C., Barthelemy, I., Servais, L., Blot, S., Voit, T.*, et al.* (2014). Serum profiling identifies novel muscle miRNA and cardiomyopathy-related miRNA biomarkers in Golden Retriever muscular dystrophy dogs and Duchenne muscular dystrophy patients. The American journal of pathology *184*, 2885-2898.

Jiang, F., Ye, X., Liu, X., Fincher, L., McKearin, D., and Liu, Q. (2005). Dicer-1 and R3D1-L catalyze microRNA maturation in Drosophila. Genes & development *19*, 1674-1679.

Jimenez-Mallebrera, C., Torelli, S., Feng, L., Kim, J., Godfrey, C., Clement, E., Mein, R., Abbs, S., Brown, S.C., Campbell, K.P.*, et al.* (2009). A comparative study of alpha-dystroglycan glycosylation in dystroglycanopathies suggests that the hypoglycosylation of alpha-dystroglycan does not consistently correlate with clinical severity. Brain pathology (Zurich, Switzerland) *19*, 596-611.

Johnson, R.P., Kang, S.H., and Kramer, J.M. (2006). C. elegans dystroglycan DGN-1 functions in epithelia and neurons, but not muscle, and independently of dystrophin. Development (Cambridge, England) *133*, 1911-1921.

Kheradpour, P., Stark, A., Roy, S., and Kellis, M. (2007). Reliable prediction of regulator targets using 12 Drosophila genomes. Genome research *17*, 1919-1931.

Kloosterman, W.P., Wienholds, E., Ketting, R.F., and Plasterk, R.H. (2004). Substrate requirements for let-7 function in the developing zebrafish embryo. Nucleic acids research *32*, 6284-6291.

Kojima, S., Chiyomaru, T., Kawakami, K., Yoshino, H., Enokida, H., Nohata, N., Fuse, M., Ichikawa, T., Naya, Y., Nakagawa, M.*, et al.* (2012). Tumour suppressors miR-1 and miR-133a target the oncogenic function of purine nucleoside phosphorylase (PNP) in prostate cancer. British journal of cancer *106*, 405-413.

Kong, Y., Liang, X., Liu, L., Zhang, D., Wan, C., Gan, Z., and Yuan, L. (2015). High Throughput Sequencing Identifies MicroRNAs Mediating alpha-Synuclein Toxicity by Targeting Neuroactive-Ligand Receptor Interaction Pathway in Early Stage of Drosophila Parkinson's Disease Model. PloS one *10*, e0137432.

Koturbash, I., Zemp, F.J., Pogribny, I., and Kovalchuk, O. (2011). Small molecules with big effects: the role of the microRNAome in cancer and carcinogenesis. Mutation research *722*, 94-105.

Kreipke, R.E., Kwon, Y.V., Shcherbata, H.R., and Ruohola-Baker, H. (2017). Drosophila melanogaster as a Model of Muscle Degeneration Disorders. Current topics in developmental biology *121*, 83-109.

Kucherenko, M.M., Marrone, A.K., Rishko, V.M., Magliarelli Hde, F., and Shcherbata, H.R. (2011). Stress and muscular dystrophy: a genetic screen for dystroglycan and dystrophin

interactors in Drosophila identifies cellular stress response components. Developmental biology *352*, 228-242.

Kucherenko, M.M., Marrone, A.K., Rishko, V.M., Yatsenko, A.S., Klepzig, A., and Shcherbata, H.R. (2010). Paraffin-embedded and frozen sections of Drosophila adult muscles. Journal of visualized experiments : JoVE.

Kucherenko, M.M., and Shcherbata, H.R. (2018a). miRNA targeting and alternative splicing in the stress response - events hosted by membrane-less compartments. Journal of cell science *131*.

Kucherenko, M.M., and Shcherbata, H.R. (2018b). Stress-dependent miR-980 regulation of Rbfox1/A2bp1 promotes ribonucleoprotein granule formation and cell survival. Nature communications *9*, 312.

Kudoh, H., Ikeda, H., Kakitani, M., Ueda, A., Hayasaka, M., Tomizuka, K., and Hanaoka, K. (2005). A new model mouse for Duchenne muscular dystrophy produced by 2.4 Mb deletion of dystrophin gene using Cre-loxP recombination system. Biochemical and biophysical research communications *328*, 507-516.

Kunkel, L.M., Hejtmancik, J.F., Caskey, C.T., Speer, A., Monaco, A.P., Middlesworth, W., Colletti, C.A., Bertelson, C., Muller, U., Bresnan, M.*, et al.* (1986). Analysis of deletions in DNA from patients with Becker and Duchenne muscular dystrophy. Nature *322*, 73-77.

Langevin, S.M., Stone, R.A., Bunker, C.H., Lyons-Weiler, M.A., LaFramboise, W.A., Kelly, L., Seethala, R.R., Grandis, J.R., Sobol, R.W., and Taioli, E. (2011). MicroRNA-137 promoter methylation is associated with poorer overall survival in patients with squamous cell carcinoma of the head and neck. Cancer *117*, 1454-1462.

Lee, R.C., Feinbaum, R.L., and Ambros, V. (1993). The C. elegans heterochronic gene lin-4 encodes small RNAs with antisense complementarity to lin-14. Cell *75*, 843-854.

Lee, Y., Ahn, C., Han, J., Choi, H., Kim, J., Yim, J., Lee, J., Provost, P., Radmark, O., Kim, S.*, et al.* (2003). The nuclear RNase III Drosha initiates microRNA processing. Nature *425*, 415-419.

Lee, Y., Kim, M., Han, J., Yeom, K.H., Lee, S., Baek, S.H., and Kim, V.N. (2004). MicroRNA genes are transcribed by RNA polymerase II. The EMBO journal *23*, 4051-4060.
Leung, A.K., and Sharp, P.A. (2007). microRNAs: a safeguard against turmoil? Cell *130*, 581-585.

Leung, A.K., and Sharp, P.A. (2010). MicroRNA functions in stress responses. Molecular cell *40*, 205-215.

Lewis, B.P., Burge, C.B., and Bartel, D.P. (2005). Conserved seed pairing, often flanked by adenosines, indicates that thousands of human genes are microRNA targets. Cell *120*, 15-20.

Lewis, B.P., Shih, I.H., Jones-Rhoades, M.W., Bartel, D.P., and Burge, C.B. (2003). Prediction of mammalian microRNA targets. Cell *115*, 787-798.

Li, F., Xu, Y., Deng, S., Li, Z., Zou, D., Yi, S., Sui, W., Hao, M., and Qiu, L. (2015). MicroRNA-15a/16-1 cluster located at chromosome 13q14 is down-regulated but displays different expression pattern and prognostic significance in multiple myeloma. Oncotarget *6*, 38270-38282.

Li, X., and Carthew, R.W. (2005). A microRNA mediates EGF receptor signaling and promotes photoreceptor differentiation in the Drosophila eye. Cell *123*, 1267-1277.

Li, X., Khanna, A., Li, N., and Wang, E. (2011). Circulatory miR34a as an RNAbased, noninvasive biomarker for brain aging. Aging *3*, 985-1002.

Li, X., Li, Y., Zhao, L., Zhang, D., Yao, X., Zhang, H., Wang, Y.C., Wang, X.Y., Xia, H., Yan, J*., et al.* (2014). Circulating Muscle-specific miRNAs in Duchenne Muscular Dystrophy Patients. Molecular therapy Nucleic acids *3*, e177.

Li, Y., Wang, F., Lee, J.A., and Gao, F.B. (2006). MicroRNA-9a ensures the precise specification of sensory organ precursors in Drosophila. Genes & development *20*, 2793-2805.

Liu, N., Landreh, M., Cao, K., Abe, M., Hendriks, G.J., Kennerdell, J.R., Zhu, Y., Wang, L.S., and Bonini, N.M. (2012). The microRNA miR-34 modulates ageing and neurodegeneration in Drosophila. Nature *482*, 519-523.

Ma, J., Shang, S., Wang, J., Zhang, T., Nie, F., Song, X., Heping, Z., Zhu, C., Zhang, R., and Hao, D. (2018). Identification of miR-22-3p, miR-92a-3p, and miR-137 in peripheral blood as biomarker for schizophrenia. Psychiatry research *265*, 70-76.

Macrae, I.J., Zhou, K., Li, F., Repic, A., Brooks, A.N., Cande, W.Z., Adams, P.D., and Doudna, J.A. (2006). Structural basis for double-stranded RNA processing by Dicer. Science (New York, NY) *311*, 195-198.

Makeyev, E.V., and Maniatis, T. (2008). Multilevel regulation of gene expression by microRNAs. Science (New York, NY) *319*, 1789-1790.

Marrone, A.K., Edeleva, E.V., Kucherenko, M.M., Hsiao, N.H., and Shcherbata, H.R. (2012). Dg-Dys-Syn1 signaling in Drosophila regulates the microRNA profile. BMC cell biology *13*, 26.

Marrone, A.K., Kucherenko, M.M., Rishko, V.M., and Shcherbata, H.R. (2011a). New dystrophin/dystroglycan interactors control neuron behavior in Drosophila eye. BMC neuroscience *12*, 93.

Marrone, A.K., Kucherenko, M.M., Wiek, R., Gopfert, M.C., and Shcherbata, H.R. (2011b). Hyperthermic seizures and aberrant cellular homeostasis in Drosophila dystrophic muscles. Scientific reports *1*, 47.

Martinez, N.J., Ow, M.C., Barrasa, M.I., Hammell, M., Sequerra, R., Doucette-Stamm, L., Roth, F.P., Ambros, V.R., and Walhout, A.J. (2008). A C. elegans genome-scale microRNA network contains composite feedback motifs with high flux capacity. Genes & development *22*, 2535-2549.

Mazaud-Guittot, S., Meugnier, E., Pesenti, S., Wu, X., Vidal, H., Gow, A., and Le Magueresse-Battistoni, B. (2010). Claudin 11 deficiency in mice results in loss of the Sertoli cell epithelial phenotype in the testis. Biology of reproduction *82*, 202-213.

McCarthy, J.J., and Esser, K.A. (2007). MicroRNA-1 and microRNA-133a expression are decreased during skeletal muscle hypertrophy. Journal of applied physiology (Bethesda, Md : 1985) *102*, 306-313.

Meijer, H.A., Smith, E.M., and Bushell, M. (2014). Regulation of miRNA strand selection: follow the leader? Biochemical Society transactions *42*, 1135-1140.

Mendell, J.T., and Olson, E.N. (2012). MicroRNAs in stress signaling and human disease. Cell *148*, 1172-1187.

Mercuri, E., and Muntoni, F. (2013). Muscular dystrophies. Lancet (London, England) *381*, 845-860.

Miska, E.A., Alvarez-Saavedra, E., Abbott, A.L., Lau, N.C., Hellman, A.B., McGonagle, S.M., Bartel, D.P., Ambros, V.R., and Horvitz, H.R. (2007). Most Caenorhabditis elegans microRNAs are individually not essential for development or viability. PLoS genetics *3*, e215.

Mok, K.W., Mruk, D.D., Lee, W.M., and Cheng, C.Y. (2012). Spermatogonial stem cells alone are not sufficient to re-initiate spermatogenesis in the rat testis following adjudin-induced infertility. International journal of andrology *35*, 86-101.

Morikawa, Y., Heallen, T., Leach, J., Xiao, Y., and Martin, J.F. (2017). Dystrophin-glycoprotein complex sequesters Yap to inhibit cardiomyocyte proliferation. Nature *547*, 227-231.

Munker, R., and Calin, G.A. (2011). MicroRNA profiling in cancer. Clinical science (London, England : 1979) *121*, 141-158.

Muntoni, F., Brockington, M., Blake, D.J., Torelli, S., and Brown, S.C. (2002). Defective glycosylation in muscular dystrophy. Lancet (London, England) *360*, 1419-1421.

Ng, S.Y., Soh, B.S., Rodriguez-Muela, N., Hendrickson, D.G., Price, F., Rinn, J.L., and Rubin, L.L. (2015). Genome-wide RNA-Seq of Human Motor Neurons Implicates Selective ER Stress Activation in Spinal Muscular Atrophy. Cell stem cell *17*, 569-584.

O'Brien, J., Hayder, H., Zayed, Y., and Peng, C. (2018). Overview of MicroRNA Biogenesis, Mechanisms of Actions, and Circulation. Frontiers in endocrinology *9*, 402.

O'Donnell, K.A., Wentzel, E.A., Zeller, K.I., Dang, C.V., and Mendell, J.T. (2005). c-Myc-regulated microRNAs modulate E2F1 expression. Nature *435*, 839-843.

O'Donnell, P.T., Collier, V.L., Mogami, K., and Bernstein, S.I. (1989). Ultrastructural and molecular analyses of homozygous-viable Drosophila melanogaster muscle mutants indicate there is a complex pattern of myosin heavy-chain isoform distribution. Genes & development *3*, 1233-1246.

Okada, C., Yamashita, E., Lee, S.J., Shibata, S., Katahira, J., Nakagawa, A., Yoneda, Y., and Tsukihara, T. (2009). A high-resolution structure of the pre-microRNA nuclear export machinery. Science (New York, NY) *326*, 1275-1279.

Olde Loohuis, N.F., Kos, A., Martens, G.J., Van Bokhoven, H., Nadif Kasri, N., and Aschrafi, A. (2012). MicroRNA networks direct neuronal development and plasticity. Cellular and molecular life sciences : CMLS *69*, 89-102.

Olivieri, F., Spazzafumo, L., Santini, G., Lazzarini, R., Albertini, M.C., Rippo, M.R., Galeazzi, R., Abbatecola, A.M., Marcheselli, F., Monti, D.*, et al.* (2012). Age-related differences in the expression of circulating microRNAs: miR-21 as a new circulating marker of inflammaging. Mechanisms of ageing and development *133*, 675-685.

Panchal, T., Chen, X., Alchits, E., Oh, Y., Poon, J., Kouptsova, J., Laski, F.A., and Godt, D. (2017). Specification and spatial arrangement of cells in the germline stem cell niche of the Drosophila ovary depend on the Maf transcription factor Traffic jam. PLoS genetics *13*, e1006790.

Pasquinelli, A.E., Reinhart, B.J., Slack, F., Martindale, M.Q., Kuroda, M.I., Maller, B., Hayward, D.C., Ball, E.E., Degnan, B., Muller, P.*, et al.* (2000). Conservation of the sequence and temporal expression of let-7 heterochronic regulatory RNA. Nature *408*, 86-89.

Perotti, M.E., Cattaneo, F., Pasini, M.E., Verni, F., and Hackstein, J.H. (2001). Male sterile mutant casanova gives clues to mechanisms of sperm-egg interactions in Drosophila melanogaster. Molecular reproduction and development *60*, 248-259.

Piccirillo, R., Demontis, F., Perrimon, N., and Goldberg, A.L. (2014). Mechanisms of muscle growth and atrophy in mammals and Drosophila. Developmental dynamics : an official publication of the American Association of Anatomists *243*, 201-215.

Porter, J.D., Khanna, S., Kaminski, H.J., Rao, J.S., Merriam, A.P., Richmonds, C.R., Leahy, P., Li, J., Guo, W., and Andrade, F.H. (2002). A chronic inflammatory response dominates the skeletal muscle molecular signature in dystrophin-deficient mdx mice. Human molecular genetics *11*, 263-272.

Rouillard, A.D., Gundersen, G.W., Fernandez, N.F., Wang, Z., Monteiro, C.D., McDermott, M.G., and Ma'ayan, A. (2016). The harmonizome: a collection of processed datasets gathered to serve and mine knowledge about genes and proteins. Database : the journal of biological databases and curation *2016*.

Ruby, J.G., Stark, A., Johnston, W.K., Kellis, M., Bartel, D.P., and Lai, E.C. (2007). Evolution, biogenesis, expression, and target predictions of a substantially expanded set of Drosophila microRNAs. Genome research *17*, 1850-1864.

Saito, K., Ishizuka, A., Siomi, H., and Siomi, M.C. (2005). Processing of pre-microRNAs by the Dicer-1-Loquacious complex in Drosophila cells. PLoS biology *3*, e235.

Schneider, M., Khalil, A.A., Poulton, J., Castillejo-Lopez, C., Egger-Adam, D., Wodarz, A., Deng, W.M., and Baumgartner, S. (2006). Perlecan and Dystroglycan act at the basal side of

the Drosophila follicular epithelium to maintain epithelial organization. Development (Cambridge, England) *133*, 3805-3815.

Selbach, M., Schwanhausser, B., Thierfelder, N., Fang, Z., Khanin, R., and Rajewsky, N. (2008). Widespread changes in protein synthesis induced by microRNAs. Nature *455*, 58-63.

Shah, M.Y., Ferrajoli, A., Sood, A.K., Lopez-Berestein, G., and Calin, G.A. (2016). microRNA Therapeutics in Cancer - An Emerging Concept. EBioMedicine *12*, 34-42.

Shcherbata, H.R., Yatsenko, A.S., Patterson, L., Sood, V.D., Nudel, U., Yaffe, D., Baker, D., and Ruohola-Baker, H. (2007). Dissecting muscle and neuronal disorders in a Drosophila model of muscular dystrophy. The EMBO journal *26*, 481-493.

Shieh, P.B., Kudryashova, E., and Spencer, M.J. (2011). Limb-girdle muscular dystrophy 2H and the role of TRIM32. Handbook of clinical neurology *101*, 125-133.

Silber, J., Lim, D.A., Petritsch, C., Persson, A.I., Maunakea, A.K., Yu, M., Vandenberg, S.R., Ginzinger, D.G., James, C.D., Costello, J.F.*, et al.* (2008). miR-124 and miR-137 inhibit proliferation of glioblastoma multiforme cells and induce differentiation of brain tumor stem cells. BMC medicine *6*, 14.

Smrt, R.D., Szulwach, K.E., Pfeiffer, R.L., Li, X., Guo, W., Pathania, M., Teng, Z.Q., Luo, Y., Peng, J., Bordey, A.*, et al.* (2010). MicroRNA miR-137 regulates neuronal maturation by targeting ubiquitin ligase mind bomb-1. Stem cells (Dayton, Ohio) *28*, 1060-1070.

Sokol, N.S., and Ambros, V. (2005). Mesodermally expressed Drosophila microRNA-1 is regulated by Twist and is required in muscles during larval growth. Genes & development *19*, 2343-2354.

Supek, F., Bosnjak, M., Skunca, N., and Smuc, T. (2011). REVIGO summarizes and visualizes long lists of gene ontology terms. PloS one *6*, e21800.

Szklarczyk, D., Franceschini, A., Wyder, S., Forslund, K., Heller, D., Huerta-Cepas, J., Simonovic, M., Roth, A., Santos, A., Tsafou, K.P.*, et al.* (2015). STRING v10: protein-protein interaction networks, integrated over the tree of life. Nucleic acids research *43*, D447-452.

Takeuchi, K., Nakano, Y., Kato, U., Kaneda, M., Aizu, M., Awano, W., Yonemura, S., Kiyonaka, S., Mori, Y., Yamamoto, D.*, et al.* (2009). Changes in temperature preferences and energy homeostasis in dystroglycan mutants. Science (New York, NY) *323*, 1740-1743.

Taylor, M.V. (2006). Comparison of Muscle Development in Drosophila and Vertebrates. In Muscle Development in Drosophila (New York, NY: Springer New York), pp. 169-203.

Tinsley, J.M., Blake, D.J., Zuellig, R.A., and Davies, K.E. (1994). Increasing complexity of the dystrophin-associated protein complex. Proceedings of the National Academy of Sciences of the United States of America *91*, 8307-8313.

Tsurudome, K., Tsang, K., Liao, E.H., Ball, R., Penney, J., Yang, J.S., Elazzouzi, F., He, T., Chishti, A., Lnenicka, G.*, et al.* (2010). The Drosophila miR-310 cluster negatively regulates synaptic strength at the neuromuscular junction. Neuron *68*, 879-893.

Tufekci, K.U., Oner, M.G., Meuwissen, R.L., and Genc, S. (2014). The role of microRNAs in human diseases. Methods in molecular biology (Clifton, NJ) *1107*, 33-50.

Ueyama, M., Akimoto, Y., Ichimiya, T., Ueda, R., Kawakami, H., Aigaki, T., and Nishihara, S. (2010). Increased apoptosis of myoblasts in Drosophila model for the Walker-Warburg syndrome. PloS one *5*, e11557.

van der Plas, M.C., Pilgram, G.S., Plomp, J.J., de Jong, A., Fradkin, L.G., and Noordermeer, J.N. (2006). Dystrophin is required for appropriate retrograde control of neurotransmitter release at the Drosophila neuromuscular junction. The Journal of neuroscience : the official journal of the Society for Neuroscience *26*, 333-344.

van Reeuwijk, J., Maugenre, S., van den Elzen, C., Verrips, A., Bertini, E., Muntoni, F., Merlini, L., Scheffer, H., Brunner, H.G., Guicheney, P.*, et al.* (2006). The expanding phenotype of POMT1 mutations: from Walker-Warburg syndrome to congenital muscular dystrophy, microcephaly, and mental retardation. Human mutation *27*, 453-459.

Vasudevan, S. (2012). Posttranscriptional upregulation by microRNAs. Wiley interdisciplinary reviews RNA *3*, 311-330.

Verma, P., Augustine, G.J., Ammar, M.R., Tashiro, A., and Cohen, S.M. (2015). A neuroprotective role for microRNA miR-1000 mediated by limiting glutamate excitotoxicity. Nature neuroscience *18*, 379-385.

Waite, A., Brown, S.C., and Blake, D.J. (2012). The dystrophin-glycoprotein complex in brain development and disease. Trends in neurosciences *35*, 487-496.

Wang, G., van der Walt, J.M., Mayhew, G., Li, Y.J., Zuchner, S., Scott, W.K., Martin, E.R., and Vance, J.M. (2008). Variation in the miRNA-433 binding site of FGF20 confers risk for Parkinson disease by overexpression of alpha-synuclein. American journal of human genetics *82*, 283-289.

Wightman, B., Ha, I., and Ruvkun, G. (1993). Posttranscriptional regulation of the heterochronic gene lin-14 by lin-4 mediates temporal pattern formation in C. elegans. Cell *75*, 855-862.

Willemsen, M.H., Valles, A., Kirkels, L.A., Mastebroek, M., Olde Loohuis, N., Kos, A., Wissink-Lindhout, W.M., de Brouwer, A.P., Nillesen, W.M., Pfundt, R.*, et al.* (2011). Chromosome 1p21.3 microdeletions comprising DPYD and MIR137 are associated with intellectual disability. Journal of medical genetics *48*, 810-818.

Wilson, K., Faelan, C., Patterson-Kane, J.C., Rudmann, D.G., Moore, S.A., Frank, D., Charleston, J., Tinsley, J., Young, G.D., and Milici, A.J. (2017). Duchenne and Becker Muscular Dystrophies: A Review of Animal Models, Clinical End Points, and Biomarker Quantification. Toxicologic pathology *45*, 961-976.

Winter, J., Jung, S., Keller, S., Gregory, R.I., and Diederichs, S. (2009). Many roads to maturity: microRNA biogenesis pathways and their regulation. Nature cell biology *11*, 228-234.

Wu, C.I., Shen, Y., and Tang, T. (2009). Evolution under canalization and the dual roles of microRNAs: a hypothesis. Genome research *19*, 734-743.

Wu, L., Fan, J., and Belasco, J.G. (2006). MicroRNAs direct rapid deadenylation of mRNA. Proceedings of the National Academy of Sciences of the United States of America *103*, 4034-4039.

Xiao, C., Calado, D.P., Galler, G., Thai, T.H., Patterson, H.C., Wang, J., Rajewsky, N., Bender, T.P., and Rajewsky, K. (2007). MiR-150 controls B cell differentiation by targeting the transcription factor c-Myb. Cell *131*, 146-159.

Xie, J., Ameres, S.L., Friedline, R., Hung, J.H., Zhang, Y., Xie, Q., Zhong, L., Su, Q., He, R., Li, M.*, et al.* (2012). Long-term, efficient inhibition of microRNA function in mice using rAAV vectors. Nature methods *9*, 403-409.

Xiong, Y., Zhou, Y., and Jarrett, H.W. (2009). Dystrophin glycoprotein complex-associated Gbetagamma subunits activate phosphatidylinositol-3-kinase/Akt signaling in skeletal muscle in a laminin-dependent manner. Journal of cellular physiology *219*, 402-414.

Yatsenko, A.S., Gray, E.E., Shcherbata, H.R., Patterson, L.B., Sood, V.D., Kucherenko, M.M., Baker, D., and Ruohola-Baker, H. (2007). A putative Src homology 3 domain binding motif but not the C-terminal dystrophin WW domain binding motif is required for dystroglycan function in cellular polarity in Drosophila. The Journal of biological chemistry *282*, 15159-15169.

Yatsenko, A.S., Kucherenko, M.M., Pantoja, M., Fischer, K.A., Madeoy, J., Deng, W.M., Schneider, M., Baumgartner, S., Akey, J., Shcherbata, H.R.*, et al.* (2009). The conserved WW-domain binding sites in Dystroglycan C-terminus are essential but partially redundant for Dystroglycan function. BMC developmental biology *9*, 18.

Yatsenko, A.S., Marrone, A.K., and Shcherbata, H.R. (2014). miRNA-based buffering of the cobblestone-lissencephaly-associated extracellular matrix receptor dystroglycan via its alternative 3'-UTR. Nature communications *5*, 4906.

Yatsenko, A.S., and Shcherbata, H.R. (2014). Drosophila miR-9a targets the ECM receptor Dystroglycan to canalize myotendinous junction formation. Developmental cell *28*, 335-348.

Yekta, S., Shih, I.H., and Bartel, D.P. (2004). MicroRNA-directed cleavage of HOXB8 mRNA. Science (New York, NY) *304*, 594-596.

Zhang, B., Wang, Q., and Pan, X. (2007). MicroRNAs and their regulatory roles in animals and plants. Journal of cellular physiology *210*, 279-289.

Zhang, H., Kolb, F.A., Jaskiewicz, L., Westhof, E., and Filipowicz, W. (2004). Single processing center models for human Dicer and bacterial RNase III. Cell *118*, 57-68.

Zhou, Y.W., Thomason, D.B., Gullberg, D., and Jarrett, H.W. (2006). Binding of laminin alpha1-chain LG4-5 domain to alpha-dystroglycan causes tyrosine phosphorylation of syntrophin to initiate Rac1 signaling. Biochemistry *45*, 2042-2052.

Zimmerman, S.G., Peters, N.C., Altaras, A.E., and Berg, C.A. (2013). Optimized RNA ISH, RNA FISH and protein-RNA double labeling (IF/FISH) in Drosophila ovaries. Nature protocols *8*, 2158-2179.

Zimmermann, C., Stevant, I., Borel, C., Conne, B., Pitetti, J.L., Calvel, P., Kaessmann, H., Jegou, B., Chalmel, F., and Nef, S. (2015). Research resource: the dynamic transcriptional profile of sertoli cells during the progression of spermatogenesis. Molecular endocrinology (Baltimore, Md) *29*, 627-642.

7 Supplementary Figures

Supplementary Figure 1. Over-expression of Dg in muscle during development results in fused muscle phenotype

Dg over-expression during the developmental stage is semi-lethal and few escapers that are analyzed have fused muscle. No muscle degeneration or the muscle atrophy was observed in these flies. Scale bar 100µm. See also Supplementary Table 4.

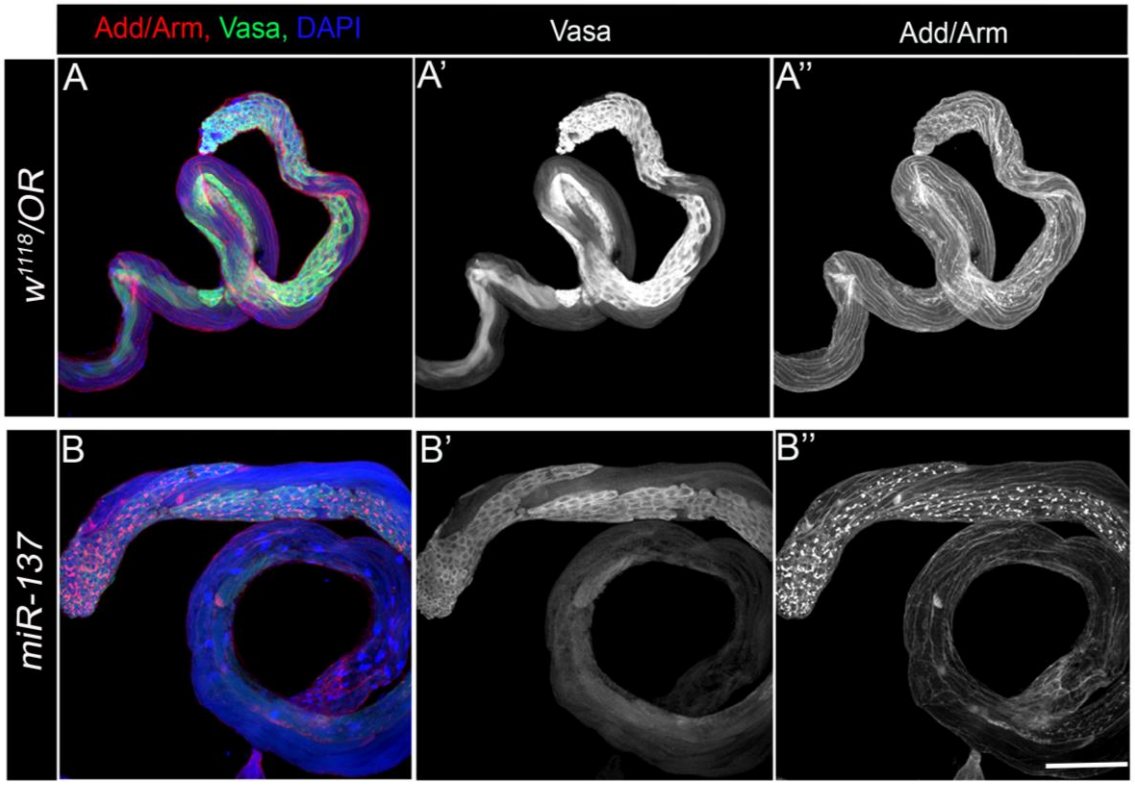

Supplementary Figure 2. *MiR-137* mutants have delayed in differentiation

Antibody staining showing dividing germline in control (A) and in *miR-137* mutant testis. Anti-Add staining was more prevalent in *miR-137* mutant testis compared to control flies indicating, germline cells are possibly differentiating slower than it has been observed for the control. Scale bar 100 µm.

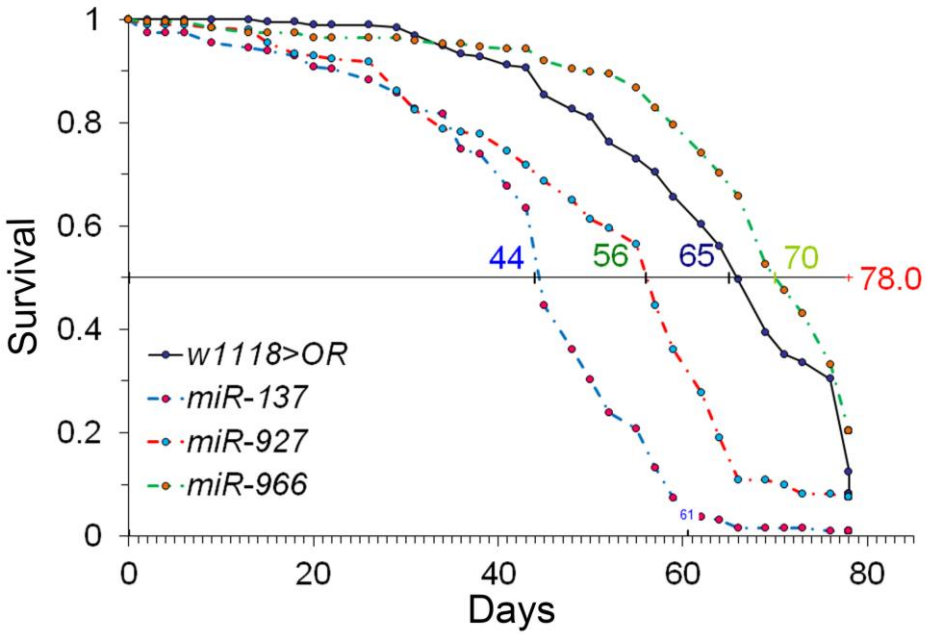

Supplementary Figure 3. Lifespan analysis on miRNA mutants

Lifespan analysis on candidate miRNA mutants showing reduced lifespan on *miR-137* (blue dashed line) and *miR-927* (red dashed line) with median survival of 44 and 56 days compared to control genotype w^{1118}>*OR* (solid black line) with median survival of 65 days. Though, *miR-966* (green dashed line) on the other hand showed extended lifespan with median survival of 70 days it is not statistical significant compared to controls. Statistics were analyzed using Log Rank Test, p-value ***<0.001).

8 Supplementary tables

Supplementary Table 1. The DGC components of *Drosophila* and its functions

***Drosophila* DGC components**	**Gene Function**	**Human homolog(s)**	**Disease association**	**% identity**	**% similarity**	**% gaps**
Dg	Actin cytoskeleton reorganization, axon guidance, establishment or maintenance of cell polarity, egg chamber formation, wing vein specification, muscle cell cellular homeostasis, regulation of glycolytic process, miRNA involved gene silencing, sarcomere organization, cytoskeleton anchoring at the plasma membrane, regulation of synaptic activity	DAG1	Limb-Girdle muscular dystrophy Congenital muscular dystrophy Pediatric autoimmune diseases	24%	35%	28%
Dys	Establishment of cell polarity, wing vein morphogenesis, wing vein specification, muscle cell cellular homeostasis, muscle organ development, neuromuscular synaptic transmission, regulation of neurotransmitter secretion, regulation of short-term neuronal synaptic plasticity	DMD UTRN	Dilated cardiomyopathy Duchenne muscular dystrophy Becker muscular dystrophy	29% 29%	47% 47%	20% 17%
Syn1	Locomotion, regulation of synaptic growth at NMJ	SNTB1 SNTB2	Myopia, Periodontitis	39% 37%	55% 52%	18% 20%

Syn2	locomotion, eye development, rhabdomere development, regulation of synaptic growth at NMJ	SNTG1	Chronic obstructive pulmonary disease	40%	59%	2%
Nos	Nervous system development, regulation of heart rate, imaginal disc development, synapse assembly, response to hormone/lipopolysaccharide, regulation of organ Growth, negative regulation of cell proliferation and DNA replication	NOS1	Colorectal cancer Hypertension Psoriasis Alzheimer	44%	59%	12%
Scg α	-	SGCE	Myoclonic dystonia	25%	45%	16%
Scg β	Muscle organ development	SGCB	Limb-Girdle muscular dystrophy	27%	45%	27%
Scg δ	Heart contraction, mesoderm development, sarcomere organization, cytoskeletal anchoring to the plasma membrane	SGCD	Limb-Girdle muscular dystrophy Dilated cardiomyopathy	39%	60%	3%
Cora	adult somatic muscle development, dorsal closure, cell adhesion in heart morphogenesis, embryonic development, establishment of the blood-brain barrier, wing hair orientation, regulation of tracheal tube size, open tracheal system, cell polarity, cell-cell junction, septate junction assembly	EPB41L3 EPB41L1 EPB41L2	Amyotrophic lateral sclerosis Colorectal cancer Mental retardation	25% 27% 36%	35% 41% 50%	43% 29% 22%

Nrx IV	Axon ensheathment, cell adhesion in heart morphogenesis, dorsal closure, the establishment of the glial blood-brain barrier, nerve maturation, presynaptic membrane assembly, septate junction assembly, regulation of tube size, an open tracheal system, synaptic vesicle docking and targeting, establishment of membrane cell polarity	CNNAP2 CNTNAP5	Alzheimer Bipolar disorder Schizophrenia Autism Cortical dysplasia-Focal epilepsy syndrome Rohn's disease	33% 32%	51% 51%	10% 9%
Yki	Border cell migration, cell proliferation, cell fate specification, Hippo-signaling, negative regulation of the apoptotic process, positive regulation of glial cell proliferation, growth, histone H3-K4 methylation, H3-K4 trimethylation, imaginal disc growth, stem cell proliferation	YAP1	Coloboma, ocular, with or without hearing impairment cleft lip/palate, and/or mental retardation MRI atrophy measures, Polycystic ovary syndrome Pubertal anthropometrics	31%	45%	34%
LanA	Axon guidance, cell adhesion, dorsal trunk growth, an open tracheal system, heart development, mesoderm development, regulation of cell adhesion, cell migration and embryonic development, negative regulation of synaptic growth at NMJ	LAMA5	Colorectal cancer Amyotrophic lateral sclerosis Cardiomyopathy Congenital muscular dystrophy	32%	47%	15%

LanB2	Basement membrane assembly, cell adhesion, endodermal digestive tract morphogenesis, extracellular matrix assembly, salivary gland morphogenesis	LAMC1	Colorectal cancer Cortical malformations Coronary heart disease Systemic lupus erythematosus Epidermolysis bullosa	42%	59%	6%
Mei-P26	Gamete generation, germ cell development, meiotic cell cycle, spermatogenesis	TRIM56 TRIM2		21% 21%	34% 35%	30% 27%
Arm	Cell adhesion, wing disc and cell morphogenesis, dorsal closure, heart formation and development, long-term memory, oogenesis, delamination, photoreceptor cell differentiation, segment polarity, somatic stem cell population maintenance, neuroblast development, nervous system development, cuticle pattern formation	CTNNB1 JUP	Hepatocellular carcinoma, Ovarian cancer Mental retardation Colorectal cancer Exudative vitreoretinopathy Medulloblastoma	67%	77%	9%
Hts	Actin filament organization, adult somatic muscle development, axon guidance, centrosome cycle, cystoblast cycle, oogenesis, female germline ring cancal formation, meiotic spindle organization, photoreceptor axon guidance, sarcomere organization, testicular fusome organization	ADD1	Cerebral palsy, spastic quadriplegia Hypertension	33% 63%	49% 76%	21% 4%

Supplementary Table 2. Relative transcript levels of *Dg*, *Dys*, and *Syn1* due to miRNA loss

Genotype	C_T *Rpl32* AVE±STDEV[a,b]	C_T *Dg*	Δ C_T	ΔΔ C_T	Relative mRNA level[a,b] AVE± SEM[a,b]
Canton-S/OR[a]	21.247 ± 0.030	25.482 ± 0.079	4.196	0	1.000 ± 0.07
Canton-S/OR[b]	16.856 ± 0.064	21.640 ± 0.206	4.784	0	1.000 ± 0.154
miR-137[b]	25.002 ± 0.027	27.922 ± 0.112	2.921	-1.863	3.638 ± 0.253
miR-252[a]	20.905 ± 0.083	23.475 ± 0.293	2.570	-1.628	3.09 ± 0.099
miR-310s[b]	15.820 ± 0.194	20.371 ± 0.084	4.555	-0.229	1.172 ± 0.141
miR-927[b]	23.734 ± 0.135	29.578 ± 0.135	5.843	1.059	0.479 ± 0.093
miR-956[a]	18.634 ± 0.061	24.515 ± 0.080	5.880	1.682	0.311 ± 0.099
miR-959C[a]	23.242 ± 0.230	25.536 ± 0.077	2.294	-1.904	3.743 ± 0.111
miR-966[b]	18.277 ± 0.310	21.176 ± 0.163	3.536	-1.248	2.375 ± 0.531
miR-975C[b]	23.889 ± 0.135	28.754 ± 0.126	4.865	0.089	0.945 ± 0.091
miR-1000[b]	25.455 ± 0.158	28.065 ± 0.079	2.610	-2.174	4.513 ± 0.103
miR-1011/+[b]	11.466 ± 0.653	14.912 ± 1.185	5.437	0.656	0.636 ± 0.129
Genotype	**C_T *Rpl32* AVE±STDEV[a,b]**	**C_T *Dys***	**Δ C_T**	**ΔΔ C_T**	**Relative mRNA level[a,b] AVE± SEM[a,b]**
Canton-S/OR[a]	16.167 ± 0.040	21.891 ± 0.040	5.438	0	1.000 ± 0.011
Canton-S/OR[b]	21.268 ± 0.030	25.482 ± 0.077	4.214	0	1.00 ± 0.070
miR-137[a]	17.931 ± 0.0126	25.482 ± 0.077	3.836	-1.641	3.118 ± 0.034
miR-137[b]	24.229 ± 0.386	27.501 ± 0.149	3.216	-0.998	1.998 ± 0.120
miR-252[a]	18.571 ± 0.105	23.524 ± 0.166	5.094	-0.383	1.304 ± 0.108
miR-252[b]	21.234 ± 0.029	24.265 ± 0.059	3.059	-1.155	2.227 ± 0.108
miR-310s[a]	19.805 ± 0.205	23.794 ± 0.106	3.917	-1.559	2.947 ± 0.04
miR-927[a]	17.546 ± 0.049	23.221 ± 0.342	5.532	0.055	0.963 ± 0.266
miR-956[b]	24.003 ± 0.031	28.451 ± 0.856	4.448	0.233	0.851 ± 0.227
miR-959C[b]	18.340 ± 0.110	23.209 ± 0.119	4.926	0.712	0.645 ± 0.046

miR-966[a]	20.720 ± 0.159	23.703 ± 0.327	3.143	-2.334	5.042 ± 0.174
miR-975C[b]	19.706 ± 0.073	23.787 ± 0.079	4.081	-0.133	1.097 ± 0.079
miR-1000[b]	18.099 ± 0.121	22.459 ± 0.225	4.359	0.149	0.905 ± 0.159
miR-1011/+[a]	16.493 ± 0.244	20.065 ± 0.040	3.479	-1.999	3.996 ± 0.213
Genotype	**C_T *Rpl32* AVE±STDEV[a,b]**	**C_T *Syn1***	**Δ C_T**	**ΔΔ C_T**	**Relative mRNA level[a,b] AVE± SEM[a,b]**
Canton-S/OR[a]	25.442 ± 0.119	26.557 ± 0.097	1.049	0	1.000 ± 0.177
Canton-S/OR[b]	16.183 ± 0.266	21.119 ± 0.175	4.939	0	1.000 ± 0.138
miR-137[a]	27.914 ± 0.286	29.786 ± 0.157	1.121	0.163	0.893 ± 0.719
miR-137[b]	17.646 ± 0.191	24.171 ± 0.098	6.525	1.586	0.333 ± 0.065
miR-252[a]	20.823 ± 0.193	23.031 ± 0.099	2.208	1.158	0.448 ± 0.187
miR-310s[b]	19.368 ± 0.137	23.831 ± 0.287	3.796	-1.14	2.209 ± 0.070
miR-927[a]	26.992 ± 0.066	28.458 ± 0.174	1.918	0.868	0.548 ± 0.528
miR-927[b]	17.419 ± 0.291	24.067 ± 0.021	6.647	1.707	0.306 ± 0.128
miR-956[a]	24.724 ± 0.182	28.898 ± 0.310	3.931	2.882	0.136 ± 0.095
miR-959C[a]	21.889 ± 0.177	27.581 ± 0.538	6.025	4.975	0.032 ± 0.078
miR-966[b]	20.593 ± 0.099	24.260 ± 0.075	3.641	-1.298	2.460 ± 0.123
miR-975C[a]	26.054 ± 0.257	28.173 ± 0.918	2.119	1.069	0.477 ± 0.174
miR-1000[a]	23.397 ± 0.464	27.631 ± 0.485	4.197	3.147	0.113 ± 0.116
miR-1011/+[b]	15.755 ± 0.161	21.192 ± 0.066	5.428	0.488	0.713 ± 0.178

[a] and [b] represent separate qPCR runs. The relative mRNA levels were calculated using the formula $2^{-\Delta\Delta CT}$. An average of two runs when applied was plotted in the graph. Average. Standard deviation (AVE±STDEV) values are based on three replicates. P values are calculated using two-tailed non-paired Student's t-test for significance testing

Supplementary Table 3. Percentage of muscle degeneration in miRNA mutants

Genotype	% of muscle degeneration			n	χ^2 test with Yate's correction	
	Mild	Moderate	Strong			
Canton-S/OR^{D7}	3.870	-	-	155	-	-
Canton-S/OR^{TS}	2.817	3.521	1.408	142	-	9.655*
Canton-S/OR^{SS}	4.167	3.333	2.500	120	-	11.534**
Canton-S/OR^{PS}	4.167	-	0.684	144	-	5.165

Canton-S/OR^{D30}	4.109	1.369	0.684	146	-	7.356
miR-137^{D7}	3.597	-	-	139	0.114	-
miR-137^{TS}	10.126	6.329	3.797	79	8.065*	17.191***
miR-137^{SS}	18.103	2.586	-	116	14.743**	18.799***
miR-137^{PS}	4.762	5.952	11.905	168	21.963***	9.429*
miR-137^{D30}	9.957	4.762	3.030	231	11.484**	20.256***
miR-252^{D7}	7.395	0.965	-	311	5.2	-
miR-252^{TS}	6.944	1.389	-	144	5.847	0.399
miR-252^{SS}	12.307	0.769	3.846	130	8.053*	0.399
miR-252^{PS}	7.692	1.183	0.592	169	2.621	9.746*
miR-252^{D30}	5.556	3.472	3.472	144	5.913	21.387***
miR-310s^{D7}	12.903	-	-	124	7.671	-
miR-310s^{TS}	4.00	2.667	1.667	300	35.523***	14.378**
miR-310s^{SS}	lethal				N/A	N/A
miR-310s^{PS}	14.110	4.294	1.226	163	12.933**	11.885**
miR-310s^{D30}	5.833	0.833	-	120	3.778	5.556
miR-927^{D7}	3.333	-	-	120	0.179	-
miR-927^{TS}	3.086	3.704	0.617	162	0.507	7.196
miR-927^{SS}	7.547	0.943	2.830	106	3.079	9.636*
miR-927^{PS}	18.717	1.069	2.139	187	18.518***	16.144**
miR-927^{D30}	7.291	5.208	2.083	96	3.282	12.624**
miR-956^{D7}	4.167	-	-	144	0.167	-
miR-956^{TS}	1.389	4.167	-	72	0.101	6.984
miR-956^{SS}	9.090	1.515	1.515	132	3.876	9.262*
miR-956^{PS}	3.125	3.906	2.343	128	3.639	7.791*
miR-956^{D30}	1.667	-	0.833	120	13.231**	3.985
miR-959C ^{D7}	13.559	0.847	0.847	236	14.963**	-
miR-959C^{TS}	5.833	-	-	120	7.35	10.983*
miR-959C^{SS}	1.923	4.807	-	104	4.615	19.802***
miR-959C^{PS}	12.962	4.321	12.963	162	31.226***	32.874***
miR-959C^{D30}	2.586	-	-	116	9.319*	16.903***
miR-966^{D7}	2.778	1.389	-	144	2.96	-
miR-966^{TS}	10.949	2.189	-	137	9.358*	8.262*
miR-966^{SS}	3.677	2.206	5.147	136	1.843	12.425**
miR-966^{PS}	15.2	2.7	-	224	14.632**	69.911***
miR-966 ^{D30}	3.333	-	-	120	8.415*	4.815
miR-975C^{D7}	-	1.438	6.475	139	3.763	-
miR-975C^{TS}	5.699	2.591	11.917	193	14.018**	16.358***
miR-975C^{SS}	2.500	5.833	8.333	120	3.122	9.941*
miR-975C^{PS}	-	-	24.432	176	29.68***	64.277***
miR-975C^{D30}	3.097	1.327	2.212	226	10.719*	7.138
miR-1000^{D7}	10.823	5.628	1.299	231	19.072***	-
miR-1000^{TS}	3.125	-	6.250	96	7.409	84.873***
miR-1000^{SS}	8.3	0.9	-	108	6.456	64.826***
miR-1000^{PS}	lethal				N/A	N/A
miR-1000^{D30}	lethal				N/A	N/A
miR-1011/+^{D7}	5.464	2.732	0.546	183	7.349	-
miR-1011/+^{TS}	6.818	5.114	2.273	176	3.634	19.635***

miR-1011/+^{SS}	8.333	0.269	-	108	3.412	5.172
miR-1011/+^{PS}	15.657	0.926	-	198	13.974**	13.513**
miR-1011/+^{D30}	5.263	4.386	0.877	114	2.854	15.489**

The frequency of muscle degeneration results was compared using the χ^2 test with 3 degrees of freedom and Yate's correction

n= number of muscles analyzed

*p<0.05, **p<0.01, ***p<0.001 represents comparison to the control at the same condition, whilst *p<0.05, **p<0.01, ***p<0.001 represents comparison within the same genotype to young age

D7 = 7 day old flies, TS= temperature stress, SS= sugar starvation, PS= protein starvation, D30= 30 day old flies

Supplementary Table 4. Percentage of muscle degeneration in selected miRNA mutants

Condition	Genotype	Experiment	% of muscle degeneration		n	% of muscle atrophy	n	AVE± SEM		
			Mild	Strong				Mild	Strong	Atrophy
Young (D7, 25°C)	*w*^{1118}/*OR*	I	11.009	0.000	109	10.092	109	10.675 ± 1.533	0.00 ± 1.052	10.370 ± 0.660
		II	10.000	0.000	132	10.000	132			
		III	11.017	0.000	130	11.017	130			
Temperature stress (D5, 33°C)		I	15.789	5.263	114	25.439	114	20.553 ± 2.653 *P***	4.512 ± 1.019 *P****	28.153 ± 1.890 *P****
		II	20.588	5.882	102	27.451	102			
		III	17.391	3.804	184	21.739	184			
Sugar Starvation (D5, 25°C)		I	12.418	1.961	153	30.065	153	15.842 ± 1.560	5.621 ± 1.249 *P****	29.660 ± 1.754 *P****
		II	14.407	2.542	118	24.576	118			
		III	14.583	2.778	144	24.306	144			
Aging (D30, 25°C)		I	31.818	6.180	178	37.640	178	27.999 ± 3.246 *P***	9.920 ± 3.147 *P***	46.896 ± 3.061 *P****
		II	21.472	12.270	163	51.534	163			
		III	25.490	8.824	204	42.647	204			
Young (D7, 25°C)	*miR-137*	I	17.308	10.577	104	28.155	103	20.291 ± 1.699 *P***	10.571 ± 1.231 *P***	35.546 ± 2.190 *P***
		II	15.436	8.725	149	21.127	142			
		III	15.789	6.579	76	26.316	76			
Temperature stress (D5, 33°C)		I	37.086	29.139	151	69.388	147	33.208± 4.671 *P** *P***	20.016± 2.270 *P** *P**	55.694 ± 3.772 *P**** *P****
		II	32.877	16.438	73	59.459	74			
		III	26.190	18.254	126	55.556	126			
Sugar Starvation (D5, 25°C)		I	13.609	6.509	169	36.095	169	19.541 ± 1.289 *P***	8.357 ± 2.90 *P*6	38.157 ± 1.392 *P*** *P***
		II	16.279	1.550	129	35.659	129			
		III	18.902	4.878	164	36.585	164			
Aging (D30, 25°C)		I	38.650	24.540	163	65.644	163	30.627 ± 5.281 *P****	20.206 ± 2.800 *P**	53.153 ± 2.463 *P****
		II	30.726	13.966	179	63.128	179			
		III	37.121	22.727	132	68.939	132			
Young		I	21.774	4.839	124	44.355	124	14.889	3.429	26.955

(D7, 25°C)	*miR-927*	II	15.104	2.604	192	30.729	192	± 3.532	± 2.782 *P***	± 8.111 *P**
		III	12.179	3.205	156	19.231	156			
Temperature stress (D5, 33°C)		I	17.424	5.303	132	20.455	132	16.178 ± 3.422	8.627 ± 2.839	31.438 ± 6.813
		II	9.333	2.000	150	17.333	150			
		III	17.910	2.985	67	43.077	65			
Sugar Starvation (D5, 25°C)		I	14.167	0.833	120	45.833	120	13.621 ± 0.355	1.201 ± 0.490 *P** *P**	40.252 ± 3.216 *P**
		II	14.054	1.622	185	34.694	196			
		III	12.644	1.149	174	40.230	174			
Aging (D30, 25°C)		I	43.262	16.312	141	57.447	141	45.255 ± 4.096 *P** *P***	11.845 ± 2.527 *P**	64.955 ± 0.951 *P** *P**
		II	53.846	12.500	104	70.192	104			
		III	38.655	6.723	119	67.227	119			
Young (D7, 25°C)	*miR-966*	I	12.717	1.734	173	23.699	173	14.872 ± 5.385	3.333 ± 3.777 *P***	38.750 ± 6.285 *P**
		II	15.179	2.679	112	37.500	112			
		III	17.500	1.250	80	25.000	80			
Temperature stress (D5, 33°C)		I	22.308	5.385	130	46.154	130	15.132 ± 1.310	1.888 ± 1.381	28.733 ± 4.399
		II	12.308	4.615	130	43.846	130			
		III	10.000	0.000	80	26.250	80			
Sugar Starvation (D5, 25°C)		I	17.683	0.610	164	42.073	164	6.533 ± 4.096 *P**	1.730 ± 2.527 *P*** *P**	43.967 ± 0.951 *P**** *P***
		II	19.255	0.000	161	44.767	172			
		III	25.926	0.617	162	45.062	162			
Aging (D30, 25°C)		I	48.780	31.098	164	79.268	164	36.897 ± 6.304 *P***	32.910 ± 6.174 *P** *P****	67.989 ± 7.431 *P** *P****
		II	28.049	43.293	164	70.732	164			
		III	33.862	24.339	189	53.968	189			
Young (D7, 25°C)		I	14.953	2.804	107	16.822	107	10.887 ± 2.232	2.221 ± 2.055	13.073 ± 2.500
		II	9.375	2.344	128	14.063	128			
		III	8.333	1.515	132	8.333	132			
Temperature stress		I	20.611	1.527	131	22.727	132	20.002 ± 2.014	3.181 ± 1.776	27.853 ± 2.564
		II	22.727	4.545	110	30.275	109			

(D5, 33°C)	*Mhc-Gal4/+*	III	16.667	3.472	144	30.556	144	*P***		*P***
Sugar Starvation (D5, 25°C)		I	24.113	1.418	141	33.333	141	19.006 ± 2.319 *P**	1.969 ± 2.556	36.705 ±4 .330 *P***
		II	16.667	2.778	108	31.481	108			
		III	16.239	1.709	117	45.299	117			
Aging (D30, 25°C)		I	34.932	6.164	146	45.205	146	32.227 ± 4.972 *P***	8.628 ± 4.280 *P***	49.220 ± 8.037 *P***
		II	37.908	11.111	153	64.706	153			
		III	23.841	8.609	151	37.748	151			
Young (D7, 25°C)	*Mhc>Dg*	I	35.938	7.031	128	39.844	128	22.856 ± 3.158	4.800 ± 6.878 *P**	34.334 ± 1.657
		II	12.632	4.211	95	20.000	95			
		III	20.000	3.158	95	43.158	95			
Temperature stress (D5, 33°C)		I	35.821	10.448	134	42.857	133	30.977 ± 5.535 *P**	6.315 ± 4.858	39.829 ± 1.692 *P**
		II	35.849	3.774	106	39.623	106			
		III	21.260	4.724	127	37.008	127			
Sugar Starvation (D5, 25°C)		I	28.846	0.000	156	66.667	156	22.497 ± 5.747	0.673 ± 5.113 *P**	67.619 ± 11.746 *P**
		II	26.263	2.020	99	66.667	99			
		III	12.381	0.000	105	31.429	105			
Aging (D30, 25°C)		I	37.815	21.008	119	64.706	119	43.057 ± 0.777 *P**	12.714 ± 3.498	59.509 ± 3.235 *P**
		II	41.667	5.952	84	53.571	84			
		III	49.689	11.180	161	60.248	161			
Young (D7, 25°C)	*Mhc>miR-137*	I	Semi-lethal • escapers with no muscles • escapers had erect wing					-	-	-
		II								
		III								
Temperature stress (D5, 33°C)		I	Semi-lethal • escapers with no muscles • escapers had erect wing					-	-	-
		II								
		III								
Sugar Starvation (D5, 25°C)		I	Semi-lethal • escapers with no muscles • escapers had erect wing					-	-	-
		II								
		III								
Aging (D30, 25°C)		I	Semi-lethal • escapers with no muscles • escapers had erect wing					-	-	-
		II								
		III								

Young (D7, 25°C)	*Mhc>miR-927*[a]	I	18.493	19.178	146	73.288	146	18.303 ± 0.883 *P**	15.854 ± 0.442 *P***	70.346 ± 2.163 *P****
		II	18.954	15.686	153	71.622	148			
		III	17.460	12.698	63	66.129	62			
Temperature stress (D5, 33°C)		I	39.634	23.780	164	86.806	144	38.583 ± 4.901 *P** *P**	28.191 ± 6.093 *P**** *P***	89.343 ± 1.582 *P**** *P****
		II	27.545	32.934	167	88.976	127			
		III	48.571	27.857	140	92.248	129			
Sugar Starvation (D5, 25°C)		I	29.358	18.349	109	82.569	109	33.227 ± 0.355 *P** *P***	13.207 ± 3.869	76.768 ± 5.801 *P***
		II	37.097	8.065	62	70.968	62			
Aging (D30, 25°C)		I	47.059	58.170	153	77.124	153	45.364 ± 4.818 *P****	39.799 ± 2.501 *P** *P**	77.438 ± 2.776 *P**
		II	40.441	32.353	136	72.794	136			
		III	48.592	28.873	142	82.394	142			
Young (D7, 25°C)	*Mhc>miR-966*	I	17.483	3.497	143	26.573	143	19.699 ± 1.728 *P**	2.010 ± 1.923	29.235 ± 1.404 *P***
		II	18.085	1.064	94	29.787	94			
		III	23.529	1.471	68	31.343	67			
Temperature stress (D5, 33°C)		I	33.824	32.353	136	95.041	121	26.230 ± 9.861	27.072 ± 3.841 *P**** *P**	79.652 ± 7.669 *P*** *P***
		II	23.438	36.719	128	72.381	105			
		III	21.429	12.143	140	71.533	137			
Sugar Starvation (D5, 25°C)		I	31.618	12.500	136	55.882	136	28.791 ± 3.333 *P** *P***	8.065 ± 1.422 *P** *P**	52.231 ± 3.776 *P** *P***
		II	27.660	4.965	141	44.681	141			
		III	27.097	10.968	155	56.129	155			
Aging (D30, 25°C)		I	37.097	16.129	124	69.355	124	40.365 ± 4.632 *P****	20.016 ± 3.908 *P*** *P****	73.194 ± 7.663 *P***
		II	48.148	22.222	108	87.963	108			
		III	35.849	21.698	106	62.264	106			
Young (D7, 25°C)		I	7.692	1.282	78	23.077	78	8.022 ± 0.665	1.152 ± 0.665	20.730 ± 1.417
		II	7.071	1.010	99	18.182	99			
		III	9.302	1.163	86	20.930	86			

Temperature stress (D5, 33°C)	*Mhc>scramble*^{sponge}	I	11.538	7.692	104	35.577	104	14.866 ± 1.081 *P**	6.374 ± 2.294 *P***	31.161 ± 2.228 *P***
		II	13.793	7.759	116	29.464	112			
		III	19.266	3.670	109	28.440	109			
Sugar Starvation (D5, 25°C)		I	8.594	1.563	128	12.500	128	17.268 ± 4.403 *P**	1.516 ± 4.337	17.619 ± 4.997
		II	21.642	2.985	134	27.612	134			
		III	21.569	0.000	102	12.745	102			
Aging (D30, 25°C)		I	20.492	7.377	122	69.672	122	30.441 ± 6.712 *P***	9.787 ± 5.191 *P***	71.722 ± 3.792 *P****
		II	32.847	8.029	137	66.423	137			
		III	37.984	13.953	129	79.070	129			
Young (D7, 25°C)	*Mhc>miR-137*^{sponge}	I	20.000	3.571	140	21.429	140	24.938 ± 3.536 *P***	4.724 ± 3.356 *P***	26.294 ± 4.394
		II	23.469	6.122	98	35.065	77			
		III	31.343	4.478	67	22.388	67			
Temperature stress (D5, 33°C)		I	24.719	8.989	89	71.910	89	25.644 ± 1.081 *P***	8.601 ± 2.294 *P***	68.684 ± 2.228 *P*** *P***
		II	24.779	8.850	113	58.036	112			
		III	27.434	7.965	113	76.106	113			
Sugar Starvation (D5, 25°C)		I	28.472	13.194	144	63.194	144	31.420 ± 2.563 *P**	10.317 ± 2.851 *P*** *P***	60.550 ± 6.616 *P*** *P***
		II	37.121	9.091	132	70.455	132			
		III	28.667	8.667	150	48.000	150			
Aging (D30, 25°C)		I	38.462	23.846	130	60.656	122	37.618 ± 4.776 *P***	27.169 ± 1.337 *P*** *P***	67.643 ± 4.976 *P***
		II	39.394	34.091	132	77.273	132			
		III	35.000	23.571	140	65.000	140			
Young (D7, 25°C)	*how-Gal4/+*	I	9.649	1.754	114	17.544	114	9.524 ±1.773	1.385 ± 1.467	19.725 ± 1.423
		II	6.923	0.000	130	19.231	130			
		III	12.000	2.400	125	22.400	125			
Temperature stress (D5, 33°C)		I	17.714	1.714	175	32.571	175	17.491 ± 0.618 *P***	1.748 ±0.137	37.029 ±2.352 *P***
		II	17.518	1.460	137	37.956	137			
		III	17.241	2.069	145	40.559	143			
Sugar Starvation		I	13.907	4.636	151	21.854	151	12.840 ± 2.628	3.505 ± 2.355	25.028 ± 2.992
		II	8.333	2.778	180	22.222	180			

(D5, 25°C)		III	16.279	3.101	129	31.008	129		*P**	
Aging (D30, 25°C)		I	32.639	8.333	144	40.972	144	31.484 ± 0.537 *P***	9.667 ± 1.807 *P***	47.212 ± 3.188 *P****
		II	27.941	14.216	204	51.471	204			
		III	33.871	6.452	124	49.194	124			
Day 7 (D7, 25°C)	*how>Dg*	I	Semi-lethal (escapers with fused muscle)					-	-	-
Day 7 (D7, 25°C)	*how>miR-137*	II	Embryonic lethal					-	-	-
Day 7 (D7, 25°C)	*how>miR-927*	III	Pupal lethal					-	-	-
Young (D7, 25°C)	*how>miR-966*	I	18.056	0.000	72	13.889	72	20.741 ± 2.381 *P***	1.852 ± 1.606	21.019 ± 4.171
		II	23.611	0.000	72	20.833	72			
		III	20.556	5.556	180	28.333	180			
Temperature stress (D5, 33°C)		I	12.308	2.308	130	26.923	130	16.678 ± 3.962	3.396 ± 2.922	30.622 ± 3.220 *P**
		II	22.222	5.556	54	37.037	54			
		III	15.504	2.326	129	27.907	129			
Sugar Starvation (D5, 25°C)		I	20.313	0.000	64	45.313	64	19.633 ± 1.608 *P**	2.288 ± 0.697 *P*** *P***	35.401 ± 9.911 *P***
		II	18.954	4.575	153	25.490	153			
Aging (D30, 25°C)		I	47.436	23.718	156	69.231	156	40.385 ± 10.18	20.986 ± 5.101	62.393 ± 6.838
		II	33.333	18.254	126	55.556	126			
Young (D7, 25°C)	*how>scramble*^{sponge}	I	14.365	1.657	181	23.316	193	13.333 ± 1.003	1.306 ± 0.633	25.179 ± 2.677
		II	12.183	0.508	197	30.457	197			
		III	13.450	1.754	171	21.765	170			
Temperature stress (D5, 33°C)		I	11.364	1.515	132	18.182	132	14.492 ± 1.915	1.503 ± 2.230	17.982 ± 0.957 *P**
		II	13.281	2.344	128	19.531	128			
		III	18.831	0.649	154	16.234	154			
Sugar Starvation (D5, 25°C)		I	17.886	3.252	123	16.260	123	18.772 ± 0.087 *P****	2.487 ± 0.507	18.418 ± 1.815 *P**
		II	18.788	2.424	165	16.970	165			
		III	19.643	1.786	168	22.024	168			
Aging		I	27.586	9.483	116	54.310	116	26.368	7.856	54.617

(D30, 25°C)		II	25.203	7.317	123	56.911	123	± 1.471 *P****	± 0.688	± 1.245
		III	26.316	6.767	133	52.632	133			
Young (D7, 25°C)	*how>miR-137^{sponge}*	I	17.606	2.817	142	30.282	142	18.928 ± 1.003 *P**	2.463 ± 0.633	28.221 ± 2.667
		II	16.892	0.000	148	20.667	150			
		III	22.286	4.571	175	33.714	175			
Temperature stress (D5, 33°C)		I	24.211	8.947	190	58.201	189	24.719 ± 3.802 *P** *P**	7.199 ± 1.964 *P**	51.826 ± 7.126 *P***
		II	28.346	9.449	127	59.677	124			
		III	21.600	3.200	125	37.600	125			
Sugar Starvation (D5, 25°C)		I	20.968	6.452	124	29.839	124	22.420 ± 1.080 *P**	4.995 ± 0.752	23.792 ± 3.034
		II	23.485	1.515	132	21.212	132			
		III	22.807	7.018	114	20.325	123			
Aging (D30, 25°C)		I	43.636	12.727	165	38.182	165	38.089 ± 2.871 *P** *P***	15.584 ± 3.000 *P**	46.548 ± 4.191 *P**
		II	37.297	10.811	185	50.270	185			
		III	33.333	23.214	168	51.190	168			
Young (D7, 25°C)	*w^{1118}/OR*	I	11.538	1.923	156	5.128	156	21.241 ± 3.289	4.041 ± 0.188	5.064 ± 0.064
		II	10.833	0.833	120	5.000	120			
Temperature stress (D5, 33°C)		I	21.428	3.571	168	32.317	164	23.183 ± 3.728	4.041 ± 0.627 *P**	30.820 ± 1.497 *P***
		II	21.053	4.511	133	29.323	133			
Sugar Starvation (D5, 25°C)		I	20.513	7.692	156	32.692	156	17.882 ± 2.186	8.815 ± 1.804 *P***	39.088 ± 2.398 *P****
		II	14.428	7.960	201	30.348	201			
		III	18.705	10.791	139	35.971	139			
Aging (D30, 25°C)		I	22.513	6.283	191	36.126	191	27.867± 4.674 *P**	9.871 ± 2.688 *P***	49.852 ± 2.060 *P****
		II	30.952	10.317	252	37.302	252			
		III	30.137	13.014	146	43.836	146			
Young (D7, 25°C)		I	25.676	12.838	148	40.541	148	24.404 ± 1.467	12.516 ± 1.887 *P****	37.207 ± 2.042 *P****
		II	20.690	13.300	203	33.498	203			
		III	26.846	11.409	149	37.584	149			
		I	31.847	17.197	157	47.134	157	34.364	18.755	49.921

Temperature stress (D5, 33°C)	*miR-137^{ko}*	II	36.552	21.379	145	56.738	141	± 2.806 *P*** *P***	± 1.368 *P*** *P***	± 3.427 *P**
		III	34.694	17.687	147	45.890	146			
Sugar Starvation (D5, 25°C)		I	26.389	10.417	144	48.6111	144	22.817 ± 1.031	12.401 ± 4.285	44.367 ± 6.333
		II	27.778	12.500	144	49.306	144			
		III	14.286	14.286	119	35.185	108			
Aging (D30, 25°C)		I	19.444	16.667	36	47.222	36	25.755 ± 5.324	20.000 ± 3.173 *P** *P**	52.489 ± 3.173
		II	29.487	25.000	156	51.079	139			
		III	28.333	18.333	120	59.167	120			
Young (D7, 25°C)	*miR-137$^{ko/Df}$*	I	16.326	11.224	98	30.612	98	20.765± 3.382 *P***	10.794± 2.220 *P***	27.689 ± 3.002 *P****
		II	23.077	5.495	182	30.769	182			
		III	22.892	15.663	166	21.687	166			
Temperature stress (D5, 33°C)		I	16.667	8.333	96	34.375	96	20.046 ± 2.650	9.398 ± 1.925 *P****	39.038 ± 3.856
		II	20.139	9.028	144	38.571	140			
		III	23.333	10.833	120	44.167	120			
Sugar Starvation (D5, 25°C)		I	26.316	6.015	133	39.850	133	24.649 ± 1.489 *P***	5.831 ± 1.913	41.592 ± 1.145
		II	26.797	5.229	153	41.177	153			
		III	20.833	6.250	48	43.750	48			
Aging (D30, 25°C)		I	33.898	8.475	112	44.915	118	34.137 ± 1.209	9.446 ± 0.238	46.416 ± 1.501
		II	34.375	10.417	96	47.917	96			
Young (D7, 25°C)	*Mhc-Gal4/+*	I	12.698	1.587	126	16.667	126	14.031 ± 0.513	0.529 ± 0.407	18.005 ± 0.515
		II	14.394	0.000	132	18.182	132			
		III	15.000	0.000	120	19.167	120			
Aging (D30, 25°C)	*Mhc-Gal4/+*	I	16.197	5.634	142	35.915	142	23.102 ± 2.658	6.101 ± 0.666 *P***	39.731 ± 2.793 *P***
		II	28.916	7.831	166	46.988	166			
		III	24.194	4.839	124	43.046	124			
Young (D7, 25°C)	*Mhc>Dg^{RNAi}*	I	29.286	5.000	151	34.416	151	28.680 ± 0.233 *P****	3.528 ± 0.608 *P***	35.518 ± 2.898 *P***
		II	28.571	1.948	154	29.091	154			
		III	28.182	3.636	110	43.046	110			

Aging (D30, 25°C)	*Mhc>Dg^{RNAi}*	I	34.409	23.118	186	77.957	186	33.373 ± 0.399 *P** *P***	18.530 ± 2.289 *P** *P***	67.781 ± 3.917 *P*** *P***
		II	33.113	12.583	151	63.758	149			
		III	32.597	19.890	181	61.628	172			

Values were obtained from the averages of 3 biological replicates. Error bars represent AVE±SEM and statistical significance was determined by two-tailed Student's t-test. *P<0.05, **P<0.01, ***P<0.001 represents comparison to control at the same condition, while *P<0.05, **P<0.01, ***P<0.001 represents comparison within the same genotype at young age.

n= number of muscles analyzed

[a] (*Mhc >miR-927*) male flies with erect wing phenotype

Supplementary Table 5. Candidate miRNAs can target *Dg in vitro*

Dg-3'UTR Reporter	Luciferase Signal (*Renilla/Firefly*) AVE±SEM	Relative Luciferase Signal AVE±SEM
Plate 1		
S3+*miR-137*	1.082 ± 0.039	1.000 ± 0.036
S3+*miR-956*	0.129 ± 0.007	0.499 ± 0.018 *P*=5.907E-02
S2+*miR-137*	0.163 ± 0.021	0.151 ± 0.018 *P*=3.0628E-05
Plate 2		
Control	0.258 ± 0.006	1.000 ± 0.022
S2+*miR-927*	0.129 ± 0.007	0.499 ± 0.018 *P*=2.68604E-06
Control	0.209 ± 0.010	1.000 ± 0.049
S2+*miR-966*	0.0798 ± 0.006	0.383 ± 0.033 *P*=4.43802E-05
Control	0.211 ± 0.012	1.000 ± 0.056
S1+*miR-137*	0.093 ± 0.006	0.443 ± 0.032 *P*=1.361E-04

Values obtained for averages of three biological replicates. Error bars represent AVE±SEM, and statistical significance was determined by two-tailed Student's t-test (*P<0.05, **P<0.01, ***P<0.001).

Control readings from respective plates were used to normalize the luciferase signals.

Supplementary Table 6. Relative *Dg* mRNA levels in adult fly muscle and testes

	Genotype	*Rpl32* C_T AVE±SEM	*Dg* C_T AVE±SEM	Δ C_T AVE±SEM	Average ΔΔ C_T	Relative mRNA level AVE± SEM
Thorax	w^{1118}/*OR*	1.64E+01 ± 3.06E-01	2.11E+01 ± 1.11E-01	4.62 ± 1.7E-01	0.93	1.000 ± 5.3E-02
		1.68E+01 ± 2.5E-02	2.11E+01 ± 4.9E-02	4.25 ± 9.9E-02	1.09	
		2.24E+01 ± 4.41-02	2.88E+01 ± 5.82E-02	6.48 ± 4.0E-02	0.93	
	miR-137^{ko}	1.79E+01 ± 2.06E-02	2.11E+01 ± 4.9E-02	3.25 ± 1.3E-02	-1.37	2.97 ± 8.0E-02 *P*= 7.121E-04
		2.15E+01 ± 6.57E-02	2.39E+01 ± 1.20E-01	2.37 ± 4.8E-02	-2.09	
		2.21E+01 ± 2.25-01	2.76E+01 ± 1.58E-01	5.24 ± 1.3E-02	-1.25	
	miR-137$^{ko/Df}$	2.36E+01 ± 2.22E-01	2.79E+01 ± 2.63E-01	4.00 ± 4.5E-02	-0.61	2.10 ± 1.1E-01 *P*= 1.577E-03 *P*=6.426E-02
		2.11E+01 ± 1.58E-0q	2.41E+01 ± 1.22E-01	2.99 ± 2.5E-02	-1.47	
		2.06E+01 ± 2.33-01	2.59E+01 ± 4.66E-02	5.35 ± 1.1E-01	-1.13	
Testes	w^{1118}/*OR*	2.08E+01 ± 2.49E-01	2.36E+01 ± 2.22E-01	1.63E ± 7.77E-02	0.01	1.000 ± 7.35E-02
		2.23E+01 ± 3.05E-01	2.42E+01 ± 3.68E-01	1.46E ± 2.13E-02	0.17	
		2.37E+01 ± 4.19E-01	2.53E+01 ± 3.86E-01	1.58E ± 9.66E-02	0.05	
	miR-137^{ko}	2.24E+01 ± 2.36E-01	2.37E+01 ± 2.24E-01	1.31 ± 9.13E-02	-0.33	3.96 ± 3.36E-02 *P*=1.020E-02
		2.13E+01 ± 2.88E-01	2.29E+01 ± 2.43E-01	1.53 ± 1.61E-02	-0.05	
		2.63E+01 ± 3.02E-01	2.75E+01 ± 1.34E-01	1.08 ± 3.76E-02	-0.40	
	miR-137$^{ko/Df}$	2.25E+01 ± 3.23E-01	2.51E+01 ± 3.03E-01	2.62 ± 5.83E-02	0.99	1.67 ± 2.25E-02 *P*=5.580E-03 *P*=2.035E-03
		2.22E+01 ± 2.51E-01	2.55E+01 ± 3.35E-01	3.33 ± 5.09E-02	1.64	
		2.46E+01 ± 2.46E-02	2.73E+01 ± 1.29E-02	2.68 ± 8.01E-03	1.05	
	tj>scramble^{sponge}	2.19E+01 ± 3.58E-01	2.32E+01 ± 3.08E-01	2.01 ± 4.49E-02	-0.07	1.000 ± 6.45E-02
		2.15E+01 ± 2.72E-01	2.35E+01 ± 4.74E-01	2.14 ± 1.52E-01	-0.06	
		2.35E+01 ± 2.59E-01	2.53E+01 ± 4.41E-02	2.09 ± 1.39E-01	-0.01	
	Dg$^{1.10G}$::*tj>miR-137*^{sponge}	2.18E+01 ± 2.57E-01	2.35E+01 ± 3.40E-01	1.64 ± 4.01E-02	-0.37	1.376 ± 3.54E-02 *P*=2.743E-03 *P*=3.926E-03
		2.18E+01 ± 2.46E-02	2.35E+01 ± 1.29E-02	1.73 ± 4.78E-02	-0.40	
		1.69E+01 ± 3.10E-02	1.84E+01 ± 4.52E-02	1.48 ± 1.48E-02	-0.60	
	tj>miR-137^{sponge}	2.46E+01 ± 4.14E-02	2.63E+01 ± 1.29E-02	2.46 ± 4.66E-02	0.45	2.33 ± 1.23E-02

		2.16E+01 ± 3.34E-01	2.47E+01 ± 5.35E-01	3.18 ± 1.16E-01	1.04	*P*=1.734E-02
		2.19E+01 ± 3.38E-01	2.48E+01 ± 5.35E-01	3.18 ± 1.11E-01	1.09	
	tj>Dg	2.28E+01 ± 2.63E-01	2.44E+01 ± 5.05E-01	1.47 ± 1.43E-01	-0.55	5.68 ± 1.48E-02 *P*=2.582E-04 *P*=7.645E-03
		2.32E+01 ± 3.89E-02	2.55E+01 ± 5.52E-01	1.53 ± 7.56E-02	-0.60	
		2.29E+01 ± 2.33E-02	2.49E+01 ± 5.01E-02	1.97 ± 7.56E-02	-0.12	

Values obtained for averages of three biological replicates. Error bars represent AVE±SEM, and statistical significance was determined by two-tailed Student's t-test (*P<0.05, **P<0.01, ***P<0.001).

Supplementary Table 7. Early somatic cell counts per testes

Genotype	Tj^+ cells AVE±SEM	Eya^+ cells AVE±SEM	$(Tj+Eya)^+$ cells AVE±SEM	Total cells AVE±SEM	n
w^{1118}/OR	56.322 ± 2.023	84.011 ± 1.204	6.389 ± 0.405	134.253 ± 3.054	24
$miR\text{-}137^{ko}$	82.204 ± 1.488 *P*=1.381E-02	80.438 ± 0.451 *P*=1.885E-01	11.062 ± 1.953 *P*=2.246E-01	151.581 ± 0.163 *P*=5.566E-02	24

Two-tailed Student's t-test with averages of three independent biological replicates was used to determine P values. *P<0.05, **P<0.01, ***P<0.001.

n= number of testes analyzed

Supplementary Table 8. Early somatic cell counts at the apical portion of testes

Genotype	Tj-positive cells	n	*P* value
w1118/OR	43.800 ± 1.110	32	-
$miR\text{-}137^{ko}$	68.559 ± 2.909	34	1.337E-03
$miR\text{-}137^{ko/Df}$	36.721 ± 2.849	31	7.736E-01
$tj/\ w^{1118}$	52.877 ± 2.133	28	-
tj>Dg	42.150 ± 1.520	22	8.093E-02
tj>miR-137	50.236 ± 0.944	27	7.736E-01
$tj>scramble^{sponge}$	39.155 ± 1.600	35	-
$tj>miR\text{-}137^{sponge}$	70.939 ± 4.521	37	3.845E-02
$Dg^{1.10G}$,$tj>miR\text{-}137^{sponge}$	39.092 ± 2.345	29	1.317E-02

Two-tailed Student's t-test with averages of three independent biological replicates was used to determine P values. *P<0.05, **P<0.01, ***P<0.001.

n= number of testes analyzed

Supplementary Table 9. Percentage of permeable testes

Genotype	% of permeable testes (AVE±SEM)	n	*P* value
Control	27.92 ± 2.5	46	-
miR-137^{ko}	88.51 ± 1.46	40	1.57E-06
miR-137$^{ko/Df}$	37.78 ± 4.70	26	4.60E-04
Dg$^{1.10G}$	85.94 ± 3.47	31	2.6E-05
tj>^{w1118}	38.83 ± 1.09	41	-
tj>Dg	69.40 ± 4.0	32	5.88E-03
tj>miR-137	41.26 ± 0.62	39	2.40E-01
miR-137$^{ko/ko}$,tj>miR-137	48.48 ± 4.67	33	1.35E-03
tj>scramble^{sponge}	38.89 ± 7.48	30	-
tj>miR-137^{sponge}	72.50 ± 0.41	40	2.85E-02
Dg$^{1.10G}$,tj>miR137^{sponge}	49.47 ± 2.55	24	3.46E-03

Two-tailed Student's t-test with averages of three independent biological replicates was used to determine P values. *P<0.05, **P<0.01, ***P<0.001.

n= number of testes analyzed

Supplementary Table 10. SJ counts and morphology on elongated spermatids

Genotype	SJ counts (AVE±SEM)	% of abnormal SJ	n
Control	18.253 ± 1.214	18.264 ± 0.024	59
miR-137^{ko}	17.309 ± 2.154 *P*=8.379E-01	51.540 ± 0.078 *P*=1.542E-03	45
miR-137$^{k/Dfo}$	21.583	30.685	8
tj>scramble^{sponge}	22.759 ± 2.059	15.184 ± 0.006	22
tj>miR-137^{sponge}	18.909 ± 0.545 *P*=1.00E-03[a]	48.446 ± 0.070 *P*=1.00E-03[a]	21
tj>^{w1118}	17.438	16.076	16
tj>miR-137	16.500	18.002	12

Two-tailed Student's t-test with averages of three independent biological replicates was used to determine P values. *P<0.05, **P<0.01, ***P<0.001.

[a] χ^2 test with Yate's correction in 1 degree of freedom was analyzed to calculate significance. *P<0.05, **P<0.01, ***P<0.001.

n= number of testes analyzed

9 Appendix

List of abbreviations

Technical abbreviations

A	ampere
AVE	average
BCA	bicinchoninic acid
bp	base pair
BSA	bovine serum albumin
C_T	threshold cycle
DAPI	4', 6-diamidino-2-phenylindole
DGRC	Drosophila Genomics Resource Center
DSHB	Developmental Studies Hybridoma Bank
ECL	enhanced chemiluminescence
EDTA	ethylenediaminetetraacetic acid
FISH	fluorescence *in situ* hybridization
NGS	normal goat serum
nt	nucleotide
PBS	phosphate buffered saline
PBT	PBS-Tween (buffer)
PBTB	PBT-blocking (buffer)
PCR	polymerase chain reaction
PFA	paraformaldehyde
qPCR	quantitative PCR
qRT-PCR	quantitative reverse transcription PCR
Rpm	revolutions per minute
RT	reverse transcriptase
RT	room temperature
S2 cells	Schneider 2 cells
SD	standard deviation
SEM	standard error of the mean
Tris	tris-hydroxymethyl-aminomethane

Biological abbreviations

AMPK	AMP-activated protein kinase
A-P axis	anterior-posterior axis
BTB	blood-testis barrier
C-terminus	carboxyl-terminus
cDNA	complementary DNA
DNAse	deoxyribonuclease
CySCs	somatic stem cells
DGC	Dystrophin-associated Glycoprotein Complex
Dme	*Drosophila Melanogaster*
DNA	deoxyribonucleic acid
Dre	*Danio rerio*
Drosophila	*Drosophila melanogaster*
dsRBD	double stranded RNA binding domain protein
E.Coli	*Escherichia coli*
ECM	extracellular matrix
GB	gonial blast
GO	Gene Ontology
GSCs	germline stem cells
hsa	*homo sapiens*
mGFP	membrane GFP
miRNA	microRNA
mmu	*mus musculus*
mRNA	messenger RNA
MTJ	myotendinos junction
PKA	cAMP-dependent protein kinase
Pol	polymerase
Pre-miRNA	precursor microRNA
Pri-miRNA	primary microRNA
RNA	ribonucleic acid
RISC	RNA-induced silencing complex
RNAi	RNA interference
RNase	ribonuclease

rRNA	ribosomal RNA
siRNA	small interfering RNA
SV	seminal vesicle
UAS	upstream activation sequence
UTR	untranslated region

Gene and protein names

act	actin
Add	adducin
Arm	armadillo
Cora	coracle
Chic	chickadee
Dg	dystroglycan
Dlg	discs large
Dys	dystrophin
Eya	eyes absent
GluR	glutamate receptor IIA
Hts	hu lo tai shao
How	held out wings
LanA/B	laminin A
Mega	mega trachea
Mei-P26	meiotic P26
MHC	myosin heavy chain
mir-310s	refers to *miR-310, miR-311, miR-312,* and *miR-313* together
miR-975C	refers to *miR-975, miR-976, miR-977* together
miR-959C	refers to *miR-959, miR-960, miR-961, miR-962* together
Nrx-IV	neurexin IV
nNOS	nitric oxide synthase
PH3	Phospho-Histone H3
Scg	sarcoglycan
Syn1	syntrophin-like 1
Tj	traffic jam
Yki	yorkie

Zfh-1	zinc finger protein 1

Symbols

°C	degree celsius
CO_2	carbon dioxide
G	gram
µg	microgram
µl	microliter
µM	micromolar
h	hour
kbp	kilo base pair
kDa	kilodalton
Mb	mega base
ml	milliliter
min	minute
mM	milli molar
NaCl	sodium chloride
NaH_2PO_4	monosodium phosphate
Na_2HPO_4	disodium phophate
NaOH	sodium hydroxide
ng	nanogram
V	volt

Acknowledgement

Foremost, I would like to thank my supervisor Halyna R. Shcherbata for giving me an opportunity to peruse my PhD under her supervision. Her continuous guidance, suggestions, and challenges has shaped me to be a better student in these 3.5 years. I not only got to realize what it takes to be a good scientist, but also a successful PI and a great human being. Some of the life lessons I took watching her closely will aspire me to be better in many ways in the years to come.

Next, I would like to thank my thesis committee members Stefan Bonn and Jörg Großhans for their suggestions, ideas, criticism and support for making this project a success. I would like to especially thank Stefan Bonn for always supporting my project and being available whenever I needed his suggestions. I would like to thank Roland Dosch, Martin Göpfert and Ahmed Mansouri for joining as my extended committee members.

My sincere gratitude to my current and previous lab mates who gave me their valuable scientific input, technical support, and especially for their company, creating a family like environment. Travis, for always motivating and helping me in every possible way to make me focus and laugh even at times of doubts and confusions. For more being a friend than just a colleague. You kept me optimistic during my times of discouragement and made weekends work a happy place to be. Ömer, for sharing his experiences as a graduating PhD student and answering all my concerns during the initial phase of my project. Mariya, for teaching me tools and techniques of the lab during my time as an intern and making me familiar with the department. Andriy, for all the help and support during the entire project. Rucha, for helping me during the final phase of my project. Jasmine, for creating $Dg^{1.10G}$ mutants that came handy on this project. To the whole Herbert Jäckle Department for their input during departmental seminars, support through reagents and technical contributions. My students, Tadas, Liezel, Daniel, and Alejandra who helped me in my project. I got an opportunity to grow as a mentor and learned a lot from them.

GGNB for giving an opportunity to learn many aspects of science. I have benefited a lot from scientific and soft skill courses throughout these years. I have enjoyed being their student representative, editorial board in GGNB times and as a part of organizing committee for WoCaNet symposium. I have come to realize many of my strengths and weakness throughout the exposures I got with these activities. I would like to acknowledge the travel grant that allowed me to present my work in international symposium.

To my friends in Göttingen, for adding healthy dosage of laughter and craziness throughout these years. Prajwal, for always listening, making tea breaks more compelling, sharing enthusiasm and frustrations and adding positivity in everyday life. Shoba, for exciting conversations about science, career and for crazy moments turning Göttingen a familiar place to be.

To my near and dear friend, Elizabeth, for making my adaptation easier since my first day in Germany. Our long conversations, life experiences always lit positivity in me. Manita, for listening to my worries and fruitful tips and a continuous reminder to taking care of myself. My childhood buddies (RSKDM), for teaching me a meaning of friendship for past 18 years. Losing one of you during these years was a shock and a realization of life beyond dreams and career.

To my family, my parents for believing in me, for always being enthusiastic to see me becoming a Doctor despite of not knowing either my project or the nature of my research. My sisters, who are my backbone. They believed so much in me that they never let me fail. Especially Priti, for taking care of our parents and home all these years. Kriti, for always encouraging me to stay on my track. My in-laws, for always motivating me to give my best. I think I stressed them more than I stressed myself during the last phase of my project. To Bhupesh and Semi for their support and accepting my absence during family engagements. To my husband Bhawesh, my life support, for his continuous support, love and for keeping up with me throughout these years. For taking care of our home, my smallest needs, for not giving up on me and not letting me give up. You truly deserve a share of my Doctor title.